Copyrighted
by
Robert Joseph Fanning
1959

Downloaded from SHAREOK. Persistent Handle URL: https://hdl.handle.net/11244/1349

THE UNIVERSITY OF OKLAHOMA

GRADUATE COLLEGE

THE DYNAMIC HEAT TRANSFER CHARACTERISTICS OF A CONTINUOUS AGITATED TANK REACTOR

A DISSERTATION

SUBMITTED TO THE GRADUATE FACULTY

in partial fulfillment of the requirements for the

degree of

DOCTOR OF PHILOSOPHY

BY

ROBERT J. FANNING

Norman, Oklahoma

1958

THE DYNAMIC HEAT TRANSFER CHARACTERISTICS OF A CONTINUOUS AGITATED TANK REACTOR

APPROVED BY

C M Slieppcevich

R L Huntington

John E Powers

Gerald Thomas

DISSERTATION COMMITTEE

TABLE OF CONTENTS

	Page
LIST OF TABLES	v
LIST OF ILLUSTRATIONS	vii
Chapter	
I. INTRODUCTION	1
II. STATEMENT OF THE PROBLEM AND REVIEW OF PREVIOUS WORK	5
III. DESCRIPTION OF EXPERIMENTAL EQUIPMENT	12
IV. EXPERIMENTAL PROCEDURE	29
V. DERIVATION OF THEORETICAL TRANSFER FUNCTIONS	56
VI. DISCUSSION OF EXPERIMENTAL AND THEORETICAL RESULTS	79
SUMMARY	107
BIBLIOGRAPHY	111
APPENDICES	
A. NOMENCLATURE	114
B. EQUIPMENT CALIBRATION DATA	119
C. DYNAMIC RESPONSE DATA	128
D. MISCELLANEOUS DATA	146
E. EXPLANATION OF BASIC PRINCIPLES	149

LIST OF TABLES

Table		Page
1.	Steady State Conditions, Arrangement Four-Water	49
2.	Processed Frequency Response Data, Arrangement Four-Water	50
3.	Steady State Conditions, Arrangement Four-Oil	51
4.	Processed Frequency Response Data, Arrangement Four-Oil	52
5.	Theoretical Transfer Functions, Arrangement One	75
6.	Theoretical Transfer Functions, Arrangement Two	76
7.	Theoretical Transfer Functions, Arrangement Three	77
8.	Theoretical Transfer Functions, Arrangement Four	78
9.	Fischer Porter Flowrator Calibration-Water	120
10.	Fischer Porter Flowrator Calibration-Water	121
11.	Fischer Porter Flowrator Calibration-Oil	122
12.	Fischer Porter Flowrator Calibration-Oil	123
13.	Bristol Recording Potentiometer Calibration	124
14.	Steady State Conditions, Arrangement One-Water	129
15.	Processed Frequency Response Data, Arrangement One-Water	130
16.	Steady State Conditions, Arrangement One-Oil	131
17.	Processed Frequency Response Data, Arrangement One-Oil	132
18.	Steady State Conditions, Arrangement Two-Water	133

Table Page

19. Processed Frequency Response Data, Arrangement Two-Water. 134

20. Steady State Conditions, Arrangement Two-Oil 135

21. Processed Frequency Response Data, Arrangement Two-Oil. 136

22. Steady State Conditions, Arrangement Three-Water 137

23. Processed Frequency Response Data, Arrangement Three-Water. 138

24. Steady State Conditions, Arrangement Three-Oil 139

25. Processed Frequency Response Data, Arrangement Three-Oil. 140

26. Effect of Agitator Speed on System Response. 142

27. Effect of Coolant Flow Conditions on System Response-Laminar Flow 143

28. Effect of Coolant Flow Conditions on System Response-Turbulent Flow 144

29. Effect of Agitator Speed on Theoretical Steady State Values of h_o 145

30. Physical Properties of Process Fluids. 147

31. Volumes and Weights of Equipment 148

LIST OF ILLUSTRATIONS

Figure		Page
1.	Front View of Sine Wave Generator	14
2.	Rear View of Sine Wave Generator	14
3.	Schematic Drawing of Experimental Continuous Agitated Tank Reactor	17
4.	Side View of Experimental Apparatus	19
5.	View of Complete System with Instruments	20
6.	View of Tank Reactor with Instruments	21
7.	Flow Diagram of Equipment Arrangement One	22
8.	Flow Diagram of Equipment Arrangement Two	23
9.	Flow Diagram of Equipment Arrangement Three	24
10.	Flow Diagram of Equipment Arrangement Four	25
11.	Flow Diagram of Sine Wave Generator Testing Equipment	32
12.	Experimental Flow Waves at Higher Frequencies	34
13.	Experimental Flow Waves at Medium Frequencies	35
14.	Experimental Flow Waves at a Lower Frequency	36
15.	Transient Response Curves, Arrangement Two, Water	40
16.	Transient Response Curves, Arrangement Four, Oil	41
17.	Selected Frequency Response Records, Arrangement Four, Water	44

Figure Page

18. Selected Frequency Response Records, Arrangement Four, Oil 45

19. Bode Diagram Comparing Oil and Water Response Curves for Equipment Arrangement Four 53

20. Experimental and Theoretical Bode Diagrams, Arrangement One, Water. 86

21. Experimental and Theoretical Bode Diagrams, Arrangement One, Oil. 87

22. Experimental and Theoretical Bode Diagrams, Arrangement Two, Water. 90

23. Experimental and Theoretical Bode Diagrams, Arrangement Two, Oil. 91

24. Experimental and Theoretical Bode Diagrams, Arrangement Three, Water. 94

25. Experimental and Theoretical Bode Diagrams, Arrangement Three, Oil. 95

26. Inlet and Outlet Cooling Water Temperature versus Coil Length. 98

27. Effect of Tank Fluid Conditions on Frequency Response Curves 99

28. Effect of Coolant Flow Conditions on Frequency Response Curves 101

29. Experimental and Theoretical Bode Diagrams, Arrangement Four, Water 104

30. Experimental and Theoretical Bode Diagrams, Arrangement Four, Oil 105

31. Calibration Curves of Fischer Porter Flowrator for Water at Various Temperatures 125

32. Calibration Curves of Fischer Porter Flowrator for Oil at Various Temperatures 126

33. Calibration Curve for Bristol Continuous Recording Potentiometer 127

Figure Page

34. Schematic Diagram of a Continuous Agitated Reactor 150

35. Block Diagram of Feedback Loop for Continuous Agitated Tank Reactor 153

36. Illustration of Method for Combining a Block Diagram 155

37. Combined Block Diagram. 156

38. Uncombined Bode Diagram Loci. 159

39. Combined Bode Diagram Loci. 160

40. Various Types of Process Transients 163

41. Graphical Analysis of a Response Curve. 164

42. Frequency Response Input and Output Waves 169

43. Example of a Nyquist Diagram. 171

THE DYNAMIC HEAT TRANSFER CHARACTERISTICS OF A CONTINUOUS AGITATED TANK REACTOR

CHAPTER I

INTRODUCTION

Modern dynamic response theory was developed to a large extent during World War II, mostly in connection with technological advancements in military equipment. Much of this information was released shortly after the war in the form of textbooks on the subject of servomechanisms theory. Since that time, developments have continued at an ever accelerating pace in problems related to aircraft, guided missile and weapons fire control. The majority of theoretical achievements has been concentrated upon position control involving mechanical, hydraulic and electronic components. Recently, chemical engineers have realized the importance of the application of servo-theory to problems in process control. The distinct possibility of some sort of advanced control method involving electronic computers has given added impetus to process control development.

To date, the majority of all chemical engineering process design has been carried out solely on a steady state basis. It is then customary to install standardized controllers on pieces of process equipment after design and installation in the hope that a wide flexibility

in controller adjustment will allow for satisfactory process control. Such methods are now being, or will in the future be, supplanted by a scientific approach to problems in plant control.

Advances in chemical plant automation by application of Systems Engineering techniques appear to be taking a definite direction. The first step is a theoretical analysis of the process in question from the standpoint of unsteady state behavior. For all but the simplest of processes this generally yields a family of differential equations describing the dynamic behavior of the given process. These equations along with those describing controller action are programmed into an analog computer. The cause and effect relationships between pertinent process and controller parameters may then be studied intensively. Optimum controller settings are readily obtained in this manner. In addition, that information vital to advanced control methods is made available.

In the development of equations suitable for analog computer programming, it is generally necessary to make a number of simplifying assumptions and approximations. The validity of certain equations employed in an overall systems analysis may then be open to question. Research directed at the development of certain valid procedures for writing accurate equations describing process dynamics is needed.

The present investigation involves a comprehensive study of the dynamics of heat transfer of a continuous agitated tank reactor. A large majority of organic chemical reactions are exothermic, thus the dynamics of reactor heat removal is of special significance. Many reactors of the batch or agitated tank type are jacketed with the inner

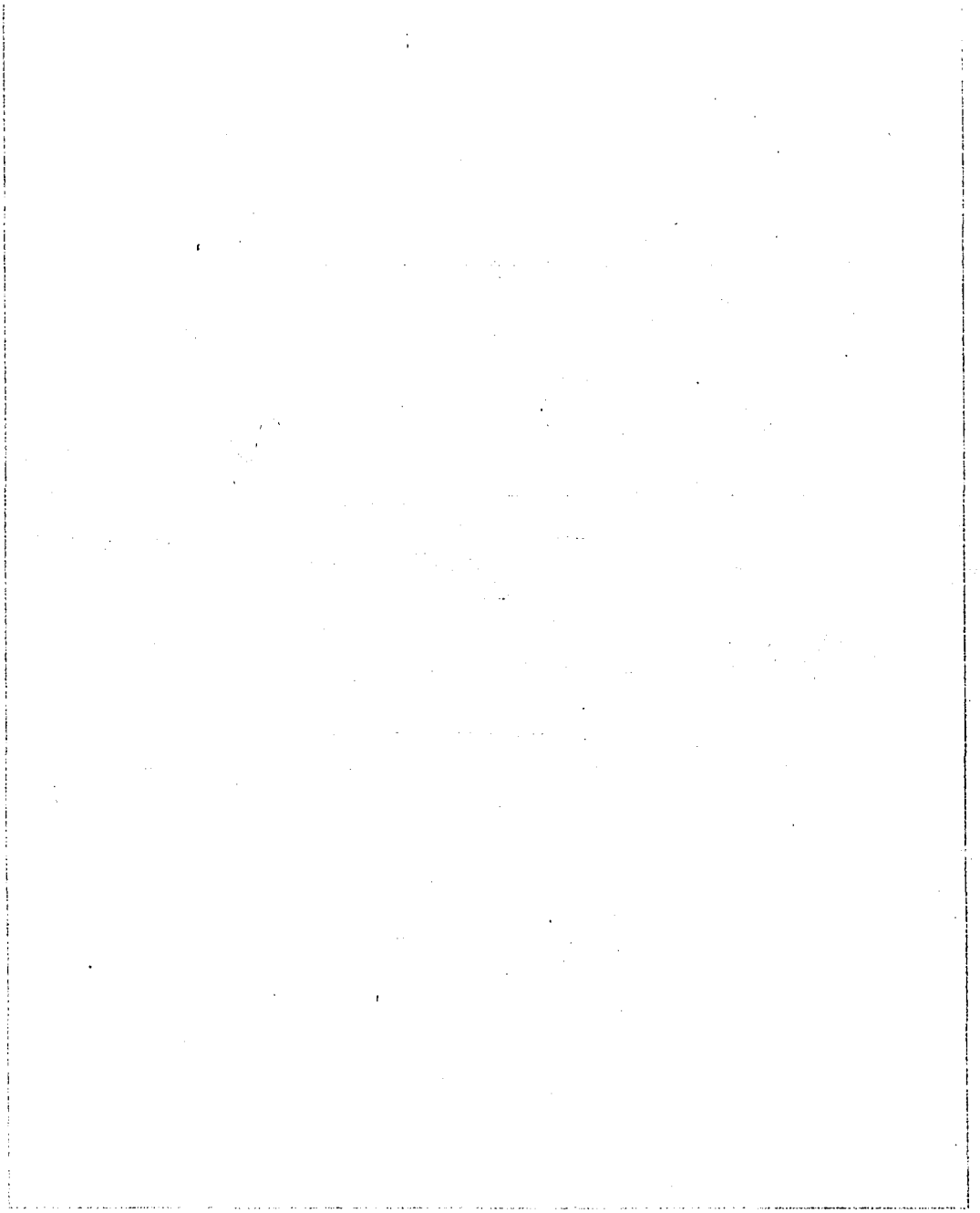
tank walls serving as a heat exchange surface. Newer designs have utilized the advantages of an internal heat transfer surface together with proper agitation and baffling to provide favorable flow patterns and effective heat transfer. The present equipment is designed along such lines with helical coils as the internal heat exchange surface.

Experimental techniques in the present work include the use of both transient and frequency response. In the collection of most frequency response data, the input sinusoid is generated by a mechanical unit constructed from a linear diaphragm control valve. Transient responses are obtained by sudden movement of the required valve. In each case the output variable is the temperature of the tank fluid. The fluctuation with time of this variable is made by a sensitive continuous recording potentiometer. A majority of experimental data is collected by the study and analysis of such records.

Time lags in the transfer of heat are basically the result of the resistance to temperature change offered by certain fluid or metal capacitances in addition to the rate of heat transfer possible under existing fluid film conditions. All capacitances are relatively easily calculated. Fluid film conditions, especially under dynamical operation, are not well known. Therefore, a complete investigation of process control problems requires a theoretical analysis supported by experimental data on specific equipment configurations.

A comparison between actual and theoretical transfer functions allows for the establishment of certain assumptions and rules regarding the derivation of theoretical equations which are accurate within engineering tolerances. It is hoped that this work may be of some practical

value from a standpoint of basic control design for similar equipment. More particularly, it is desired that it will serve as a stimulant toward future work in the dynamic analysis of all types of process equipment.



CHAPTER II

STATEMENT OF THE PROBLEM AND REVIEW OF PREVIOUS WORK

Objectives of Process Dynamic Studies

Contrary to many of the more recent articles treating the general subject of process control development, this investigation does not cover a closed-loop analysis. In the present work, no attempt is made to devise methods and procedures for a predetermination of proper controller settings with a given set of process parameters. Although such work is of major importance, it is believed that more is to be gained in this particular instance by experimental and theoretical investigations involving open loop process dynamics.

A closed loop analysis involves cases wherein the entire control loop is studied as a unit. An open loop investigation involves the isolated study of any one or all of the individual components of a process control loop such as the controller, valve, sensing element and the process itself. Investigation of the dynamic characteristics of individual loop components is more of a basic nature and the answers obtained here are of value when considering closed loop situations.

The term "process dynamics" connotes the characteristics displayed by a given piece of equipment during conditions which change with time. If it is desired to know the manner in which a unit of process

equipment will respond, it is then reasonable to impose a change of some sort upon it and note the following response with time. One of the newer methods for characterizing or rating a piece of process equipment from the standpoint of dynamics is to oscillate periodically one of the process variables and note the effect upon a related variable. Such a procedure is referred to as the frequency response technique. Numerous recent textbooks in the field of servomechanisms theory adequately cover the subject of frequency response analysis. Most of these however are concerned with servo-theory applied to position control as contrasted with process control (5, 11, 38). At present, there are very few references which cover the subject of modern process control theory exclusively (8, 50). Included in the Appendix of the present work is a short coverage of servo-theory as it specifically concerns the problem under investigation.

In any dynamic study of a chemical process or unit operation whether it be experimental or theoretical, relationships between two or more pertinent process variables and time must be obtained. In the case of a purely theoretical approach, these relationships generally take the form of ordinary or partial differential equations. Such equations are employed in the programming of an analog computer for simulation of the process. If experimental frequency response techniques are used, the desired relationships are obtained in the form of transfer functions which relate the forced process variable, the forcing process variable and time.

In the development of the mathematical model of a process suitable for simulation on an analog computer, it is generally necessary to

make certain simplifying assumptions. This limitation is necessary because of the space available on the computer and because of the extreme complexity of many chemical processes, particularly those involving heat and mass transfer. There is then definite need for the establishment of experimental proof which will either refute or confirm the use of certain simplifying procedures in equations making up the mathematical model (20, 43).

Previous Investigations

Literature in the field of the dynamics of chemical process equipment is relatively meager because of the recent interest of chemical engineers in this area. Virtually all work of either experimental or theoretical nature has appeared since 1953. One of the earliest publications was that of Stanton and Hoyt (35) concerning the dynamics of a commercial-size, continuous fractionating unit. Williams and Rose (44) presented a very comprehensive theoretical study of a five plate, two component continuous fractionating column. Here, a total of 17 simultaneous differential equations were derived describing the equipment dynamics. The effect of various control and process parameters on column response was studied with the aid of an analog computer. Ceaglske and Eckman (9) described the dynamic analysis of a pressure process utilizing experimental transient and frequency response techniques.

Worley and McKnight (28) were interested in the response characteristics of a plate-type heat exchanger. By experimental and analytical methods, they were able to develop the transfer function describing

the relationship between the exhanger effluent temperature and the brine coolant input temperature. Cohen and Johnson (12) as well as Mozley (30) investigated the dynamics of small, single-pass, concentric-tube heat exchangers. Here also, the subject of interest was the exchanger effluent temperature when forced by variations in temperature of the shell-side fluid. Williams and Young (47) studied the system dynamics of a single control loop wherein the process was a shell and tube heat exchanger. The equations describing the dynamics of the exchanger were obtained by a method of compartmentalization. Response of the control loop was studied by simulation on an analog computer.

The response characteristics of a Dubbs oil cracking furnace were described by Laspe (24). The fuel gas flow rate was varied sinusoidally by means of a sine-wave generator and the response of the oil effluent temperature noted. By trial and error fitting of the resulting Bode diagram, an experimental transfer function was obtained.

In the field of continuous agitated systems, the work available from references has been almost entirely of a theoretical nature. Mason (27) presented a quantitative treatment of the dynamics of a small, steam-heated kettle. The transfer function concept was not at that time in common use and response characteristics were obtained in the time domain by classical solution of the describing differential equations. Aries and Amundson (49), then later Bilous, et. al. (4) developed theoretical equations relative to the dynamics of continuous agitated tank reactors. Both articles are to be commended for their mathematical excellence.

Literature references on the subject of process dynamics are, at present, relatively few in number. Considerable stress has been placed

on a theoretical analysis followed by solution on an analog computer. As regards the control dynamics of continuous agitated tank reactors, virtually all the information available is of a theoretical nature.

Control Methods For Continuous Agitated Tank Reactors

The continuous agitated tank reactor is extensively used in the process industries in the synthesis of many and varied products. Among processes employing such equipment are those for the production of synthetic rubber, linear polyethylene, polyvinyl chloride and many others. The reactions involved are usually exothermic and reaction temperatures must often be carefully controlled in order to produce quality products at the desired reaction rate. A number of different methods for continuously removing the heat evolved are now in use. Probably the oldest type of equipment is the conventional jacketed reactor through which a suitable coolant is passed. A more recently applied method consists of passing the coolant, in liquid form, through some sort of internal heat transfer surface. A variation of the latter method is to utilize the heat of vaporization of a volatile coolant within internal coils. Such a method is employed extensively throughout, for example, the entire synthetic rubber industry. Another method gaining in application by process designers is that of immersing tubular reactor coils within a pressure vessel containing a suitable volatile coolant. Again, removal of the heat of reaction is effected by evaporation of the coolant.

In most cases, reaction temperature control is achieved by application of any one or combinations of the following: (1) varying the liquid coolant flow rate, (2) varying the rate of fresh feed, catalyst, or re-

cycle flow to the reactor, and (3) controlling the back pressure and therefore the temperature of a volatile coolant whether it be located within internal tubes or on the shell side of a tubular reactor.

Specific Objectives of the Present Investigation

The present investigation is directed at determining the control dynamics of a small, continuous agitated tank-type unit equipped with helical heat transfer coils. Experimental and theoretical dynamic studies were made with coils acting both as a heat source and a heat sink; however, the latter study was stressed because of the reasons which were previously discussed. Here, the system is in effect a distributed one since the temperature of the coolant changes with length of cooling tube traversed.

The most important transfer function developed was that obtained by sinusoidally varying the coolant flow rate and noting the response of the reactor effluent temperature. These tests were experimentally conducted for various fluids charged, various conditions of fluid turbulence both outside and within the coolant coils, and for different coil sizes. The response under these variable conditions was noted and comparisons made with theoretical transfer functions whose derivations were obtained using different assumptions.

The present work differs from published work available on agitated reactor units in that it includes experimental data. In the field of conventional heat exhangers where experimental dynamic data are presented, the forcing variable is generally fluid temperature instead of flow rate. A mathematical analysis involving the latter process variable

is more complex and uncertain because of the variation in heat transfer film coefficient with rate of coolant flow. However, system response to a change in coolant flow rate is of more value because reactor temperature control is often achieved, as previously mentioned, by the manipulation of a coolant flow control valve.

In summarizing, it may be stated that the present investigation is directed toward supplying experimentally corroborated information which may be used in adequately describing the dynamics of heat transfer of a continuous agitated tank reactor equipped with an internal heat transfer surface. It represents the initial portion of a long-range research program aimed at acquiring a better understanding of the control characteristics of continuous chemical reactors in general.

CHAPTER III

DESCRIPTION OF EXPERIMENTAL EQUIPMENT

Sine Wave Generator

It was realized at the beginning of the investigation that some satisfactory method must be available for imparting a sinusoidal movement to certain process variables. For the change in liquid flow rate, this may be accomplished with reasonable accuracy by manual methods using a stop watch and a flow indicating device. However, beyond a frequency of about 1.5 cycles per minute, hand methods result in too much wave distortion. Some relatively simple, inexpensive device had to be developed which would permit oscillations up to five cycles per minute or even higher if necessary. The most satisfactory arrangement consisted of a linear motor control valve with stem driven by a small, geared-down induction motor.

The basic portion of the sine-wave generator, consists of a 1/2 inch IPT Research Control Valve with ATC top works. The trim is constructed of stainless steel with bronze valve body tested to 150 psig W.P. Trim bevel is such that the valve is linear through the lower 80 percent of stem travel. In construction of the generator, the top half of the diaphragm body was removed together with diaphragm and spring. The cast aluminum housing which had served as the lower half of the dia-

phragm body was then used to support the device which imparted a harmonic translational motion to the valve stem. This device is made of a rotational power source and Scotch yoke together with connecting gears. The driver consists of a Merkle-Korff SG-10 induction motor attached to a gear reduction housing. Motor gear-train output speed is 1 RPM and maximum output torque is 10 lb.in. Appropriate gear sets connect the motor output drive to the Scotch yoke drive. The arrangements of gears are such that yoke drive speeds of 0.1, 0.25, 0.5, 1.0, 2.5 and 5 cycles per minute are obtainable. The range can easily be increased by exchange with a motor of higher speed. The free end of the valve stem is screwed into the Scotch yoke drive block and secured by lock nut. Variable, periodic, up-and-down motion is thereby imparted to the valve stem. Since the valve trim is linear at least throughout the bottom portion of its movement, it would be expected that a sinusoidal wave of bulk fluid flow would pass through the valve body. A variable amplitude of stem movement is obtained by installing yoke drive throws of varying radii. Throughout most of this work, a peak to valley stem travel of 1/8 inch was used. The valve plug location for steady state operation is continuously adjustable. Figures 1 and 2 consist of front and rear photographs of the wave generator. Details of construction are on file in the Chemical Engineering Department, University of Oklahoma.

Continuous Agitated Tank Reactor and Auxiliaries

Design of the agitated tank is such as to approximate geometrically many larger types used in industry. The tank is constructed

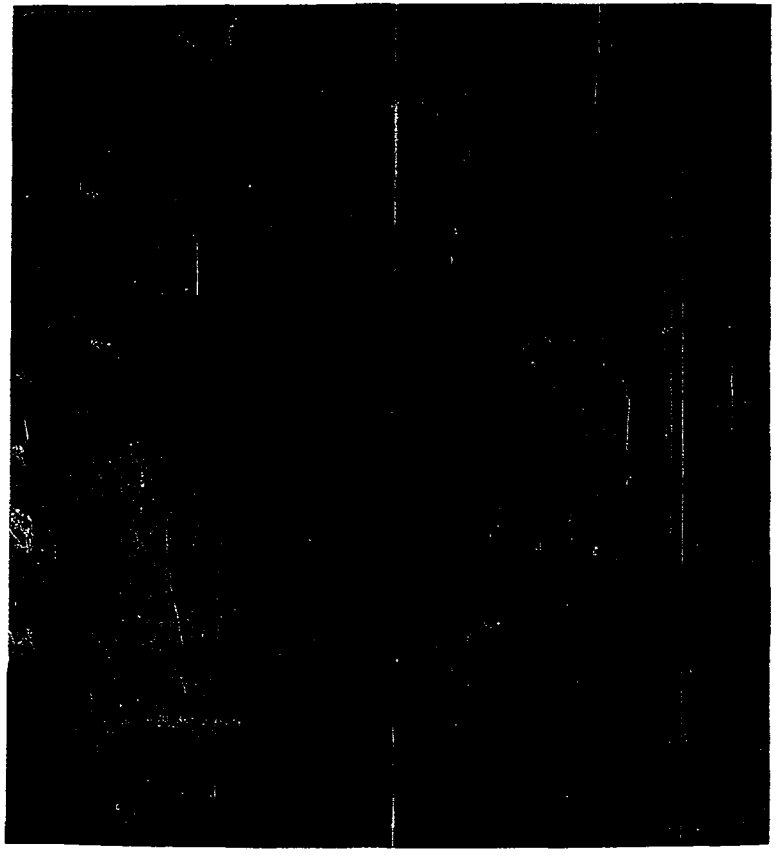


Figure 1 - Front View of Sine Wave Generator

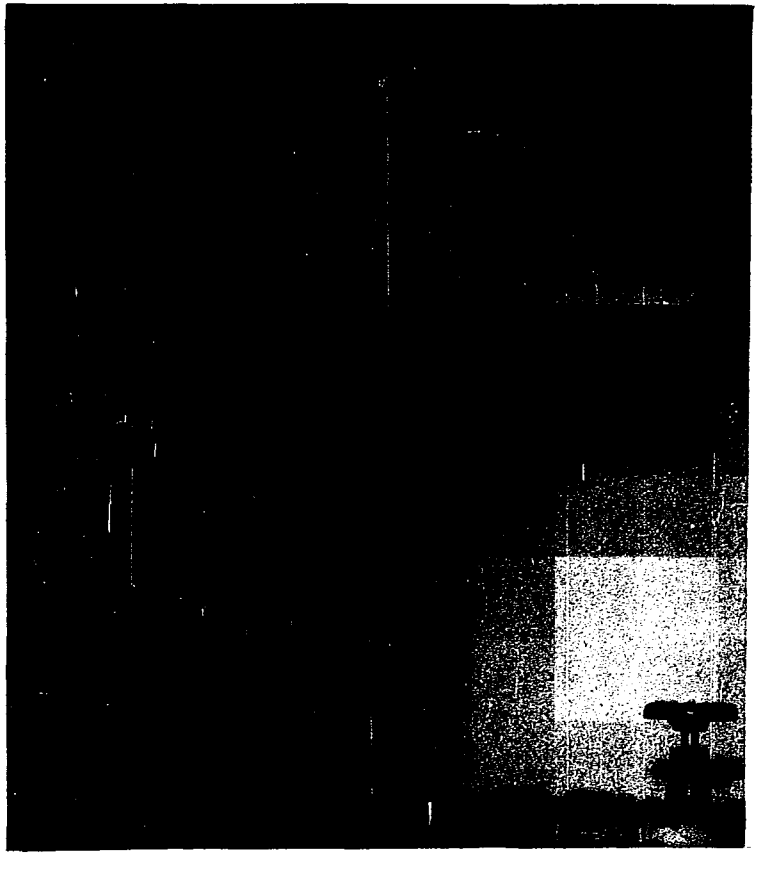


Figure 2 - Rear View of Sine Wave Generator

of 14 gauge 316 stainless steel. Diameter and total height are 12 and 15 inches respectively. Four 1-inch baffles are spot-welded 90° apart at the inner periphery of the tank. The lower edge of the top outlet is 12-inches from the tank bottom. A 5/8-inch plywood annulus rests on the top ends of the baffles and extends flush with top of the tank. This is to provide overall strength together with coil, thermocouple and thermometer support. The entire tank rests on a 1 7/8-inch combination plywood and fiberboard insulation mat of the same diameter as the tank. Outside insulation consists of a 2-inch thick layer of fiber-glass insulation glued to the outside tank wall with sodium silicate solution. This in turn is covered with aluminized heavy insulating paper. Bonding with aqueous sodium silicate was also used here to prevent any slippage.

Two sets of copper heat transfer tubes were used during the course of the experimentation. These sets are identical as to tube diameter, wall thickness and coil diameter. The coil sets contain a different number of coil turns. Coil A consists of 3.5 turns of 5/8-inch type L copper tubing with a total surface area of 135.01 square inches. Coil B consists of 7.5 turns of same type tubing with a total exposed surface area of 264.83 square inches. The copper tubing inside coil diameter is approximately five inches. With such a small diameter, a method had to be devised for wrapping straight tubing without introducing excessive distortion into the coils. A previous trial with 1/2-inch tubing wrapped on an 8-inch diameter mandril indicated that without support within the tube, the finished-coil tube cross section is in the form of an ellipse instead of a circle. A satisfactory method was

eventually devised for obtaining coils with very slightly distorted cross-sections. This consisted of first packing the straight tube as tightly as possible with jeweler's sand. With a 5-inch steel pipe acting as the form, the tubing was snugly wrapped by means of a metal turning lathe. The final result was an accurately wound coil section with low distortion. Inside coil volume, coil displacement volume, coil weight and area were all carefully measured as they are of major importance in the derivation of theoretical transfer functions. Entrance of a straight length of copper tubing through the bottom of the tank to connect with the coils is effected by means of a specially-machined "O"-ring fitting. This arrangement proved satisfactory and very little leakage was experienced. Figure 3 shows a simplified sectional drawing of the finished continuous agitated tank with its fittings.

The tank agitator consists of a Model CV-4, 1/4 H.P. direct drive "Lightnin" portable mixer equipped with a 1/4 H.P. variable speed brush shifting type motor of 1/4 H.P. capacity, wound for operation on 110/220 volt, 60 cycle, single phase current. Output speed of the motor and agitator is 1750 RPM, adjustable down to about 100 RPM. This speed may be reduced further by connecting the motor in series with a continuously adjustable transformer. The agitator, shaft and impeller were purchased as a unit. The shaft is of type 304 stainless steel of suitable length to allow positioning of the impeller one turbine diameter off-bottom. The impeller is a 4-inch pilot plant turbine type closely modeled from commercial size installations. The impeller location in the tank was fully adjustable; however, in accordance with recommended

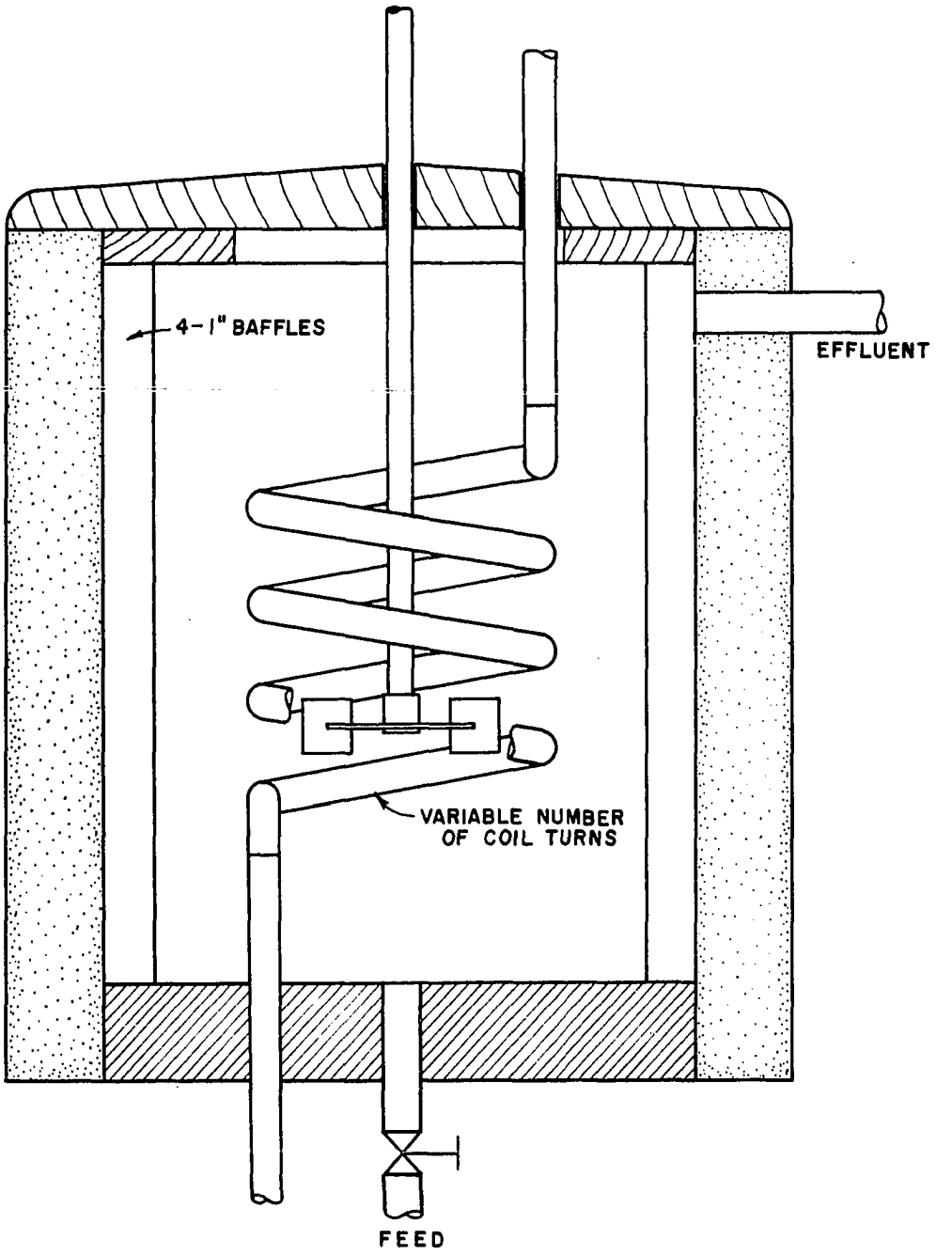


Figure 3 - Schematic Drawing of Experimental Continuous Agitated Tank Reactor

mixing theory for this type installation, the impeller was positioned at one turbine diameter (4-inches) from the tank bottom through all runs. The agitator installation was quite heavy and had to be mounted on a heavy, modified A-frame support.

The fluid under test is not pressured out of the system but instead overflows from an 1/2-inch opening near the top of the tank. The arrangement as described is not the most desirable, however, it can be made to operate satisfactorily if the tank is mounted at a position at least three feet above a fluid effluent storage tank. In this manner, a definite siphoning effect is realized and fluid may be withdrawn from the tank at rates up to 5 GPM depending upon fluid viscosity. The tank fluid level remains essentially constant for small changes in feed rate so that the result is substantially the same as if the fluid were forced from the tank by pressure.

Figures 4, 5 and 6 clearly show the tank together with all auxiliaries. Figures 7, 8, 9 and 10 are schematic drawings for the four different equipment arrangements tested. The feed supply unit consists of a 55 gallon barrel lagged with 1-inch aluminum-sheathed fiber glass insulation. Heat transfer surface for heating or cooling of the feed barrel contents is provided by 5/8-inch copper tubing with approximately 2.8 sq. ft. of surface. The piping details are such that either steam or cooling water may be admitted to the tubes. Adequate feed barrel mixing is obtained by a clamp-on type agitator equipped with a marine-type impeller. The fluid under study flows from the bottom of the barrel to the suction side of a small feed pump. This pump is a Goulds 1/4 H.P., 1750 RPM centrifugal with a capacity of approximately 10

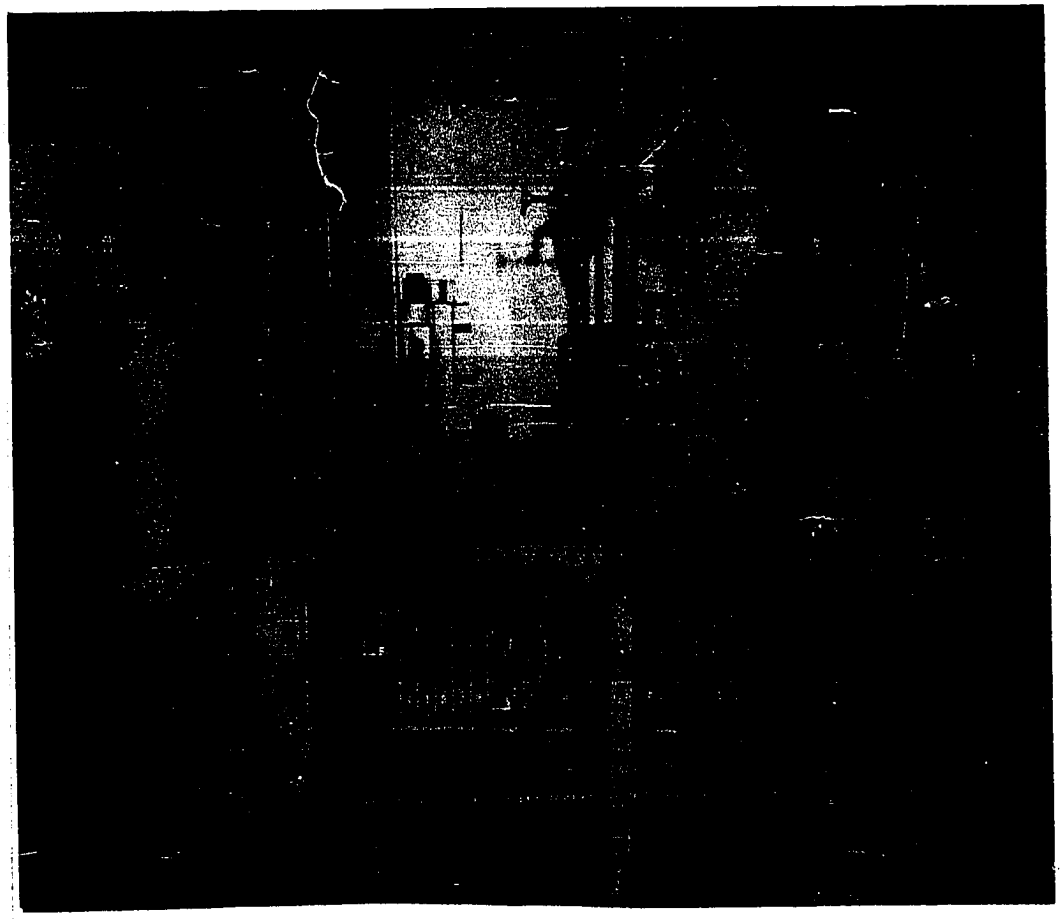


Figure 4 - Side View of Experimental Apparatus Without Continous Recording Equipment

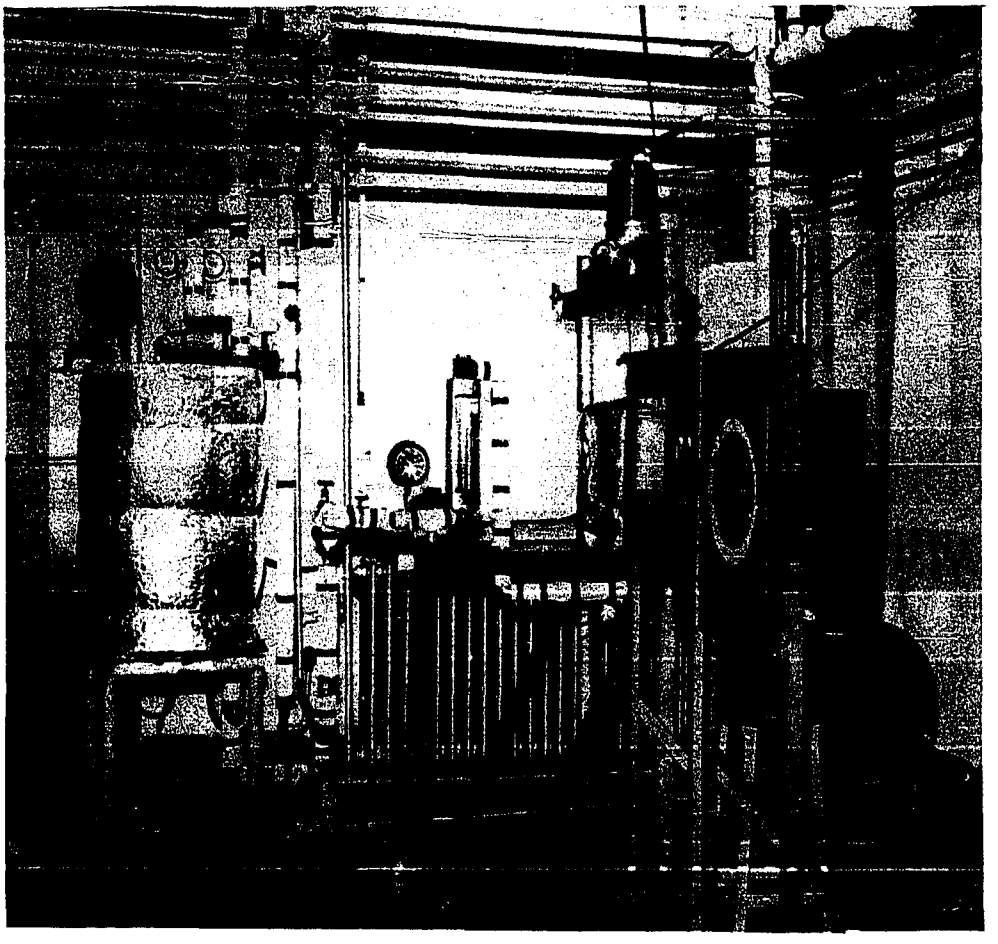


Figure 5 - View of Complete System with Instruments

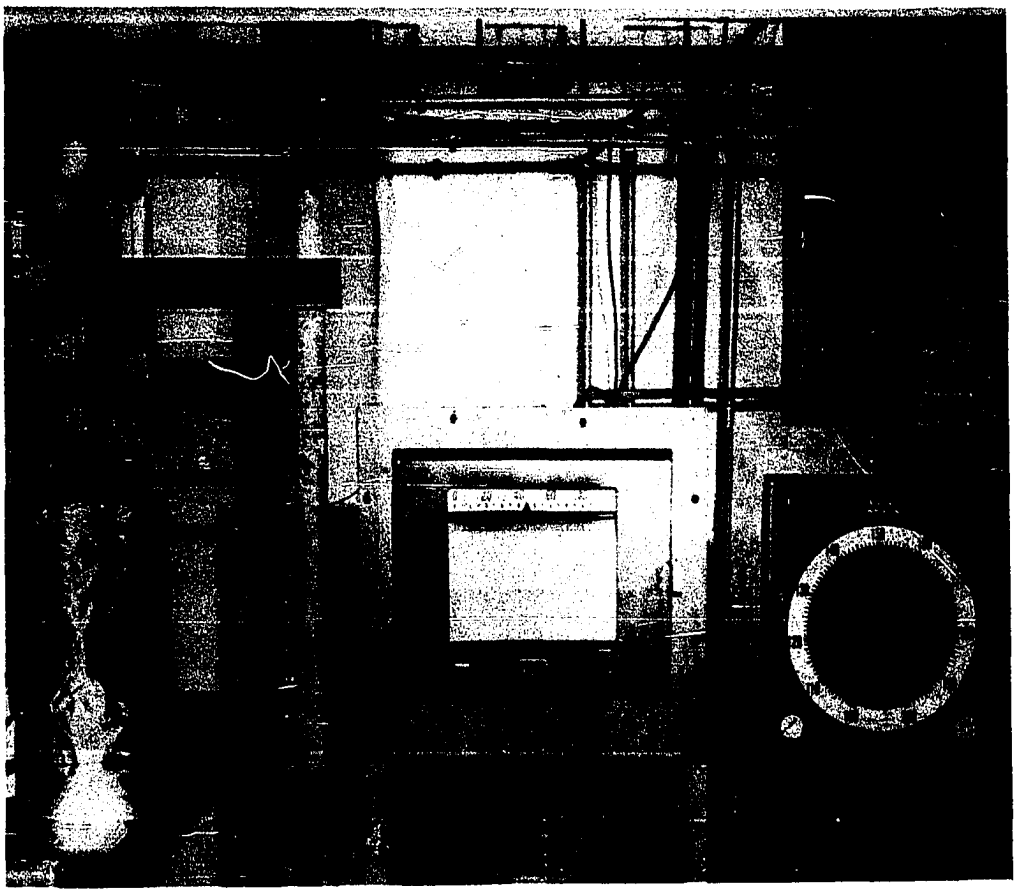


Figure 6 - View of Tank Reactor with Instruments

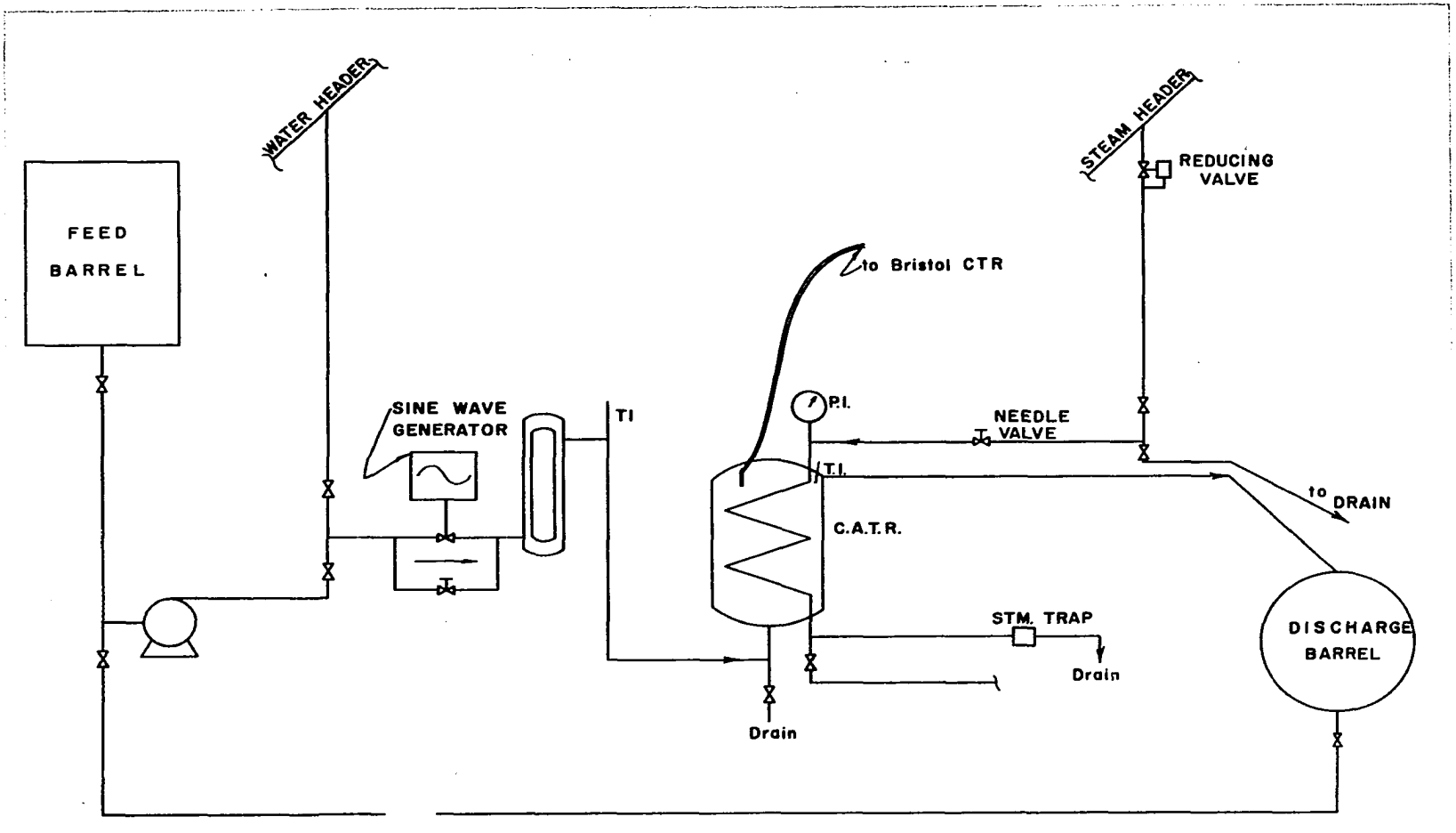


Figure 7 - Flow Diagram of Equipment Arrangement One

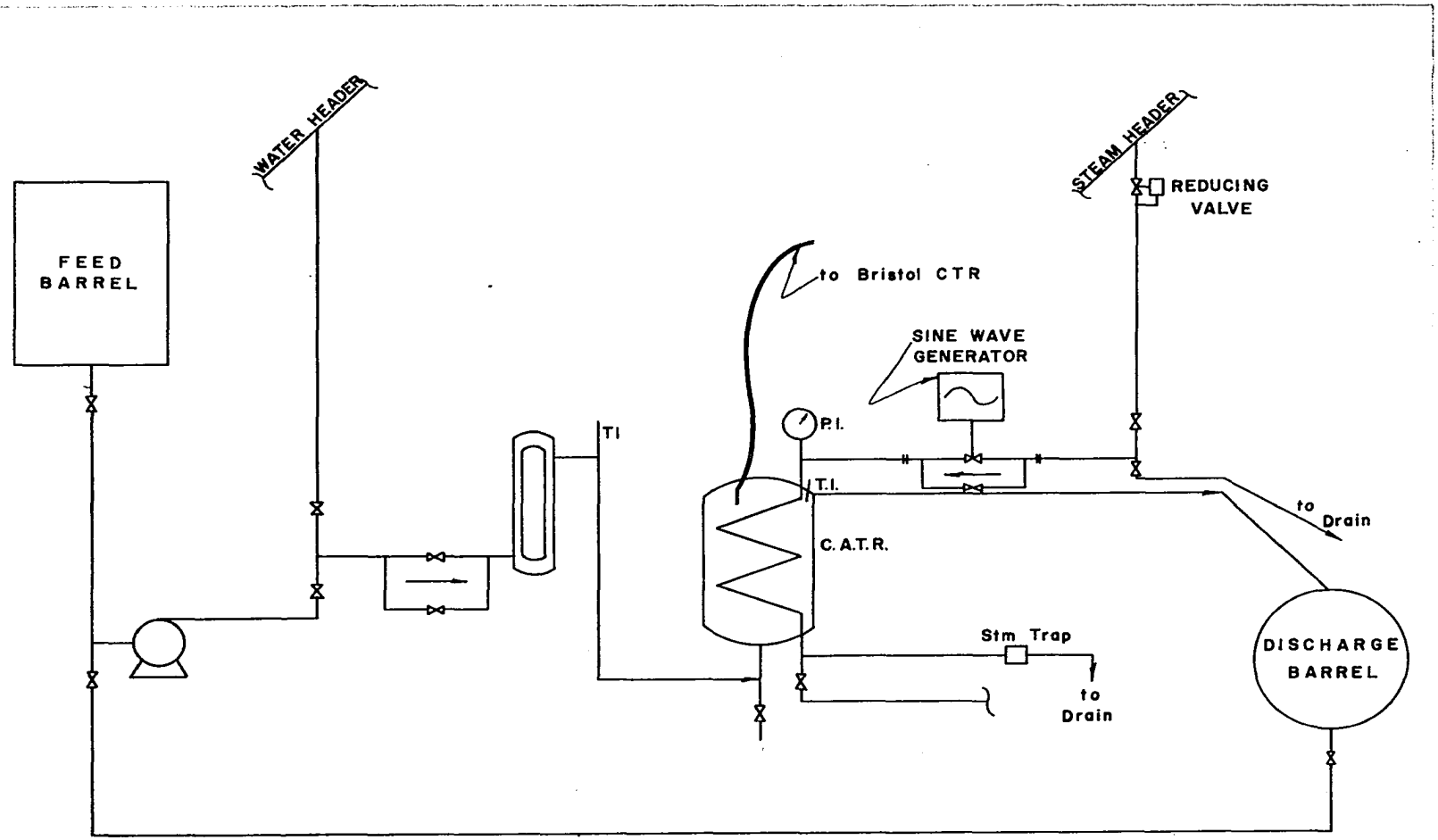


Figure 8 - Flow Diagram of Equipment Arrangement Two

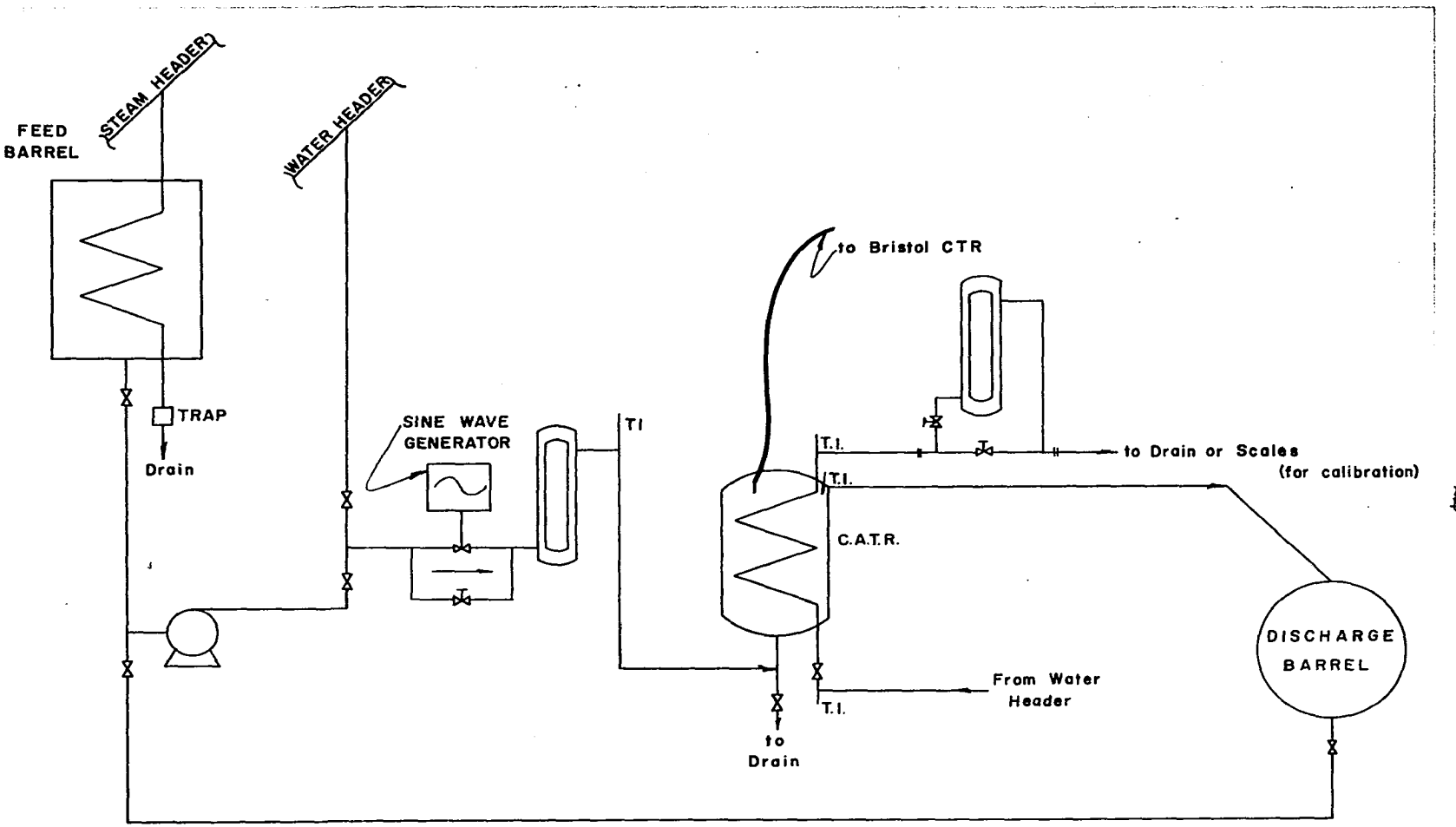


Figure 9 - Flow Diagram of Equipment Arrangement Three

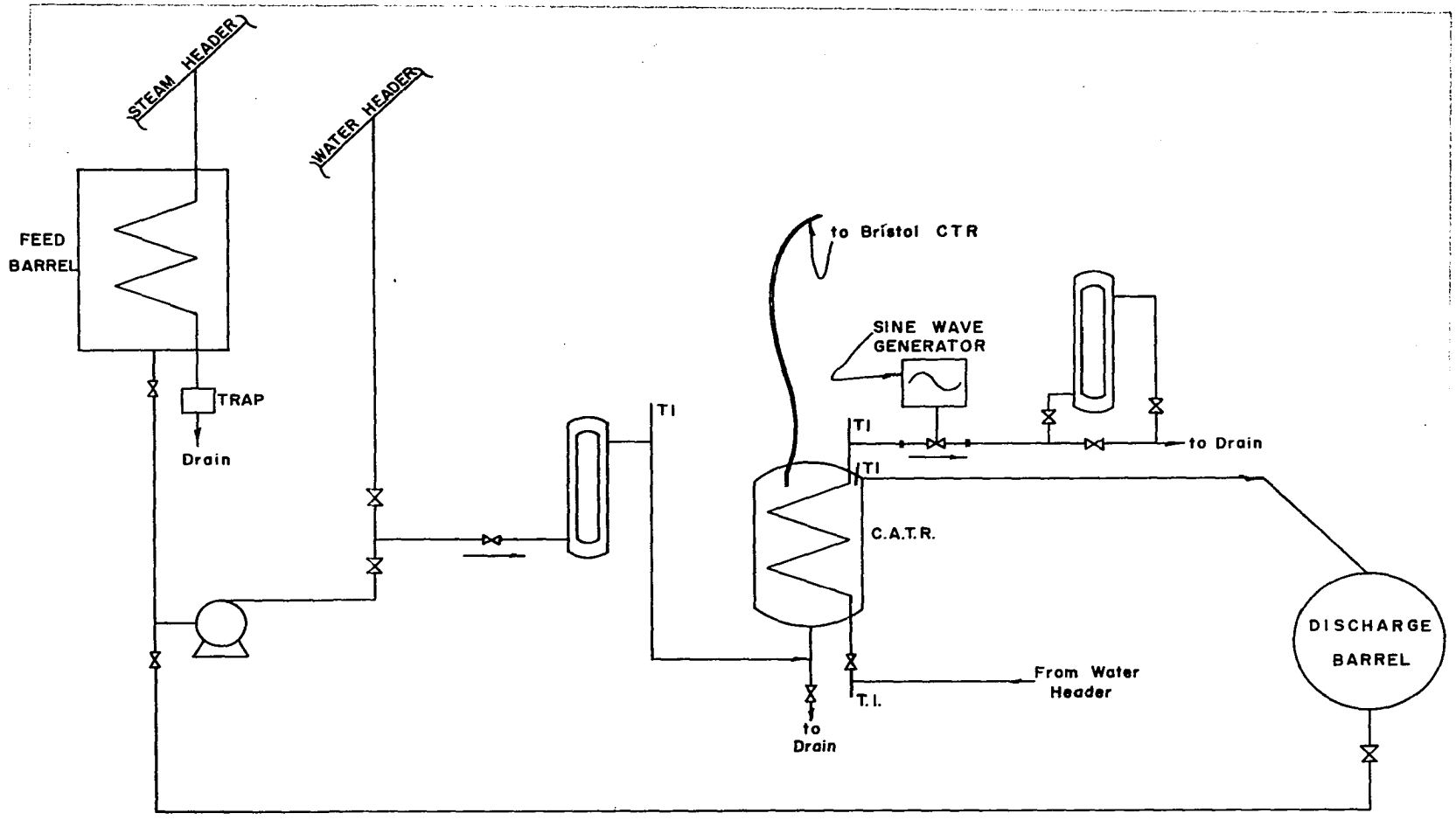


Figure 10 - Flow Diagram of Equipment Arrangement Four

GPM when pumping against a 20-ft. head. The fluid passes from pump discharge into the feed control section. This amounts to a parallel piping arrangement with facility for mounting the sine wave generator in one branch. The other branch includes a 3/8-inch needle valve for raising steady state feed level or applying a manual flow sine wave. From this section the fluid passes through a flow rate measuring unit thence into the bottom of the continuous agitated tank reactor. The feed rate measuring device is a Fischer Porter series 1700 "Flowrator" meter with a maximum water flow capacity adjustable to 6.6 or 8.3 GPM. The lower adjustment was used in this work. For equipment arrangements 3 and 4, a 0.6 GPM (maximum) Fischer Porter "Flowrator" is present for measuring coolant flow rate. Most of the connecting piping is 1/2-inch galvanized iron pipe with appropriate fittings.

Fluid from the continuous agitated tank reactor passes by means of a 45 degree discharge line into a one-barrel effluent reservoir. Polyethylene pipe connects the outlet line and tank reactor so as to minimize heat losses by conduction. The piping is arranged in order to allow recycling of the effluent into the feed barrel by means of the feed pump. The effluent may also be sewered if desired. Calibrated Mercury-in-glass thermometers are installed at the necessary positions to enable recording of steady state inlet and tank reactor fluid temperatures. For Equipment Arrangements Three and Four where tank reactor coils act as a heat sink, the same type thermometers measure cooling water temperatures at the entrance and outlet to the cooling coils.

Equipment Arrangements One and Two allow for the heating of tank contents by steam condensation. Steam supply in the mains averages

approximately 70 psig (saturated). Calculations showed that this pressure was too high for certain phases of the investigation. A steam pressure reducer was then installed in the line connecting the header and the steam control manifold section. The latter is constructed much the same as for the fluid feed control section. Such an arrangement then allows for wide flexibility in steam flow rates and pressures to the tank coils. Steam lines are of course heavily insulated as are fluid feed lines.

In this investigation, the output or forced variable is the tank reactor fluid temperature for all four equipment arrangements. In order to conduct a transient and frequency response study, a satisfactory method had to be at hand for the continuous recording of tank fluid temperatures. For frequency response determinations, an extremely sensitive temperature measurement must be available if good results are to be produced, particularly at the higher frequencies. For a portion of the transient response work, a Brown "Electronik" Type 152 temperature recorder was employed. Circular chart speed is four minutes per revolution with a temperature range of 100F to 200F. Transient response reaction curves were developed by taking temperature changes with time directly from the circular chart and plotting these on rectangular coordinate paper. Although satisfactory transients may be obtained in this manner, the method is in general tedious and unwieldy. It has been used recently by some investigators in the study of process dynamics on commercial - size units.

Most of the experimental dynamic data was collected by use of a Bristol model 560 high-speed "Dynamaster" continuous recording poten-

tiometer with strip chart. Full scale deflection is obtained by a one-millivolt signal. A careful calibration of this instrument against a calibrated mercury-in-glass thermometer showed that pen deflection versus indicated temperature relationship is linear and that each chart division (100 divisions per instrument span) corresponds to 0.444°F when the thermocouple junction is copper constanton. Since the approximate fluid temperature in the tank was always available, it was not necessary that the absolute value of temperature be recoverable from strip chart records. However, some method was necessary for positioning the Bristol output indicator since experiments were carried out over a fairly wide mean temperature range. The method for positioning made use of a Leeds Northrup Type 8662 portable potentiometer equipped with a cold junction compensator. The lead terminals from the latter were connected in series with the copper wire in the thermocouple. With such an arrangement, the Bristol recording pen could be positioned at any desired chart location by manipulation of the portable potentiometer balancing knob. Figure 10 shows a view of all special electronic equipment used in the investigation.

CHAPTER IV

EXPERIMENTAL PROCEDURE

Calibrations

Much of the experimental data was taken from tapered-tube, plummet-type flow indicators. Such meters are generally supplied by the manufacturer with calibration curves. Since the experimental procedure called for metering over a considerable range of rates and temperatures with fluids of widely differing physical properties, it was decided that calibration under actual experimental conditions would be advisable. Calibration curves for the reactor feed rotameter were obtained at oil feed temperatures of 83, 107, 120 and 139F over a flow rate range of approximately 2 to 26 lbs./min. A plot of the data showed that the curves for the three higher temperatures were superimposed except at the very low rates. For this reason, it was felt unnecessary to collect data at higher oil temperatures. For the same rotameter, curves were developed for water at reactor feed temperatures of 77 and 170F throughout a flow range of approximately 4 to 38 lbs./min. Although the curves did not coincide, they were very close which demonstrated that for both fluids a feed temperature variance of a few degrees would contribute very little error in the flow values indicated.

The method of calibration consisted of noting the amount of

time required to collect a given weight of meter effluent. Timing starts and stops were taken "on the fly" so that kinetic energy effects of the fluid falling into the weigh container would cancel. Either duplicate or triplicate runs at the same rates were always made with the final results tabulated from the average. It should be pointed out that exceptionally good repeatability was experienced for most of the runs. All the data in addition to the calibration curves are listed in Appendix B. It will be noted that except at the low ranges for oil, plummet heights and flow rates are related linearly. This is important in the manual generation of flow rate sine waves.

As previously stated, absolute values of temperature from a continuous recorder are usually not required for an investigation such as this. However, the temperature change represented by a given increment of chart range is sometimes desired. For this reason, two calibration curves with supporting data for the Bristol continuous recorder are presented in Appendix B. The data were taken at intervals of about one month in order to ascertain the effect, if any, of instrument drift brought about by a difference in atmospheric conditions, weakened amplifier tubes, etc. Points for the curves were obtained by bringing the tank contents up to the desired steady state temperature as indicated by a calibrated mercury-in-glass thermometer, then noting the corresponding reading on the instrument strip chart. Intervals of 10 degrees were used with four sets of instrument readings made at each temperature. Average strip chart values were then plotted against temperature. An investigation of the plot will show that the relationship is again linear. This is to be expected in view of the fact that over this range, tempera-

ture and potential from a copper-constantan thermocouple are directly related by a constant of proportionality. The plot also shows that there is very little difference between the curves for the different times at which the data were taken. The points are perhaps within the range of experimental accuracy; therefore, the conclusion is that the instrument is sufficiently reliable for the present work. This is quite important since a large portion of the processed data has its source in the instrument strip chart recordings.

Sine Wave Generator

Successful frequency response analysis depends upon the generation of an accurate sine wave input function. A distorted input wave together with the usual inherent system non-linearities can very easily result in a misinterpretation of experimental data. It was therefore imperative to check carefully the actual flow wave produced by the mechanical wave generator. According to theoretical design, the generator could be expected to develop a perfect sinusoidal wave of fluid flow rate if the conditions of absolute valve linearity, constant motor RPM, and zero slippage and backlash in the mechanical linkages prevailed. These hypothetical conditions also call for constant fluid pressure upstream from the generator. It was known that such a combination of ideal conditions probably would not exist; therefore, several experimental determinations were carried out in order to determine the amount of deviation from ideality.

Figure 11 illustrates the method employed in testing the mechanical sine wave generator:

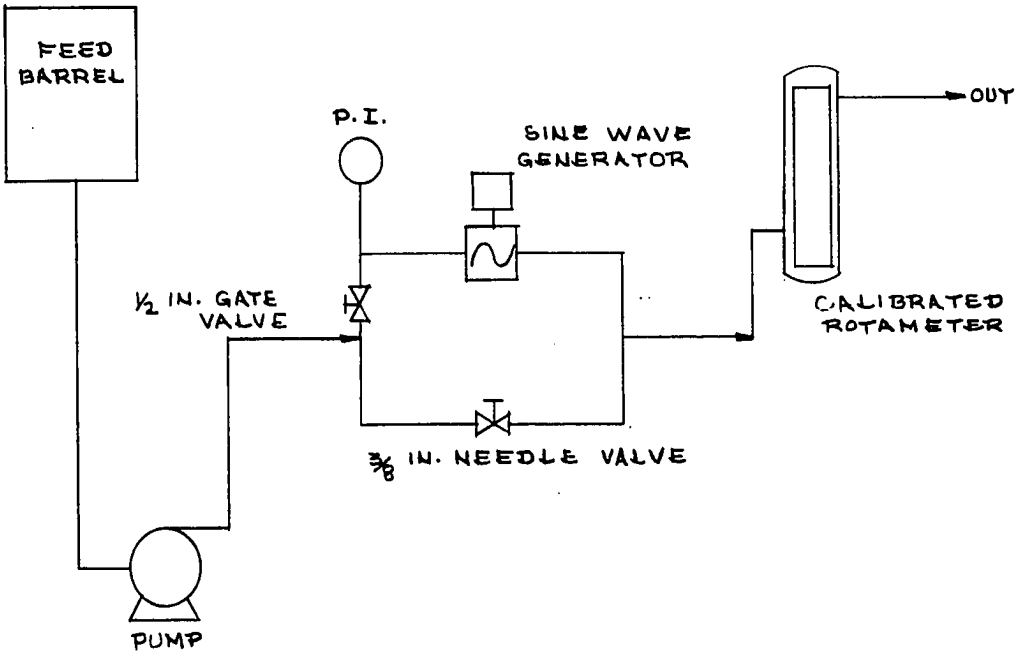


Figure 11

Experimental data desired were rate of fluid flow versus time. As previously stated, the relationship between rotometer plummet height and fluid flow rate is almost perfectly linear; therefore, a sinusoidal variation of the plummet represents the same type of function for flow rate. The generator was equipped with a 1/8-inch Scotch yoke drive for all tests. The peak to valley travel of the valve stem was then 0.25 inches. Data were collected for frequencies of 0.1, 0.25, 0.5, 1.0 and 5 cycles per minute. At the beginning of a run at each frequency, the feed barrel was filled with water at the temperature of the mains. The generator valve stem position was adjusted so that the valve plug was snugly seated at the lower-most travel of the stem. The stem was then driven to its mean position by switching the motor drive on and off. The

desired position was indicated by a pointer attached midway up the valve stem. The generator should always first be set in this manner at the beginning of any frequency response determination. The piping arrangement as shown in Figure 11 is such that the desired flow rate level from which the sine wave is generated may be realized by the principle of superposition on manipulation of the 3/8-inch bypass needle valve. With the latter, the feed rate was arbitrarily adjusted to 16.25 lbs./min (30 plummet units) and the generator was switched on. By means of a stop watch, plummet readings were taken at time intervals of about 10 seconds for the lower frequencies and at somewhat shorter intervals at the higher frequencies. A plot of plummet readings versus time then gave the desired information.

For most of the runs an entire barrel of fluid was passed through the generator. As expected, there was a gradual downward drift in the periodic plummet movement brought about by the decrease in fluid head at the feed source. It was found that such drift could be corrected by adjusting the plummet upward (by means of the bypass valve) to its proper position at the bottom of each wave. Although downward drift with falling fluid head was quite noticeable, there was relatively little attenuation of the wave during the runs. Figures 12, 13, and 14 show plots of the experimental data at various frequencies. The solid lines indicate theoretical sine waves at the frequency in question. As may be seen, the mechanically-generated sine waves of fluid flow are very good approximations of the theoretical curves.

Frequency and Transient Response Experimentations

In simple terms, the dynamic characteristics of a process may

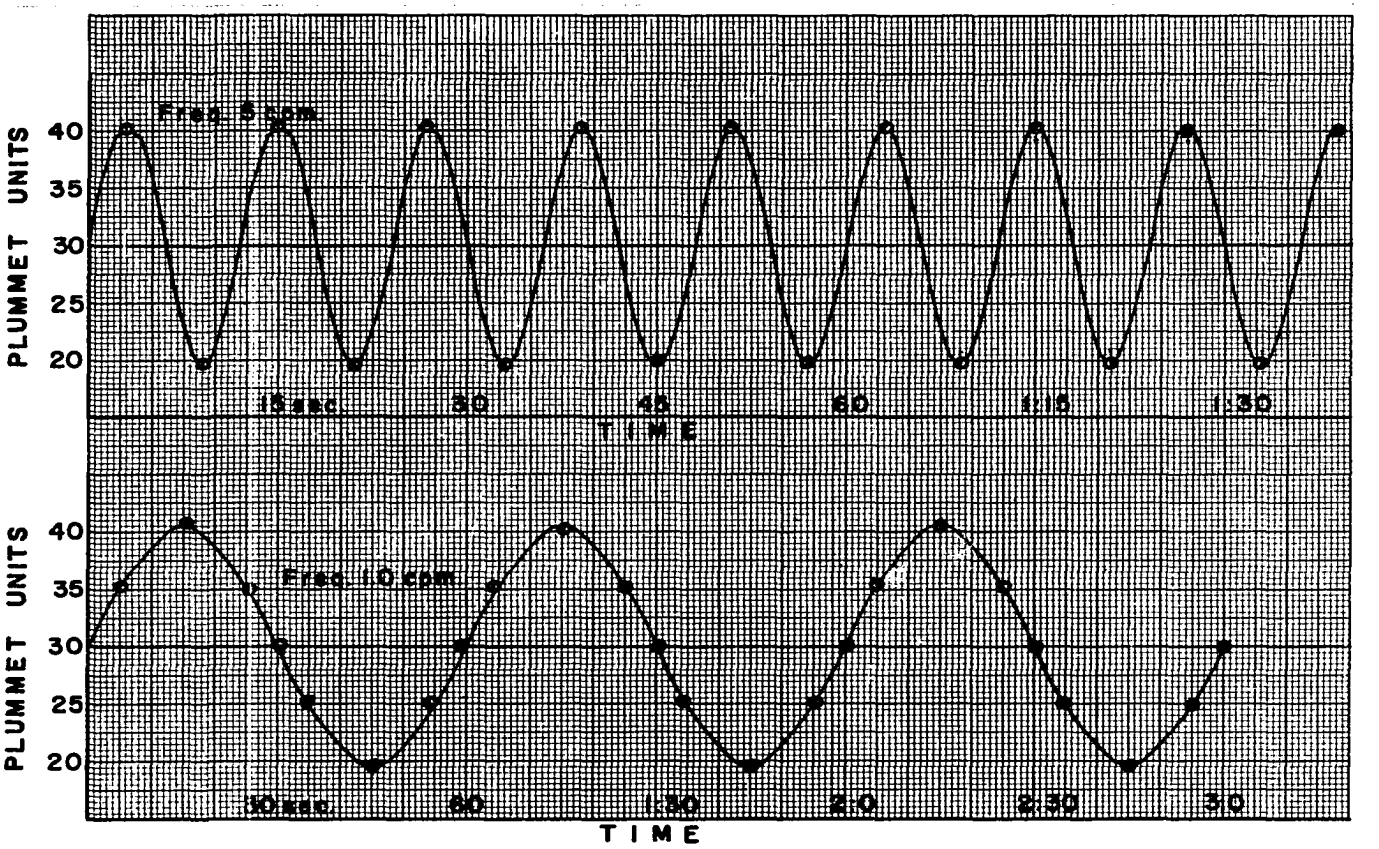


Figure 12 - Experimental Flow Waves at Higher Frequencies

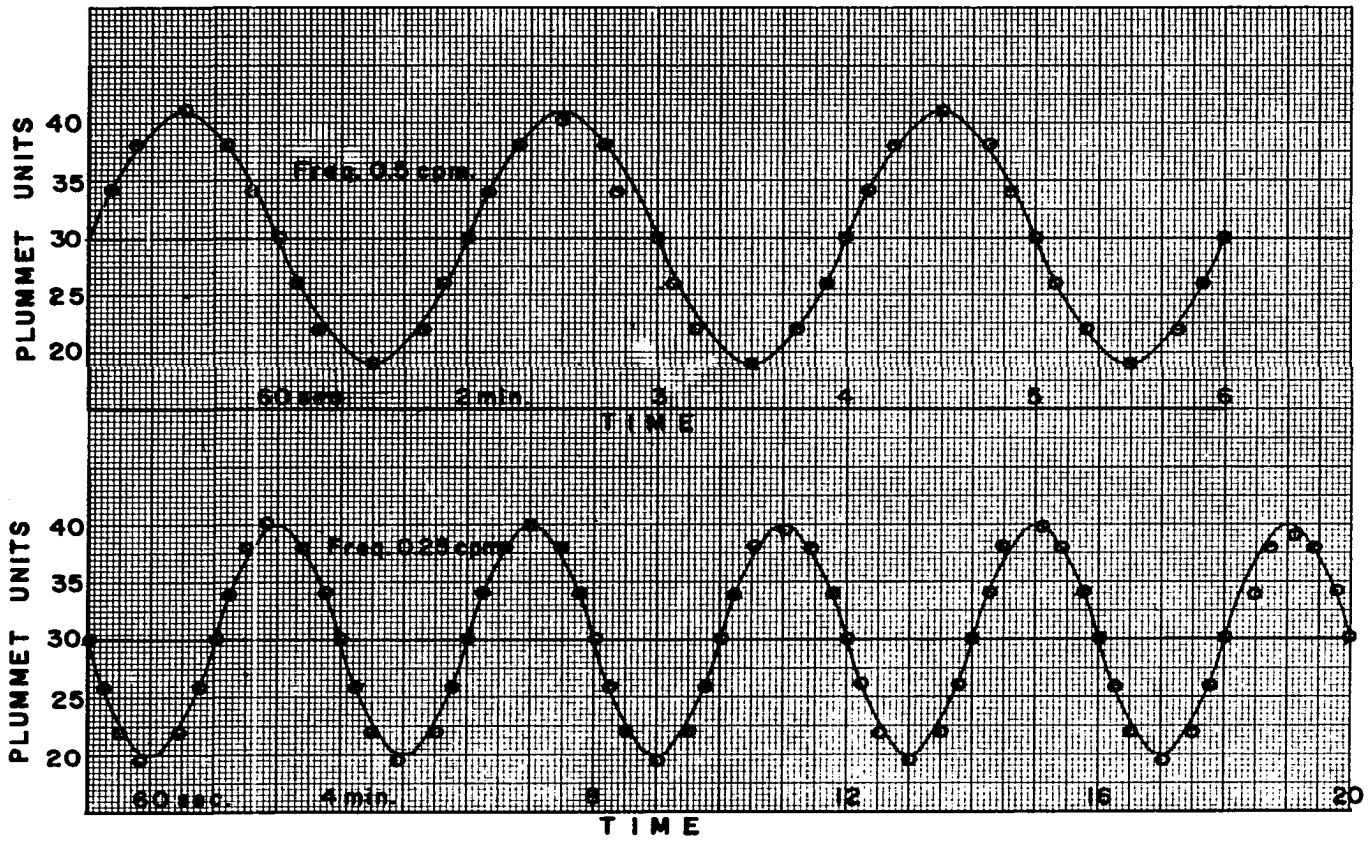


Figure 13 - Experimental Flow Waves at Medium Frequencies

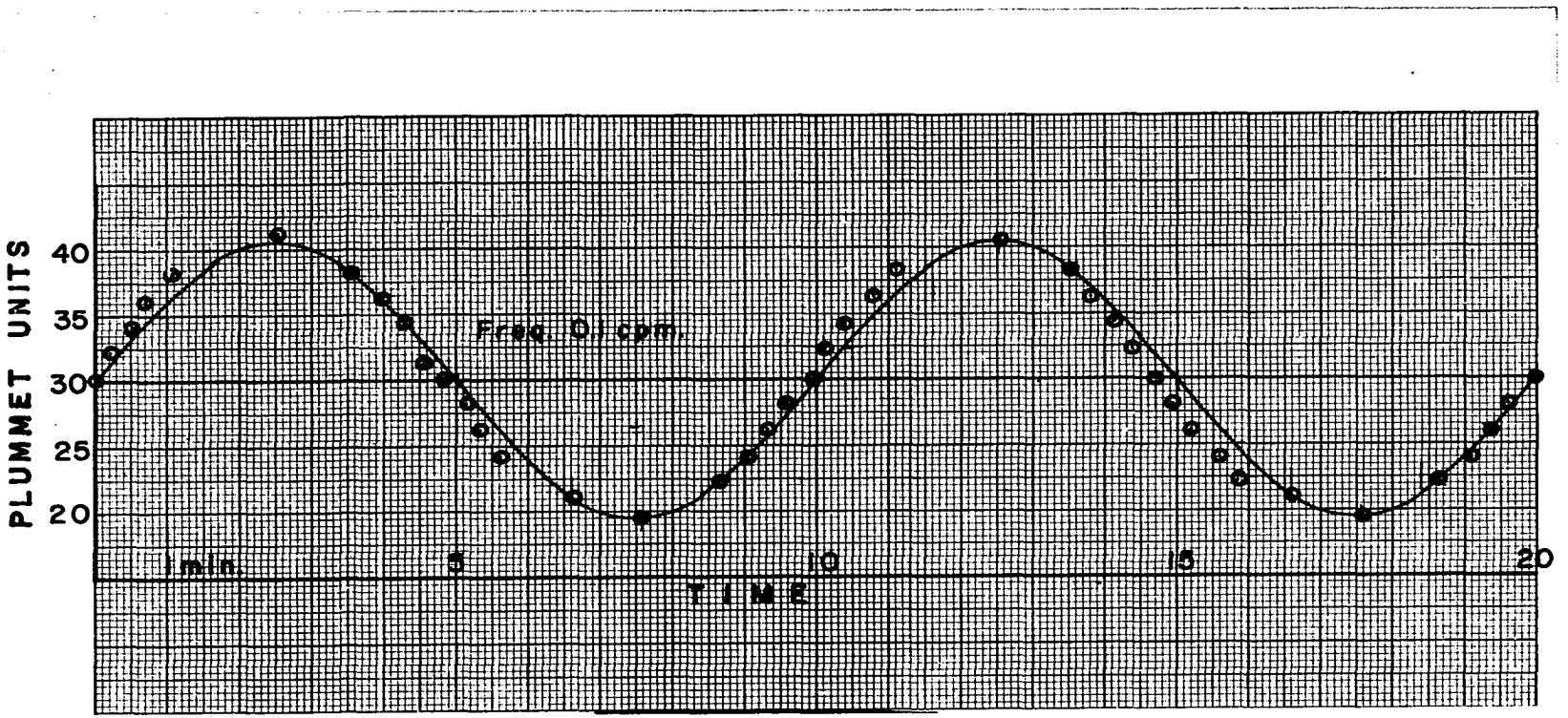


Figure 14 - Experimental Flow Waves at a Lower Frequency

be said to consist of the time and manner of reaction of one process variable when a related variable is changed with some function of time. The experimental portion of this work consisted of obtaining in graphical but quantitative terms information which would conveniently describe such reactions. The following four basic transfer functions were studied experimentally and theoretically:

Equipment Arrangement	Coils	Transfer Function
One	Heat Source	$\frac{\theta_r(j\omega)}{W_f} = f_1(j\omega)$
Two	Heat Source	$\frac{\theta_r}{\theta_s}(j\omega) = f_2(j\omega)$
Three	Heat Sink	$\frac{\theta_r}{W_f}(j\omega) = f_3(j\omega)$
Four	Heat Sink	$\frac{\theta}{W_w}(j\omega) = f_4(j\omega)$

Equipment Arrangement Four is by far the one of most interest since most chemical reactions are exothermic. Heat removal from the reactor is then necessary either by cooling water jackets or an internal surface containing a coolant of some sort. Because of its practical value and the fact that its transfer function is of more interest mathematically, equipment arrangement four was selected as the subject of special study.

In each frequency response evaluation, the first step was to determine, sometimes by trial and error, the optimum amplitude over which the input variable should be forced by the wave generator. The amplitude was always kept as low as possible commensurate with con-

venient chart interpretation at the higher frequencies. In a continuous agitated tank reactor during a rapid exchange of heat, there is continuous movement of liquid filaments of slightly different temperature past the temperature sensing element. This results in considerable "noise" or small erratic variations in the output of the chart recorder. The lower limit of chart interpretation occurs at that point where sinusoidal variations of the output variable θ are of the same order of magnitude as overall system noise.

After selection of a convenient input wave amplitude, the next step in the experimental procedure was to obtain chart records of the steady state gains. For example, in a special study of Arrangement Four, the selected sine wave of input coolant flow was the range of 0.38 - 0.48 - 0.60 GPM. After obtaining conditions of steady state operation with coolant flow at 0.48 GPM, the latter rate was suddenly raised to 0.60 GPM. The resulting trace of the drop in θ was then filed as the system transient response under those particular conditions of operation. The maximum deviation of θ between initial and final conditions constituted the steady state gain for <u>one-half</u> of the input wave. The procedure was then carried out for the other half of the input wave. Coolant flow rate at a steady state of 0.48 GPM was suddenly lowered to 0.38 GPM and the resulting trace of the rise in θ noted. The transient is complete when steady state conditions prevail under the new set of process conditions. Again the difference between these steady state values of θ make up the gain for the other half of the input wave. For convenience, these are referred to here as positive and negative steady state gains. If the process is precisely linear in the range of the applied unit step

functions, the transient response curves will be mirror images of each other. The amount of deviation from this symetrical condition was used as a measure of the degree of non-linearity at that particular operating level. Frequency response analysis is based upon the presumption of linear systems; however, it will be later shown that much valuable information may be derived from such an analysis even when the system is substantially non-linear provided the proper range of input wave is applied.

Figure 15 shows the strip chart records for Equipment Arrangement Two using water as the tank fluid. As may be seen, the curves are quite similar in shape. Figure 16 illustrates the degree of non-linearity at one particular range of operation for Equipment Arrangement Four. Here, the curves differ in that one is considerably flatter than the other. In this case, oil was the system fluid. It is to be pointed out that the chart trace noise level for water is appreciably higher than for oil. This is expected in view of the fact that with higher rates of heat exchange, there is a wider range of temperature in adjacent, minute liquid filaments.

Appendix E explains that considerable information of a qualitative nature may be acquired from a cursory study of a system's transient response. For example in Figure 15, the tank fluid temperature θ begins to rise sharply very soon after the steam temperature θ_s is suddenly raised. The system transfer function can then be expected to approach first order. On the other hand, the curves in Figure 16 show no tendency to change at all until about 15 seconds after the forcing step function has been applied to the coolant flow rate. After a change does

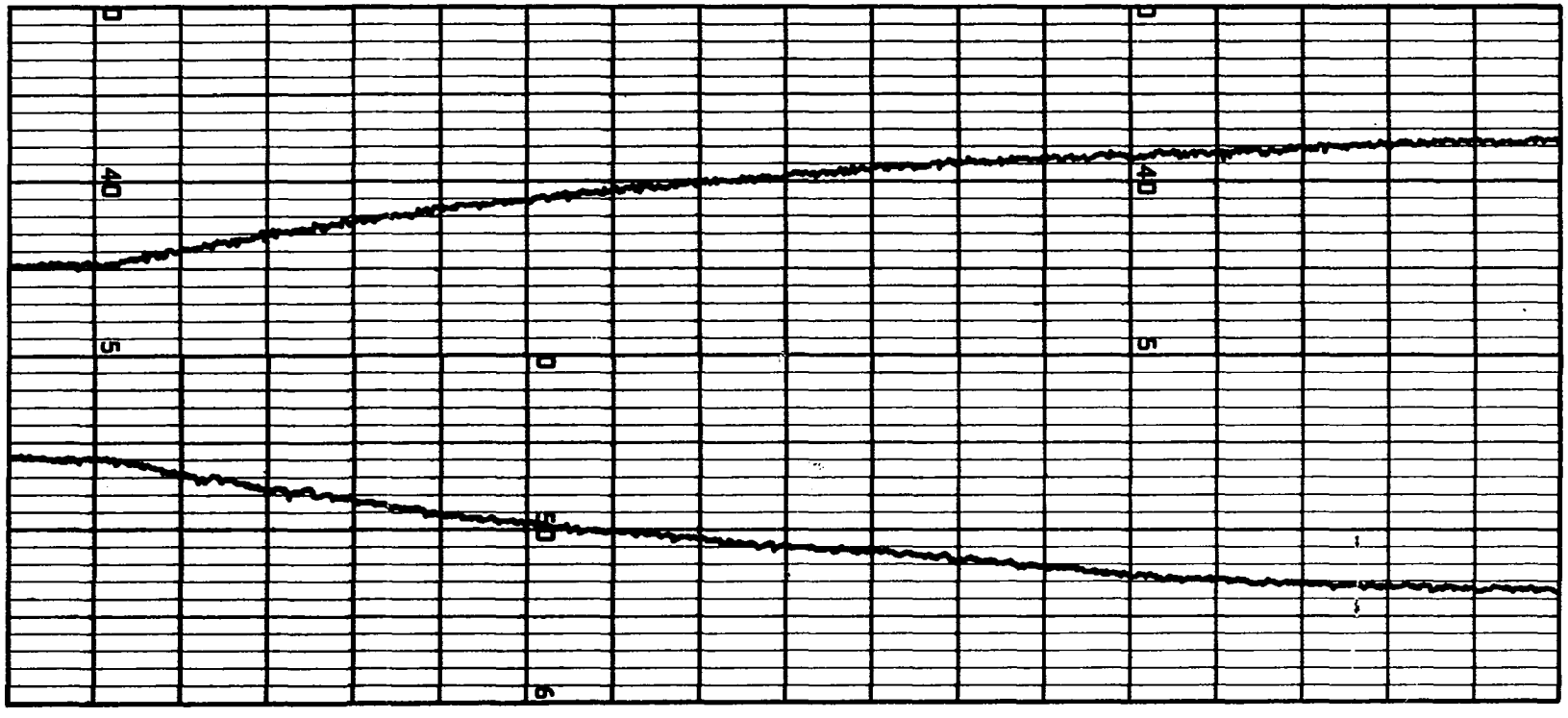


Figure 15 - Transient Response Curves, Arrangement Two, Water

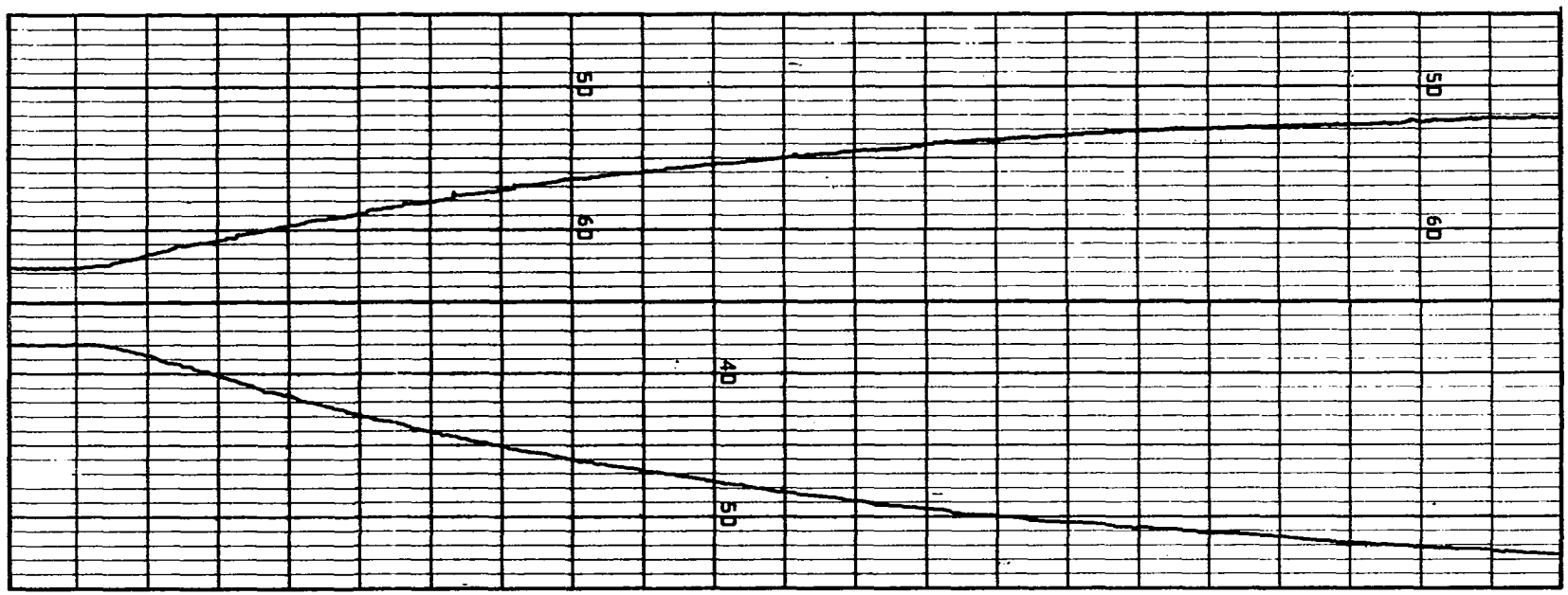


Figure 16 - Transient Response Curves, Arrangement Four, Oil

begin it is gradual and asymptotic in nature. In this case, the transient curve shows that some sort of time delay is present which will result in a system transfer function that is of second or higher order. The difficulty with a transient analysis is that it does not lend itself easily to the acquiring of accurate quantitative information regarding process dynamics. Such information is readily obtained from frequency response.

All of the experimental frequency response determinations were carried out in much the same manner even though each equipment arrangement involved a different forced process variable. The desired range of generator stem travel was set either by application of previous experience or by trial and error. Inlet feed rates and temperatures, steam back-pressures or cooling water rates were then selected according to the schedule of the experimental program. The feed pump was turned on and the system was allowed to reach steady state conditions as indicated by a straight trace drawn by the instrument chart pen. It was always attempted to reach steady state conditions as soon as possible in order that the larger portion of the feed barrel would remain for the frequency response section of the run. Throughout most of the runs a chart speed of one inch per minute was used. At a given time, the run was begun by switching on the sine wave generator at the same instant that a beginning mark was written on the strip chart. In much of the frequency response work done to date, multi-channel strip chart recorders were employed so that a sinusoidal trace of the forced variable could be made on the same chart with the output variable. This lends itself to ease in interpretation of phase lags. Such equipment was not available in this work; it

was therefore necessary to devise an alternate scheme.

It was first decided that since previous tests showed the generator capable of supplying dependable, correctly-timed periodic motion, the input wave could be penciled in with the recorded output wave provided care was taken in marking the beginning of a run. In practice, however, this method was slow, inconvenient and in some cases, inaccurate. A much more satisfactory method consisted of the following: at the instant the input variable arrived at its peak and/or valley position in its sinusoidal motion, a fine mark was made on the instrument output wave and labeled as to whether it represented a peak or valley in the input variation. Such a method called for the services of two individuals; however, for the present investigation, wherein frequencies no higher than five cycles per minute were required, the procedure proved quite satisfactory. The method is of course limited depending upon the speed of the process under investigation.

A large part of the present investigation is based upon the interpretation of frequency response data. For this reason, the analysis of all strip chart recordings was given considerable time and care. Figures 17 and 18 present batteries of response records at selected frequencies for water and oil respectively. The recordings were taken for Equipment Arrangement Four. The records as listed in the above figures are the only ones shown from all four equipment arrangements. Over 175 separate transient and frequency response determinations were made and the inclusion of all is of course prohibited by space limitations. All information is on file in the Chemical Engineering Department, University of Oklahoma. Methods for interpretation of frequency and transient

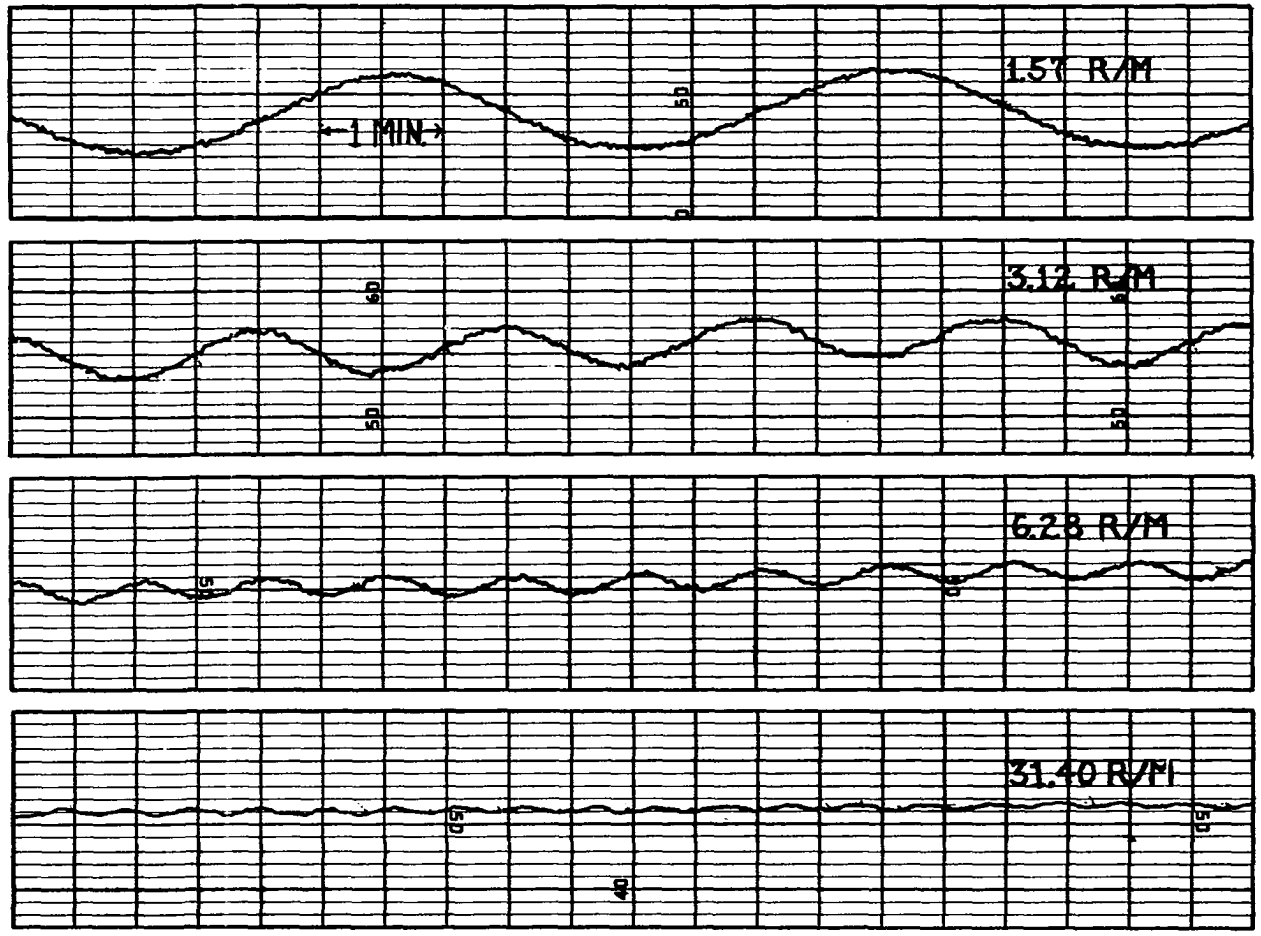


Figure 17 - Selected Frequency Response Records, Arrangement Four, Water

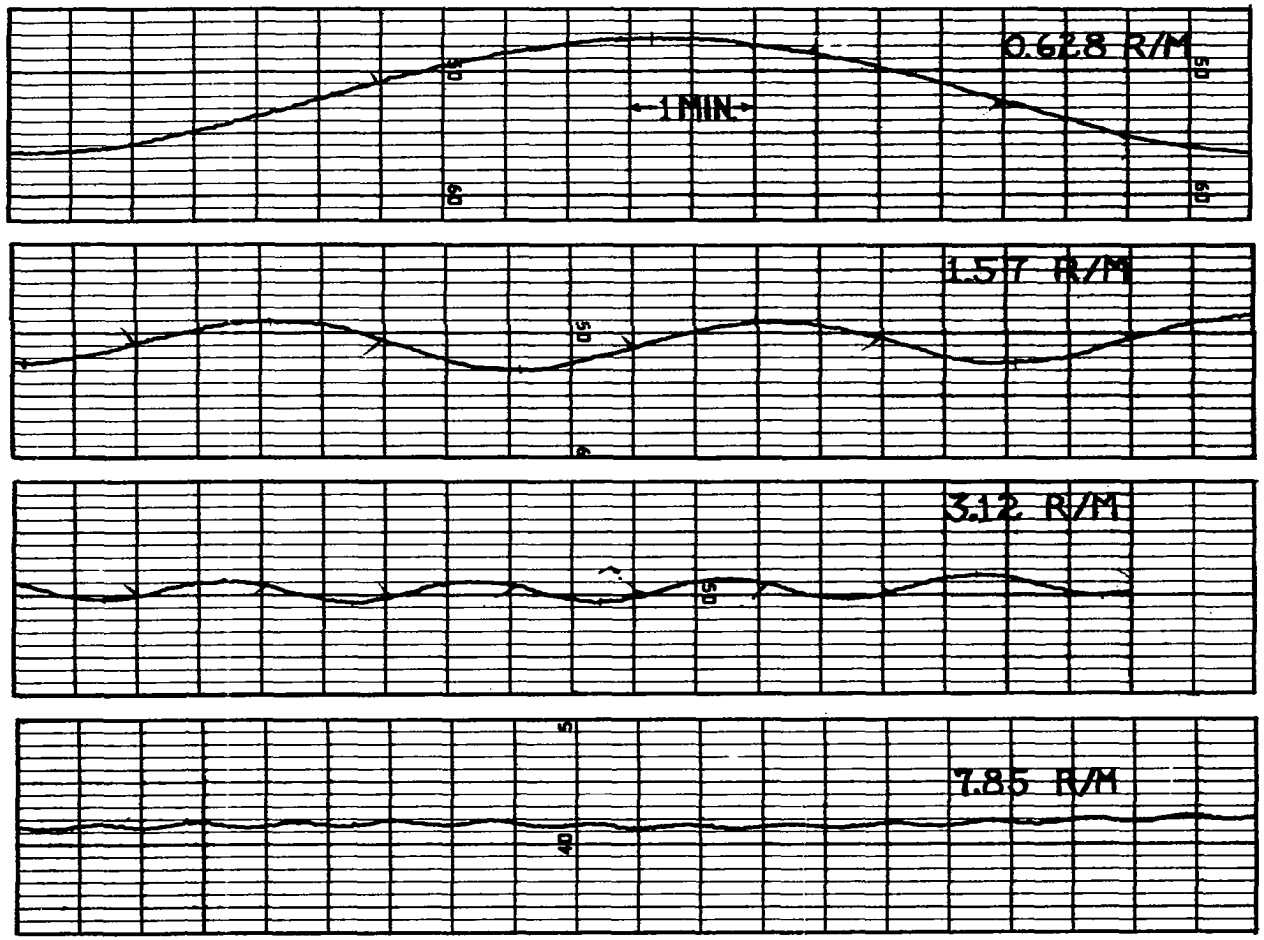


Figure 18 - Selected Frequency Response Records, Arrangement Four, Oil

response records were basically the same for all four general transfer function types.

From the standpoint of analysis of frequency response records, magnitude ratio is generally defined as the ratio of output to input distances from the wave means to wave peaks. However, it was found in this investigation that the output wave could be analyzed faster and more accurately by measuring the total distance in chart divisions between wave peaks and valleys. These distances are unique for each individual frequency. The mathematical expression for a standardized magnitude ratio as briefly discussed in Appendix E will be listed here for further study:

$$\text{Magnitude Ratio} = \frac{\left[\frac{\Delta\theta}{\Delta W_w}\right] F = F}{\left[\frac{\Delta\theta}{\Delta W_w}\right] F = 0} \qquad \text{(IV-1)}$$

This magnitude ratio represents that for the case where tank reactor fluid temperature θ is forced by a sinusoidal change in cooling water flow rate, W_w. As concerns the present work, the above equation may be easily simplified when it is considered that W_w for a given response spectrum was a fixed quantity at all frequencies. Thus the equation may be effectively reduced to the following:

$$\text{Magnitude Ratio} = \frac{(\Delta\theta)_{F = F}}{(\Delta\theta)_{F = 0}} \qquad \text{(IV-2)}$$

The numerator of this expression represents the average total distance between peaks and valleys of the output wave at any frequency

F. The denominator represents the numerical sum of the positive and negative steady state gain or transient curves. In actual record analysis distances in chart divisions were rarely converted to temperatures since the magnitude ratio remained the same in either case.

In the case of very low frequencies of 0.0667 and 0.05 cycles per minute, only two values for $(\Delta\theta)_{F=F}$ could be obtained since no more than three complete input cycles were possible. At the usual rate of feed charged, the feed reservoir capacity was such as to allow a maximum of approximately forty minutes of operation. For higher frequencies, the system was cycled up to 25 times. In the latter instances enough data were available to allow the calculation of statistical averages for $(\Delta\theta)_{F=F}$. Here, from 6 to 20 magnitudes were carefully estimated by means of dividers and a finely graduated measuring rule. The numerical average of all magnitudes was then recorded, usually in chart divisions, as the table value for $(\Delta\theta)_{F=F}$. Sections of response curves which showed decided drift, flattened waves or highly distorted waves were generally excluded from numerical analysis.

The measurement of average phase lags proceeded along much the same lines except that here, it was necessary to estimate the point in time where the maximum (or minimum) of the output sine wave appeared. At the higher frequencies, this is quite difficult to accomplish accurately, especially with a high noise level present. Furthermore, an error in marking of a given distance represents a larger error in phase lag for high frequencies than for low if the same chart speed is used throughout. Special care was therefore given in the all phase lag determinations. Nevertheless, Bode diagrams of the experimental data show

phase lag data to be somewhat more erratic than magnitude ratio data, particularly at the higher frequencies. It would appear that better accuracy would result from using faster chart speeds at the higher frequencies. Under such conditions, the output wave was often so distended and flat that an estimation of wave peaks was made more approximate. Under some experimental conditions, it was felt that more accurate values for phase lags resulted from the use of faster chart speeds. The latter was then dictated by the experimental transfer function sought and the conditions of operation. The numerical average value of phase lag at a given frequency was estimated as before by carefully measuring the distance between input and output peaks with dividers, converting this average into inches and thence into degrees according to the particular impressed input frequency.

By application of the methods just described, transient response as well as frequency versus magnitude ratio and phase lag data are collected. With such information, the system is completely characterized from the experimental standpoint. For purposes of clarification and illustration, raw and finished frequency response data are presented in Tables 1, 2, 3 and 4. The remainder of the data is located in Appendix C. The first two tables represent data for water feed while the last two are for oil. The information is a portion of that collected for equipment arrangement number four. Figure 19 shows the data for both fluids plotted on the same diagram for comparison. The difference in attenuation and phase lag for the same equipment when fluids of different physical properties are processed is striking.

Only brief passing mention was made in the preceding discussion

TABLE 1

Steady State Conditions for Equipment Arrangement Four
Cooling Water Rate Forcing
Process Fluid - Water

Run No.	Radians / Minute	Water Feed °F		Cooling Water °F	
		θ_f	θ	θ_{w_i}	θ_{w_o}
A-62	0.420	170.2	142.0	75.7	120.5
A-63	0.628	170.1	142.5	75.1	121.8
A-72	1.048	170.0	143.9	74.7	118.5
A-64	1.570	170.5	142.8	75.3	122.8
A-73	2.515	170.5	144.0	74.7	118.9
A-65	3.120	170.4	142.1	75.3	121.0
A-74	4.190	170.5	144.0	75.0	119.4
A-66	6.280	170.8	142.1	75.3	120.5
A-75	7.850	170.0	143.9	73.5	119.1
A-76	12.560	170.2	144.1	73.2	119.5
A-68	15.710	170.1	141.0	74.8	120.0
A-69	31.400	170.1	141.7	74.5	122.2

Parameters: Coolant Flow, Steady State: 8.12 lb./min.

Coolant Flow Forcing Range: 4.63-8.12-11.61 lb./min.

Water Feed Rate: 13.18 lb./min.

Agitator RPM: 200

TABLE 2

Processed Frequency Response Data, Equipment Arrangement Four
Cooling Water Rate Forcing
Process Fluid - Water

Run No.	Radians / Minute	Steady State Gain		Average Amplitude		Magnitude Ratio	Phase Angle, Degrees
		Chart Divs.	°F	Chart Divs.	°F		
A-62	0.420	27.9	12.4	18.9	8.42	0.678	- 56
A-63	0.628	27.9	12.4	15.8	7.03	0.566	- 66
A-72	1.048	29.2	13.0	9.80	4.36	0.338	- 75
A-64	1.570	27.9	12.4	6.33	2.82	0.227	- 86
A-73	2.515	29.2	13.0	4.25	1.89	0.146	- 87
A-65	3.120	27.9	12.4	3.14	1.39	0.112	-103
A-74	4.190	29.2	13.0	2.40	1.07	0.082	-103
A-66	6.280	27.9	12.4	1.48	0.66	0.053	-109
A-75	7.850	29.2	13.0	1.25	0.56	0.0427	-119
A-76	12.560	29.2	13.0	0.70	0.31	0.024	-120
A-68	15.710	62.8	27.9	1.15	0.51	0.0183	-127
A-69	31.400	62.8	27.9	0.473	0.21	0.00753	-176

TABLE 3

Steady State Conditions for Equipment Arrangement Four
Cooling Water Rate Forcing
Process Fluid - Oil

Run No.	Radians / Minute	Oil Feed °F		Cooling Water °F	
		θ_f	θ	θ_{w_i}	θ_{w_o}
B-34	0.314	174.2	147.2	74.2	119.1
B-35	0.420	176.8	148.5	74.4	120.2
B-36	0.628	175.0	147.8	74.5	119.4
B-41	1.048	175.0	147.0	74.2	121.3
B-37	1.570	174.8	147.8	74.8	119.6
B-42	2.520	173.0	146.2	73.9	120.0
B-38	3.121	175.0	147.9	73.9	119.9
B-43	4.200	173.8	148.0	86.9	125.0
B-39	6.280	175.4	148.9	74.3	120.9
B-44	7.850	173.0	147.2	74.6	120.5
B-45	12.560	174.0	147.0	73.8	120.0

Parameters: Coolant Flow, Steady State: 0.24 GPM

Coolant Flow Forcing Range: 0.12-0.24-0.42 GPM

Oil Feed Rate: 7.2 lb./min.

Agitator RPM: 200

TABLE 4

Processed Frequency Response Data, Equipment Arrangement Four
Cooling Water Rate Forcing
Process Fluid - Oil

Run No.	Radians / Minute	Average Amplitude Chart Divs.	Average Amplitude °F	Magnitude Ratio	Phase Angle, Degrees
B-34	0.314	14.95	6.65	0.610	-56
B-35	0.420	12.55	5.48	0.510	-68
B-36	0.628	8.10	3.61	0.330	-84
B-41	1.048	6.10	2.71	0.248	-95
B-37	1.570	2.84	1.63	0.115	-103
B-42	2.520	2.10	0.93	0.0854	-122
B-38	3.121	1.42	0.63	0.0580	-131
B-43	4.200	0.80	0.36	0.032	-150
B-39	6.280	0.45	0.20	0.018	-165
B-44	7.850	0.20	0.089	0.0081	-179
B-45	12.560	0.07	0.031	0.0028	-197

Parameters: Total Steady State Gain: 24.6 Cht. Divs. or 10.94 Degrees

Coolant Flow Forcing Range: 0.12-0.24-0.42 GPM

Oil Feed Rate: 7.2 lb./min.

Agitator RPM: 200

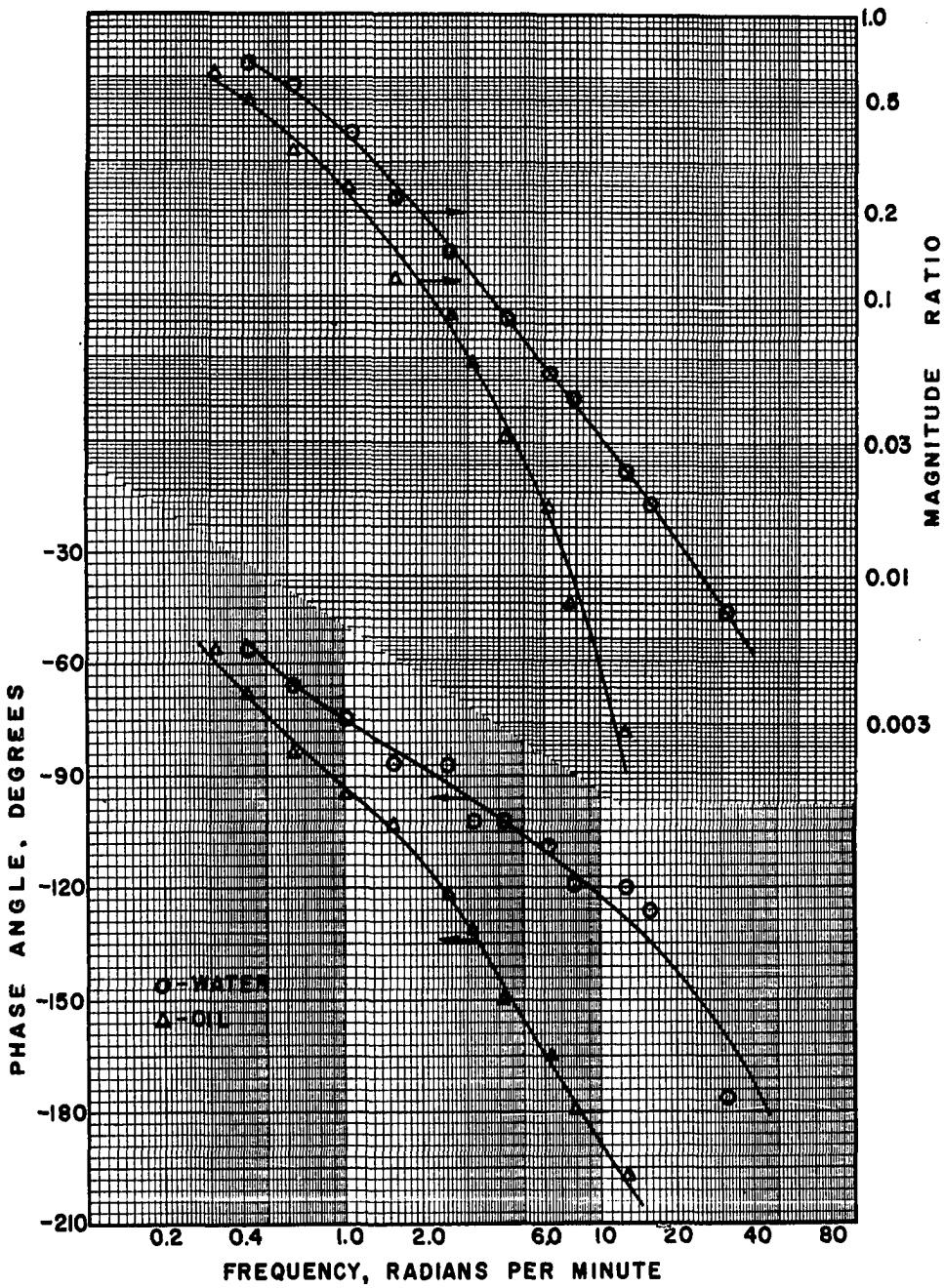


Figure 19 - Bode Diagram Comparing Oil and Water Response Curves for Equipment Arrangement Four

relative to the difficulties encountered in collecting and interpreting frequency response data. In the interest of developing better methods for obtaining dynamic process data, some of the more serious difficulties will be reviewed at this point: In any frequency (or transient) response analysis, great care should be exercised in insuring constancy of those process parameters supposedly being held constant. For example in the present investigation it was very difficult to hold feed temperatures within ± 0.5F of the initial steady state temperature, particularly when the feed rates were being varied sinusoidally. Even if the insulated feed reservoir remained relatively constant, the feed temperature changed with sinusoidally varying flow rates because of losses in the connecting lines. These too were insulated. Such changes in temperature were at times sufficient to affect the output wave. The mean value of the latter would sometimes drift as much as two degrees during certain portions of a run. Accurate analysis cannot be made during steep drifts of the output wave.

Excessive drift was experienced a number of times. These are no doubt attributable to a combination of changes in process parameters. In addition to fluctuations of feed temperature, cooling water temperatures were subject to arbitrary fluctuations. Again, this was particularly noticeable during changes of coolant flow rate. The situation was aided considerably by sewering a side stream of cooling water throughout the runs. Some difficulties were also met with the coils acting as a heat source. Although the steam back-pressure could be regulated with reasonable accuracy, it was known that the steam quality sometimes changed appreciably. This in turn affected the overall heat transfer

coefficient and the system response. In any case, where it was known that varying parameters had affected a response curve sufficiently to render interpretation uncertain, the run was repeated.

A non-linear process response also calls for careful planning of the experimental frequency response routine. One of the objectives of this thesis was that of attempting to establish the degree of accuracy in the characterization of a non-linear process by frequency response analysis. For the case of equipment arrangement four with oil as the charge fluid, it was observed that the steady state gain was appreciably less for a sudden increase in coolant flow than it was for a sudden decrease of the same magnitude under the desired conditions of oil feed. It was found however that if an unsymmetrical periodic wave input range of 20 - 40 - 70 plummet units were applied, the output wave was almost sinusoidal in nature and readily interpretated. The input wave, however, must be generated either by hand methods or by a specially constructed mechanical generator. A later discussion demonstrates that the resulting experimental transfer function agrees well with the theory.

CHAPTER V

DERIVATION OF THEORETICAL TRANSFER FUNCTIONS

Prior Methods

In characterizing a process system dynamically, either one of two broad avenues of approach are generally undertaken. These have been briefly mentioned in the course of subject coverage but will be discussed in more detail at this point. The graphical or empirical approach consists of collecting a large amount of experimental transient and/or frequency response data, then constructing response and attenuation curves. If enough data of reasonable accuracy are collected, it may be assured from a statistical standpoint that the resulting curves represent the process characteristics within a close degree of approximation. Such curves may then be fitted by the various methods available and a quantitative expression for the system transfer function obtained. The transfer function is then expected to be quite accurate for the particular set of process conditions under which the data were taken. It would seem that such a method of dynamical analysis would be satisfactory under certain conditions.

It is sometimes necessary to know the transfer function describing two process variables when such a relationship involves a complexity of staged and pure dead time lags. The describing differential

equations must then be partial and probably non-linear - - a combination most difficult to handle by classical methods. Such a set of equations would also have to be modified by certain simplifying assumptions before use in an analog computer. On the other hand, the experimentally obtained approximate transfer function is often not of especially complicated construction and is suitable in its unmodified form for computer programming.

The disadvantage of such a procedure is that it would be of limited value in synthesis. Unless a proposed process design called for equipment of precisely the same construction and operation, the experimental transfer function would be of questionable value. Furthermore, for existing equipment, large changes in the levels of operation could affect the transfer function to such an extent as to make it valueless. If this were found to be the case, new transfer functions or at least new time constants for the existing transfer function would have to be obtained experimentally at the various levels of assumed operation.

A second method of approach in obtaining the dynamic characteristics of a given piece of equipment is a theoretical analysis followed by sufficient experimentation to verify or refute all or certain areas of the theoretical analysis. The present thesis is based in the main, upon such a procedure. The present work has shown that often, a dynamical analysis can be made to follow an organized plan. It is first established as to what variable is to be controlled and the variable manipulated in order to effect such control. The left side of the transfer function is then defined. Various dynamic material and energy balances are then written so that sufficient equations are at hand to relate

properly the variables in question. At some point in the mathematical manipulations, the equations are transformed into the functional domain by the Laplace transformation. From here, usually algebra is all that is required to derive the desired expression.

Only the basic procedure has been described in obtaining theoretical transfer functions. The type and complexity of the process involved renders each separate case an entity in itself. For this reason, several ramifications of the general outline as described above have been employed in the derivation of theoretical transfer functions. Some of these will be discussed briefly at this point.

Bilous, Block and Piret (4) have recently developed a variety of interesting theoretical transfer functions in their analysis of frequency response relations for a continuous agitated tank reactor. One of the transfer functions of chief concern was that between feed and product concentration for the above type system. The basic equations were developed in the usual manner by employing material and energy balances together with simple reaction kinetics. Three differential equations are then derived showing the change of feed concentration x, product concentration y and temperature θ with time. The rate of formation of y is some function of x and θ. For non-steady state operation around a point, three new variables X, Y and Z are introduced. These are defined as:

$x = x_s + X$ $\qquad$ s = Steady State Value

$y = y_s + Y$ $\qquad$ R = Reaction Rate

$\theta = \theta_s + Z$

Also, $R(x,\theta) = R(x_s,\theta) + \frac{\partial R(x_s,\theta)}{\partial x}X + \frac{\partial R}{\partial \theta}(x_s,\theta_s)Z$

The new values of x, y, θ and $R(x,\theta)$ are substituted into the original three equations and the desired combination of forced and forcing variables obtained by simultaneous solution of the defining differential equations. Process variables held constant for a particular solution of a transfer function are treated as identically zero. With such a solution, the partial derivatives actually become a part of the transfer function; however, this posed no particular problem in the construction of (in this case) Nyquist diagrams since only a constant first derivative was assumed.

Williams and Young (45) developed theoretical equations describing the dynamics of a baffled, multipass shell and tube heat exchanger. The response of the exchanger alone was described by a battery of ten ordinary, linear, differential equations. Consideration of a multipass, tube and shell heat exchanger will show that it is a highly distributed unit of process equipment and that fluid temperatures in both tube and shell sides are changing with distance as well as time when forced by one of the inlet streams. The method these authors employed in deriving equations of the ordinary type was by use of a "lumping" process. As regards fluid temperatures, the exchanger was separated into ten different compartments; five for the tube-side fluid and five for the shell-side fluid. It was assumed that perfect mixing occurred in each individual compartment and that each compartment was represented by a temperature which, if varied, could change only with time. No consideration was given to the non-linear variation of film coefficient with changes in flow behavior. Furthermore, all metal capacitances were disregarded. Conservation of computing equipment was cited as the reason

for certain areas of simplification. In this particular heat exchanger study, an analog computer was used in obtaining a controller constant-exchanger stability type of solution. The result of such work is of practical value since controller settings are easily ascertained for given process conditions.

The general method of transfer function development by Mozley (30) was similar to that just described. The problem here was also one of heat exchange except that the equipment was less complex. The exchanger consisted of two long concentric pipes with cold water in the annulus and hot water in the inner pipe. Various temperature ratio transfer functions were developed employing the "lumping" method as previously explained. Consideration was given neither to inner nor outer pipe wall dynamics. The mathematical methods applied in this paper are somewhat unique in that the final form of the various transfer functions includes all equipment constants and process parameters. Such a procedure allows for easy observation of any changes in the latter upon the attenuation or phase shift curve. The relatively simple transfer functions as derived by Mozley are of the type which would be most readily applied in actual control situations.

Takahashi (36) and later Cohen and Johnson (12) analyzed heat exchange processes from a more rigorous mathematical standpoint. The latter co-workers carried out experimental and theoretical investigations upon, again, a concentric pipe heat exchanger but with condensing steam as the heat source in the annulus. Differential dynamic balances were made yielding partial differential equations defining the system during unsteady state conditions. The lumping concept was not employed here;

rather, the defining partial differential equations were changed to the ordinary type by elimination of the independent variable of time during the Laplace transformation. The resulting ordinary differential equations contained the complex variable s which was considered as a constant throughout the remainder of the integration. Of interest in such a method of analysis is that the final forms of the transfer functions relating output temperature to steam or to input temperature contained the familiar pure dead time components modified by a more complicated exponential function of s.

A very early mathematical treatment of continuous agitated tanks undergoing heat exchange is presented by Mason in his "Quantitative Analysis of Process Lags" (27). The analysis was based upon a "fictitious" thermal resistance defined as equal to the temperature level divided by a constant heat flux. The transfer function concept was not in general use at the time and all solutions of derived differential equations were carried out by classical methods. The work is of value in pointing out the factors which are dominant in the response of this type of equipment.

Derivations

In the present work, emphasis has been placed upon analytical methods because of their value in synthesis as well as analysis of process control systems. Experimental corroboration is relied upon in order to help provide certain rules about which an analytical approach to similar problems may be built. The general method of derivation of transfer functions proceeds much along the same lines as those previously discussed. In certain cases where partial differential equations

describe the physical system, linearization is accomplished by averaging initial and final values of the pertinent dependent variables. It has been pointed out previously that most of the prior development of theoretical transfer functions has involved temperatures or other intensive properties. Mathematically, such derivations are often somewhat simpler and easier to handle when compared with transfer functions involving other important process variables such as, for example, flow rates.

In this work four different equipment arrangements (and therefore transfer functions) were studied. The general method of approach in all derivations was the same. For this reason, Arrangements Two and Four will be analyzed thoroughly and a final summary in the form of tables will present all the finished derivations for each arrangement. This should allow for a saving in space with no sacrifice in clarity. The first derivation is for Arrangement Two with steam temperature forcing tank fluid temperature. Assumptions are as follows for a first derivation:

Derivation 1

A. The steam is saturated and condensing at all points within the coils. Its pressure (and therefore temperature) may be varied with time but does not vary from point to point in the coils at any particular instant of time.

B. Copper coil and tank wall dynamics are considered as significant in the derivation.

C. Thermocouple well dynamics are considered as negligible and therefore disregarded.

A dynamic energy balance over the copper tubes for a very small increment of time Δt yields:

$$\text{Input} = h_s A_s(\theta_s - \theta_c)\Delta t \quad \text{BTU}$$

$$\text{Output} = h_f A_f(\theta_c - \theta)\Delta t \quad \text{BTU}$$

$$\text{Accumulation} = C_c \Delta\theta_c \quad \text{BTU}$$

These are easily combined by the equation

$$\text{Input} - \text{Output} = \text{Accumulation}$$

to yield: $$\frac{d\theta_c}{dt} + \frac{1}{T_2}(\theta_c - \theta) = \frac{1}{T_1}\theta_s - \theta_c) \qquad \text{V-1}$$

where: $T_1 = \frac{C_c}{h_s A_s}$, $T_2 = \frac{C_c}{h_f A_f}$, $C_c = (M)(c_p)$

For the reactor fluid, the result is:

$$\text{Input} = W_f c_p \theta_f \Delta t \quad \text{BTU}$$

$$\text{Input} = h_f A_f(\theta_c - \theta)\Delta t \quad \text{BTU}$$

$$\text{Output} = W_f c_p \theta \Delta t \quad \text{BTU}$$

$$\text{Output} = h_t A_t(\theta - \theta_t)\Delta t \quad \text{BTU}$$

$$\text{Accumulation} = C_f \Delta\theta \quad \text{BTU}$$

By treating these expressions in the same manner as before, the following differential equation is obtained:

$$\frac{d\theta}{dt} + \frac{1}{T_4}(\theta - \theta_t) + \frac{1}{T_5}(\theta - \theta_f) = \frac{1}{T_3}(\theta_c - \theta) \qquad \text{V-2}$$

where: $T_3 = \frac{C_f}{h_f A_f}$, $T_4 = \frac{C_f}{h_t A_t}$, $T_5 = \frac{C_f}{W_f c_p}$

A dynamic balance over the reactor tank walls yields:

$$\text{Input} = h_t A_t(\Theta - \Theta_t)\,\Delta t \qquad \text{BTU}$$

$$\text{Output} = 0$$

$$\text{Accumulation} = C_t \Delta\Theta_t \qquad \text{BTU}$$

The resulting differential equation is:

$$\frac{d\Theta_t}{dt} + \frac{\Theta_t}{T_6} = \frac{\Theta}{T_6} \qquad \text{V-3}$$

where: $T_6 = \dfrac{C_t}{h_t A_t}$

Equations V-1, V-2 and V-3 may now be transformed by the Laplace transformation. The initial conditions imposed are that the deviation of all temperatures from steady state conditions is zero at $t = 0$. Also, in applying the Laplace transformation, any system temperature which does not vary with changes in other temperatures is identically zero. This is true of Θ_f, the temperature of the fluid entering the vessel, which is held constant throughout all experimental dynamic testing. Upon rearranging and transforming, the equations as listed above become:

$$s\underline{\Theta}_c + \underline{\Theta}_c \left[\frac{1}{T_1} + \frac{1}{T_2}\right] = \frac{\underline{\Theta}_s}{T_1} + \frac{\underline{\Theta}}{T_2} \qquad \text{V-4}$$

$$s\underline{\Theta} + \underline{\Theta} \left[\frac{1}{T_3} + \frac{1}{T_4} + \frac{1}{T_5}\right] = \frac{\underline{\Theta}_c}{T_3} + \frac{\underline{\Theta}_t}{T_4} \qquad \text{V-5}$$

$$s\underline{\Theta}_t + \frac{\underline{\Theta}_t}{T_6} = \frac{\underline{\Theta}}{T_6} \qquad \text{V-6}$$

Sub-bars refer to transformed quantities. The following substitutions are then made:

$$\frac{1}{T_7} = \frac{1}{T_1} + \frac{1}{T_2} \quad , \quad \frac{1}{T_8} = \frac{1}{T_3} + \frac{1}{T_4} + \frac{1}{T_5}$$

Upon rearranging, the equations are ready for solution simultaneously for the desired transfer function. The final forms of the individual equations are:

$$\underline{\theta}_c = \left[\frac{1}{T_7 s + 1}\right] \left[K_1 \underline{\theta}_s + K_2 \underline{\theta}\right] \qquad \text{V-7}$$

$$\underline{\theta} = \left[\frac{1}{T_8 s + 1}\right] \left[K_3 \underline{\theta}_c + K_4 \underline{\theta}_t\right] \qquad \text{V-8}$$

$$\underline{\theta}_t = \frac{1}{T_6 s + 1} (\underline{\theta}) \qquad \text{V-9}$$

where: $K_1 = \frac{T_7}{T_1}$, $K_2 = \frac{T_7}{T_2}$, $K_3 = \frac{T_8}{T_3}$, $K_4 = \frac{T_8}{T_4}$

Equations V-7 and V-9 are substituted into equation V-8. Upon rearrangement and substitution of $j\omega$ for s, the final transfer function form of the equation is shown as follows:

$$\frac{\theta}{\theta_s}(j\omega) = \frac{(1 + T_6 j\omega)}{A(j\omega)^3 + B(j\omega)^2 + C(j\omega) + D} \qquad \text{V-10}$$

where:

$$A = \frac{T_6\ T_7\ T_8}{K_1 K_3}$$

$$B = \frac{T_6\ T_7 + T_6\ T_8 + T_7\ T_8}{K_1 K_3}$$

$$C = \frac{T_6 + T_7 + T_8 - K_2\ K_3\ T_6 - K_4\ T_7}{K_1 K_3}$$

$$D = \left[\frac{1 - K_4}{K_1 K_3}\right] - \frac{K_2}{K_3}$$

The second derivation for this arrangement proceeds along much the same lines. However, a considerably different transfer function is derived because of the difference in assumptions. These are as follows for Derivation 2.

Derivation 2

A. Steam temperatures - same as previously.

B. It is assumed here that the influence of wall dynamics is insignificant.

C. The effect of the thermocouple well is assumed to be significant.

A dynamic balance over the coils yields the same equation as previously; however, analysis of the reactor fluid and thermocouple well is of course modified. The three defining differential equations are as follows:

$$\text{Coils:} \quad \frac{d\theta_c}{dt} + \frac{1}{T_2}(\theta_c - \theta) = \frac{1}{T_1}(\theta_s - \theta_c)$$

$$\text{Fluid:} \quad \frac{d\theta}{dt} + \frac{1}{T_9}(\theta - \theta_r) + \frac{1}{T_5}(\theta - \theta_f) = \frac{1}{T_3}(\theta_c - \theta) \qquad \text{V-11}$$

$$\text{Well:} \quad \frac{d\theta_r}{dt} + \frac{\theta_r}{T_{10}} = \frac{\theta}{T_{10}} \qquad \text{V-12}$$

New time constants are:

$$T_9 = \frac{C_f}{h_r A_r}, \quad T_{10} = \frac{C_r}{h_r A_r}, \quad \frac{1}{T_{11}} = \frac{1}{T_3} + \frac{1}{T_5} + \frac{1}{T_9}$$

When these equations are rearranged and transformed, the following are obtained:

$$\underline{\theta}_c = \frac{1}{T_7 s + 1} (K_1 \underline{\theta}_s + K_2 \underline{\theta}) \qquad \text{V-7}$$

$$\underline{\theta} = \frac{1}{T_{11} s + 1} (K_5 \underline{\theta}_c + K_6 \underline{\theta}_r) \qquad \text{V-12}$$

$$\underline{\theta}_r = \frac{1}{T_{10} s + 1} \underline{\theta} \qquad \text{V-13}$$

These equations must be solved for $\frac{\theta_r}{\theta_s}(j\omega) = f(j\omega)$ because the thermowell temperature θ_r is the one recorded. If it is assumed that the well provides a small but significant lag, the recorded temperature is not the same as θ, the tank fluid temperature.

Solution of the above set of equations for the desired transfer function yields the expression as presented below:

$$\frac{\theta_r}{\theta_s}(j\omega) = \frac{K_1 K_6}{E(j\omega)^3 + F(j\omega)^2 + G(j\omega) + H} \qquad \text{V-14}$$

where: $$T_{11} = \frac{1}{T_3} + \frac{1}{T_5} + \frac{1}{T_9},$$

$$K_5 = \frac{T_{11}}{T_3}, \quad K_6 = \frac{T_{11}}{T_9}$$

and: $$E = T_7 T_{10} T_{11}$$

$$F = T_{10} T_{11} + T_7 T_{10} + T_7 T_{11}$$

$$G = T_7 + T_{10} + T_{11} - K_2 K_5 T_{10} - K_6 T_7$$

$$H = 1 - (K_2 K_5 + K_6 T_7)$$

An inspection of equations V-10 and V-14 will show that the process transfer function is altered in character to an appreciable extent depending upon assumptions made in its derivation. For example,

in equation V-10, the net limiting phase angle is -180 degrees while for equation V-14, it is -270 degrees. Thus, it may be appreciated that for the purely analytical approach to control dynamics without supporting data, it may be difficult to decide which assumptions are valid, which factors may be disregarded and those that must be retained. Furthermore, if results of any benefit are to be realized, the analog computer must be programmed with reasonably accurate transfer functions.

Derivations for the most important equipment arrangement will now be considered. In Arrangement Four, hot reactor feed is continuously pumped through the system during which time a portion of its heat is removed by cooling water flowing through internal coils. It is desired to study the dynamics of heat removal as a result of change in coolant rate of flow only. Throughout all runs with this arrangement, the temperature signal source was a bare thermocouple junction thus obviating any assumptions in this regard. The true temperature history of the cooling water must be represented by a partial differential equation since its temperature changes with time as well as length of coil traversed. Using the same technique of dynamic balance (in this case over a small length) and finite increments the following partial, non-linear differential equation was derived:

$$\frac{\partial \theta_w}{\partial t} + \frac{\partial \theta_w}{\partial x} V + \left[\frac{1}{T_{12}}\right] \theta_w = \left[\frac{1}{T_{12}}\right] \theta \qquad \text{V-15}$$

where: θ_w = Cooling water temperature

x = Length of coil in direction of flow

V = Cooling water velocity

$$T_{12} = \frac{A_o \rho c_p}{U \pi d}$$

In order to obtain the transfer function desired, $\frac{\theta}{W_w}(j\omega)$, the second partial derivative would have to be assigned a constant average value. Another method which amounts to essentially the same thing consists of defining a single cooling water temperature in the following manner:

$$\bar{\theta}_w \triangleq \frac{\theta_{wi} + \theta_{wo}}{2} \qquad \text{V-16}$$

or

$$\theta_{wo} = 2\bar{\theta}_w - \theta_{wi}$$

The key assumptions considered in effecting the first derivation for Arrangement Four are as follows:

Derivation 1

1. All metal capacitances are ignored as being negligible in affecting the dynamics of heat removal.
2. The two capacitances taken into account are those of the vessel fluid and the cooling water holdup.
3. An overall heat transfer coefficient is employed. Its value is assumed to be constant during the sinusoidal fluctuations of cooling water flow rate and equal numerically to its value at mean steady state conditions.

From a dynamic balance over the cooling water, the following equation

is produced in the same manner as before:

$$\frac{d\bar{\theta}_w}{dt} + \frac{2}{T_{13}}\bar{\theta}_w + \frac{1}{T_{14}}\bar{\theta}_w - \frac{1}{T_{14}}\theta = 2K_7W_w \qquad V\text{-}17$$

where: $T_{13} = \frac{C_w}{\bar{W}_w c_p}$, $T_{14} = \frac{C_w}{U A_a}$, $K_7 = \frac{\theta_{wi} c_p}{C_w}$

This equation may be simplified by defining a new time constant in the following manner:

$$\frac{1}{T_{15}} = \frac{2}{T_{13}} + \frac{1}{T_{14}}$$

The final equation is then:

$$\frac{d\bar{\theta}_w}{dt} + \frac{\bar{\theta}_w}{T_{15}} - \frac{\theta}{T_{14}} = 2K_7W_w \qquad V\text{-}18$$

By similar methods of dynamic balance, the following equation is derived for the tank fluid:

$$\frac{d\theta}{dt} + \frac{1}{T_{17}}\theta = \frac{1}{T_{16}}\bar{\theta}_w \qquad V\text{-}19$$

where: $\frac{1}{T_{17}} = \frac{1}{T_5} + \frac{1}{T_{16}}$, $T_{16} = \frac{C_f}{U A_a}$, $T_5 = \frac{C_f}{W_f c_p}$

Equations V-17 and V-18 are transformed as before by the Laplace transformation. Again, the initial condition that all parameters are at zero variation from steady state conditions at $t = 0$ must be applied. After solution simultaneously, the final form of the transfer function is obtained as:

$$\frac{\theta}{W_w}(j\omega) = \frac{2K_7/T_{16}}{(j\omega)^2 + \left[\frac{T_{17} + T_{15}}{T_{17}T_{15}}\right] j\omega + \frac{1}{T_{15}T_{17}} - \frac{1}{T_{14}T_{16}}} \qquad V\text{-}20$$

The preceding treatment has produced a relatively simple second order transfer function with a limiting phase lag of -180 degrees. Comparison with experimental results will prove whether or not the assumptions made in its derivation are justifiable. It would appear intuitively that the most serious assumption is the one neglecting the capacitance of the internal mass of metal separating hot and cold fluids. A certain amount of time would always be necessary to change the temperature of the metal internals. Such thinking could be taken to an extreme wherein the internal tubes or coils constituted a large portion of the entire system mass and were of thick-walled construction because of the need for pressuring the coolant. It is a simple matter mathematically to take into account any capacitance. The uncertainty is in determining proper values to be applied to fluid resistances in the transfer of heat under dynamical conditions. For the case under study, both inside coil and outside coil film coefficients must be available because of the demands of the derivation. Both are subject to change with time and location as flow rates and temperatures vary simultaneously. A second derivation for Arrangement Four was carried out with the following key assumptions:

Derivation 2

1. The internal metal heat transfer coil is considered as offering sufficient lag so as to affect control dynamics at the medium and higher frequencies.

2. All other metal capacitances are neglected.
3. The outer film coefficient of heat transfer h_o is considered as remaining essentially constant during dynamical operation and equal numerically to its value at mean steady state conditions.
4. The inside film coefficient of heat transfer h_i is considered as remaining essentially constant during sinusoidal fluctuations of flow rate and equal numerically to its value at steady state conditions. Such values were obtained by difference from experimental overall coefficients and the outside coefficients as listed above.

On applying the assumptions as outlined together with a cooling water temperature as defined by equation V-16, the following differential equations were derived when dynamic balances were made over the cooling water, heat transfer coils and tank fluid:

Cooling Water: $$\frac{d\bar{\theta}_w}{dt} + \frac{1}{T_{19}}\bar{\theta}_w - \frac{1}{T_{18}}\theta_c = 2K_7W_w \qquad \text{V-21}$$

Coils: $$\frac{d\theta_c}{dt} + \frac{1}{T_{22}}\theta_c = \frac{1}{T_{20}}\theta + \frac{1}{T_{21}}\bar{\theta}_w \qquad \text{V-22}$$

Tank Fluid: $$\frac{d\theta}{dt} + \frac{1}{T_{23}}\theta = \frac{1}{T_{23}}\theta_c \qquad \text{V-23}$$

New time constants are defined by:

$$T_{18} = \frac{C_w}{h_iA_i}, \quad T_{20} = \frac{C_c}{h_oA_o}, \quad T_{21} = \frac{C_c}{h_iA_i}, \quad T_{23} = \frac{C_f}{h_oA_o}$$

$$\frac{1}{T_{19}} = \frac{2}{T_{13}} + \frac{1}{T_{18}} \quad , \quad \frac{1}{T_{22}} = \frac{1}{T_{20}} + \frac{1}{T_{21}}$$

Equations V-21, V-22 and V-23 are transformed as before, then solved simultaneously for the required transfer function. The final equation is:

$$\frac{\theta}{W_w}(j\omega) = \frac{2K_9 K_{10}/T_{23}}{I(j\omega)^3 + J(j\omega)^2 + L(j\omega) + M} \qquad \text{V-24}$$

where: $K_9 = \frac{T_{22}}{T_{21}}$, $\frac{1}{T_{24}} = \frac{1}{T_5} + \frac{1}{T_{23}}$, $K_{10} = \frac{c_p\theta_f +$

$c_p\overline{W}_f + h_f A_f$

$$I = T_{22}$$

$$J = \frac{T_{22}T_{19} + T_{24}(T_{22} + T_{19})}{T_{19}T_{24}}$$

$$L = \frac{T_{19} + T_{22} + T_{24}}{T_{19}T_{24}} - \left[\frac{K_9}{T_{18}} + \frac{K_8}{T_{23}}\right]$$

$$M = \frac{1}{T_{19}\,T_{24}} - \left[\frac{K_8}{T_{19}\,T_{23}} + \frac{K_9}{T_{18}\,T_{24}}\right]$$

Several of the more important transfer functions have been derived. During the course of this investigation, a total of eleven expressions were obtained by analytical methods for the four equipment arrangements tested. In Tables 5 to 8 these theoretical transfer functions are listed according to the particular equipment arrangement they represent. Each is assigned a number for ease in reference. A complete listing of all time constants is located in the Appendix. In the following chapter, the coefficients for most of the expressions are

assigned numerical values and the resulting functions plotted on Bode diagrams for comparison with experimental data.

TABLE 5

Theoretical Transfer Functions for Equipment Arrangement One
Coils Acting as Heat Source - Fluid Feed Rate Forcing

No.	Transfer Functions	Key Assumptions
1.	$\frac{\Theta_r}{W_f}(j\omega) = \frac{K_8}{T_8\, j\omega + 1}$	a. All metal capacitances negligible b. Negligible steam film resistance
2.	$\frac{\Theta_r}{W_f}(j\omega) = \frac{K_9}{\frac{T_{10}T_{25}(j\omega)^2 + (T_{10} + T_{25})\, j\omega + 1}{T_{25}} - \frac{1}{T_9}}$	a. Vessel wall and coil dynamics disregarded b. Thermocouple well dynamics considered c. Negligible steam film resistance

TABLE 6

Theoretical Transfer Functions for Equipment Arrangement Two
Coils Acting as Heat Source - Steam Temperature Forcing

No.	Transfer Functions	Key Assumptions
3.	$\frac{\theta_r}{\theta_s}(j\omega) = \frac{T_8/T_3}{T_8(j\omega) + 1}$	a. All metal capacitances negligible b. Negligible steam film resistance
4.	$\frac{\theta_r}{\theta_s}(j\omega) = \frac{T_6(j\omega) + 1}{\frac{T_6T_8}{K_3}(j\omega)^2 + \frac{T_6T_8}{K_3}(j\omega) + \frac{1 - K_4}{K_3}}$	a. Reactor wall dynamics considered b. Coil and T.C. well disregarded
5.	$\frac{\theta_r}{\theta_s}(j\omega) = \frac{T_6(j\omega) + 1}{A(j\omega)^3 + B(j\omega)^2 + C(j\omega) + D}$	a. Wall and coil dynamics considered b. T. C. well dynamics disregarded c. Negligible steam film resistance
6.	$\frac{\theta_r}{\theta_s}(j\omega) = \frac{K_1K_s}{E(j\omega)^3 + F(j\omega)^2 + G(j\omega) + H}$	a. Reactor wall dynamics disregarded b. Coil and T. C. well considered c. Negligible steam film resistance

TABLE 7

Theoretical Transfer Functions for Equipment Arrangement Three
Coils Acting as Heat Sink - Fluid Feed Rate Forcing

No.	Transfer Functions	Key Assumptions
7.	$\frac{\theta}{W_f}(j\omega) = \frac{K_9 K_8}{T_8 j\omega + 1}$	a. Metal or cooling water capacitances not considered
8.	$\frac{\theta}{W_f}(j\omega) = \frac{K_7(T_{14}j\omega + 1)}{\frac{(T_{27}j\omega + 1)(T_{14}j\omega + 1)}{T_{27}} - \frac{1}{T_{16}}}$	a. All metal dynamics disregarded b. Cooling water and vessel fluid capacitances considered c. Overall coefficient of heat transfer employed
9.	$\frac{\theta}{W_f}(j\omega) = \frac{K_7 T_8 T_2 T_{21}(T_{18}j\omega + 1)(T_{26}j\omega + 1) - T_2 T_{26}}{T_2 T_{21}(T_8 j\omega + 1)(T_{18}j\omega + 1)(T_{26}j\omega + 1) - T_2 T_{26}(T_8 j\omega + 1) + T_3 T_{21} T_{26}(T_{18}j\omega + 1)}$	a. Vessel fluid, metal coils cooling water dynamics considered b. Vessel wall dynamics disregarded c. Overall coefficient of heat transfer employed

TABLE 8

Theoretical Transfer Functions for Equipment Arrangement Four
Coils Acting as Heat Sink - Cooling Water Rate Forcing

No.	Transfer Functions	Key Assumptions
10.	$\frac{\theta}{W_w}(j\omega) = \frac{2K_{10}/T_{16}}{(j\omega)^2 + \left[\frac{T_{17} + T_{15}}{T_{17}T_{15}}\right](j\omega) + \frac{1}{T_{15}T_{17}} - \frac{1}{T_{14}T_{16}}}$	a. Metal capacitances ignored b. Fluid dynamics only considered c. Overall coefficient employed
11.	$\frac{\theta}{W_w}(j\omega) = \frac{2K_9K_{10}/T_{23}}{I\,(j\omega)^3 + J(j\omega)^2 + L(j\omega) + M}$	a. Coil capacitance as well as fluid capacitances taken into account b. Individual film coefficients employed

CHAPTER VI

DISCUSSION OF EXPERIMENTAL AND THEORETICAL RESULTS

The method of attack in theoretical equation development was demonstrated in the preceding chapter. Many of the equations appear unduly complex with an excessive amount of time being required merely for substitution into equation constants. It is true that simple process transfer functions are desirable for any type of control study. However, it must be realized that even for a relatively simple process unit such as the one under study, the dynamical relationship between certain process variables may be of a complex nature. With regard to Arrangement Four, the process transfer function or as it is sometimes called, the process equation may be represented diagramatically as follows:

$$\theta = \left[\begin{array}{c}\text{Process Transfer} \\ \text{Function}\end{array}\right] W_w$$

This states that a given change in cooling water flow rate multiplied by the process transfer function will describe the amount and manner in which the tank temperature will change. The process transfer function may be represented in general mathematical terms by the following expression:

Process Transfer Function = f {

1. Liquid Capacitances
2. Metal Capacitances
3. Feed Rates
4. Physical Properties of Fluids
   a. Temperature of operation
   b. Pressure of operation
5. Vessel Fluid Conditions
   a. Agitator RPM
   b. Equipment Geometry
6. Coil Fluid Conditions
   a. Laminar Flow
   b. Turbulent Flow

An accurate experimental frequency response determination takes into account all the effects and counter-effects of the many variables so that a true pictorial representation of process characteristics is at hand, provided system non-linearity is not too great. Even here, good approximations may be obtained. For highly non-linear systems, transfer functions are usually restricted to levels of operation adjacent to that from which the experimental data were taken. In the derivation of theoretical expressions, an attempt is made to take into account all factors considered to have a substantial influence. When certain parameters vary appreciably within the range of the forcing upset, such variations are considered. A comparison between experimental and theoretical results usually points up correct and incorrect assumptions. The simplest transfer function which compares favorably with the experimental

results is then selected as representative. Certain basic rules are thereby established for writing analytical expressions covering cases of similar nature.

Most theoretical investigations show that usually three or fewer time constants are dominant; however, the present work has shown that several supposedly insignificant lags sometimes react together in such a manner as to have a decided effect upon the Bode curves, particularly at medium and higher frequencies. Since these small time constants as well as the larger ones usually contain film coefficients of heat transfer, the following discussion will explain, in detail, the source of these coefficients.

Heat Transfer Coefficients

At the outset of the problem, it was known that some sort of correlation must be available for estimating outside heat transfer film coefficients. One of the objectives of this work was to determine if such coefficients heretofore always obtained under steady state conditions, would be sufficient for the continually varying state. The amount of work done on heat transfer problems relative to agitated reactor vessels is meager compared with the multitude of correlations available for circular conduit heat transfer. A search of the literature indicated that Chilton, et.al. (10) were among the first to do work in this particular field. In this paper, several correlations were presented but none were felt to be applicable because of the geometry of their equipment. The correlations of Cummings and West (13) were rejected for the same reason. Dunlap and Rushton (14) obtained steady state heat transfer

data from equipment larger but similar to that of the present investigation except that vertical tube baffling was employed.

The correlation of Oldshue and Gretton (32) was finally selected as the one most suitable for the present study. Although their agitated vessel was four times larger in diameter, its geometric configuration was very much the same as the one used in these experiments. The heat transfer surface was in the form of a closely-spaced helical coil with small baffle clearance. Turbine geometry was very similar. The correlation which these investigators recommend is listed below:

$$\frac{h_o d}{k} = 0.17 \left[\frac{ND^2\rho}{\mu}\right]^{0.67} \left[\frac{c_p \mu}{k}\right]^{0.37} \left[\frac{D}{T}\right]^{0.1} \left[\frac{d}{T}\right]^{0.5} \qquad \text{VI-1}$$

This correlation was employed throughout all calculations. It has been applied, for example, in Table 29 where the numerical relationship between impeller speed and outside film coefficient, h_o was desired.

Physical properties of the oil used in the present investigation were supplied by the blender, Cato Oil and Grease Company of Oklahoma City, Oklahoma. The water tested came from the University of Oklahoma mains and all physical properties were obtained from the Chemical Engineer's Handbook. Physical properties of both fluids at key temperatures are listed in the Appendix.

Heat transfer to other parts of the reactor tank as well as the thermocouple well was assumed to be governed by the same film coefficient as that calculated for the helical coils. This should be a reasonable assumption since with adequate agitation, the condition of fluid turbulence was comparable. A conservative figure of 2400 BTU/(hr.) (sq.ft.)^{o}F was used for the steam film coefficient h_s in the limited

number of cases requiring it. This is in accordance with recommendations in the Chemical Engineer's Handbook. Its effect on any theoretical transfer function was slight because of the much greater outside film resistance. Time constants involving an overall coefficient of heat transfer U were encountered in several derivations. Its numerical value was calculated directly from steady state conditions existing prior to the imposition of a forcing function. For example, the data from Tables 1 and 3 may be employed in calculating an overall U at the average level of operating conditions.

Several correlations are available for estimating an inside coefficient of heat transfer h_i for different conditions of pipe flow. It was felt however that a more accurate value would be realized by direct computation from the experimental data. An overall value for U was established as described previously at the steady state conditions existing prior to the initiation of a run. Knowledge of all parameters also allowed the computation of h_o using equation VI-1. With a knowledge of coil areas and coil thickness, h_i was readily obtained from the basic heat transfer equation defining the overall film coefficient. This, of course, yields a steady state value of h_i under prevailing conditions. With regard to Arrangement Four where coolant flow rate is continually changing, the value of h_i could not be expected to remain constant. Its degree of variation from mean steady state conditions determines whether or not a critical error is introduced by treating it as constant in the theoretical development.

An inspection of the composition of theoretical time constants will reveal that many contain a capacitance term C (with applicable sub-

script) in the numerator. This term is in the units of BTU/°F and is obtained by multiplying the mass in question by its specific heat. It was therefore necessary to know accurately the tank volume and mass as well as coil volume and mass. All these values were obtained by actual measurement. In addition, it was necessary to know both inside and outside coil heat transfer surface together with tank inner surface. These values were calculated since equipment configuration made physical measurement impractical. All such numerical values are listed in the Appendix.

First Three Arrangements

The first transfer function tested experimentally involved the change in tank fluid temperature resulting from a change in fluid feed rate. Substitution of constants into the theoretical equations listed in Table 5 yielded the following expressions with numerical values for the two fluids tested:

Transfer Function No.	Fluid	Composition
1.	Water	$\frac{\theta_r}{W_f}(j\omega) = \frac{3.260}{2.407\ j\omega + 1}$
1.	Oil	$\frac{\theta_r}{W_f}(j\omega) = \frac{7.280}{3.70\ j\omega + 1}$
2.	Water	$\frac{\theta_r}{W_f}(j\omega) = \frac{1.642}{0.0096(j\omega)^2 + 1.005\ j\omega + 0.5306}$
2.	Oil	$\frac{\theta_r}{W_f}(j\omega) = \frac{4.889}{0.0098\ (j\omega)^2 + 1.005\ j\omega + 0.287}$

Note that it is not actually necessary to calculate the process gains because of the manner in which the magnitude ratios have been defined. With this definition, the magnitude ratio at zero frequency is always one. At each individual frequency, the process gains therefore cancel. Figures 20 and 21 present plots of theoretical transfer functions 1 and 2 for water and oil respectively. The curve representing the particular transfer function is designated by its assigned number. Points obtained from experimental frequency response determinations are shown as small circles.

A comparison between experimental points and theoretical curves is of interest. The first general observation is the marked difference in equipment response depending upon the type of fluid flowing through the system. This is even more sharply noticeable during actual response runs. With regard to attenuation, it may be stated that both fluids react in an approximate first order manner. In fact, the experimental points for water indicate a slope between -1 and zero. This cannot be explained except that it was among the first frequency response data taken and therefore subject to more inaccuracies. At the higher frequencies, the oil attenuation points begin to drop off indicating the effect of a small secondary lag. The experimental points for both phase diagrams also show definite first order tendencies with that for water the most marked. Again, phase angles for both fluids drop beyond the limiting -90 degrees for a first order transfer function at the higher frequencies. The rate of phase lag increase is considerably higher for oil than for water. Lag introduced by the same thermocouple well is then of much more importance for a fluid of high viscosity. This may be intui-

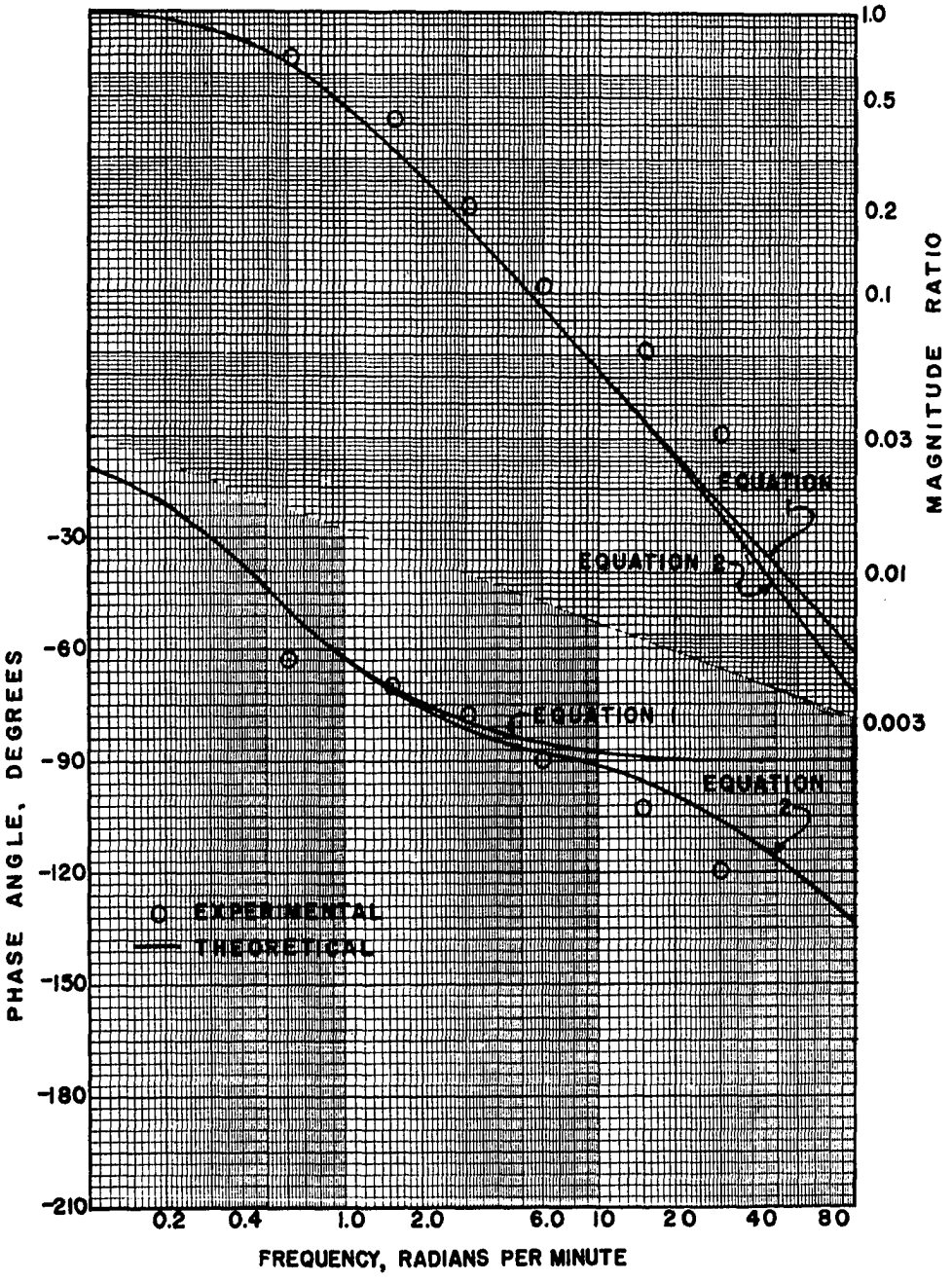


Figure 20 - Experimental and Theoretical Bode Diagrams, Arrangement One, Water

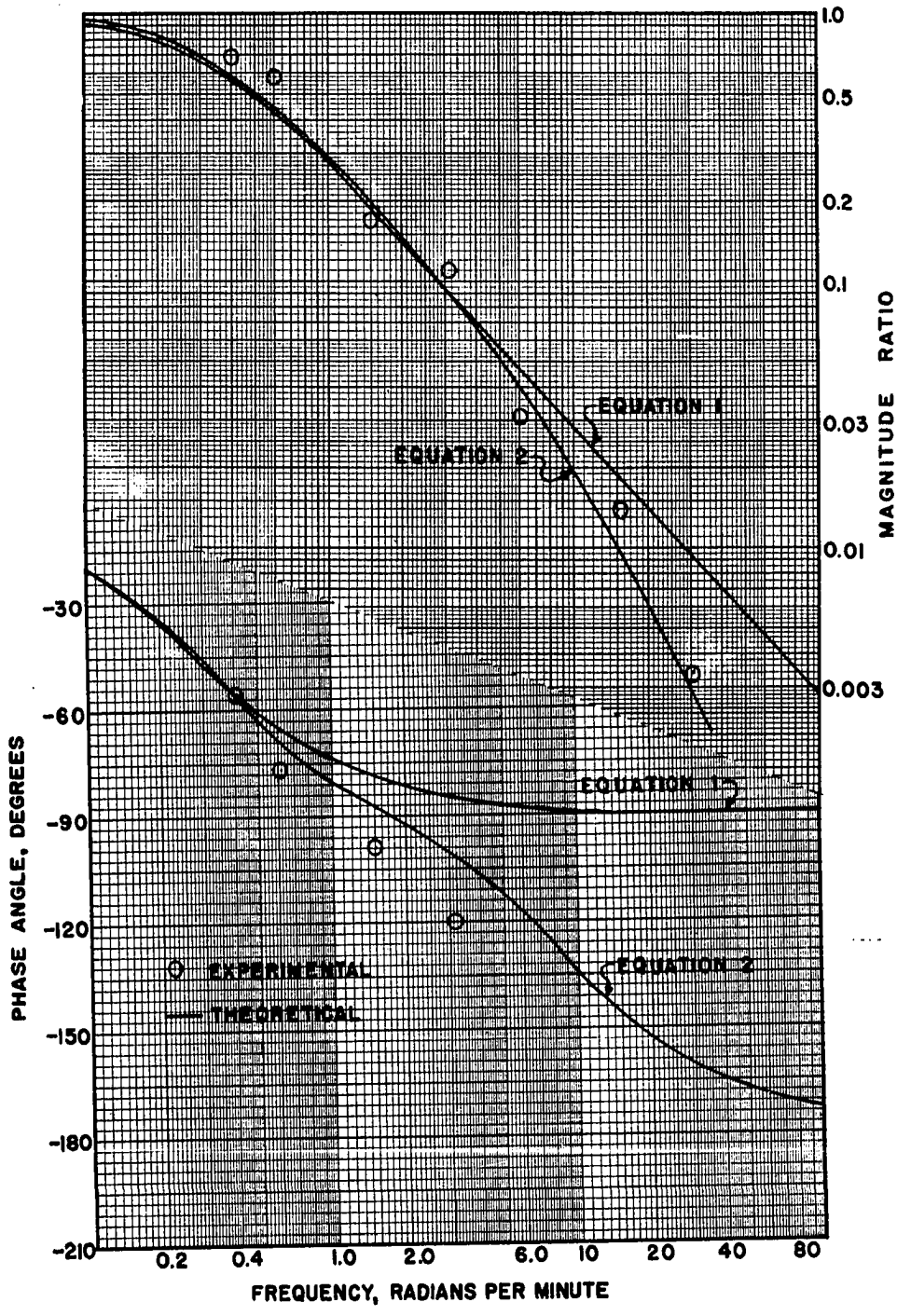


Figure 21 - Experimental and Theoretical Bode Diagrams, Arrangement One, Oil

tively deduced but the actual quantitative effect is illustrated by the information displayed in Figures 22 and 23.

In summarizing, it may be stated that system dynamics can be represented for both fluids by a simple first order transfer function (equation 1) up to frequencies of about three radians per minute. For oil as the process fluid, theoretical equation 2 must be employed at frequencies any higher than this if reasonable phase lag accuracy is to be expected. In accordance with the theory, experimental observations indicate first order behavior for both fluids if all measurement and recording lags are reduced to very small quantities in comparison with the dominant lags.

The dynamics of Equipment Arrangement Two wherein reactor tank fluid is forced by changes in steam temperature could be of practical value in control problems involving the cyclic heating and mixing of paints, varnishes and a multitude of other applications. This particular arrangement afforded an excellent opportunity to investigate the effect of outer wall dynamics. The two theoretical equations plotted are listed in their numerical forms below. Assumptions made in the derivations are listed in Table 6.

Transfer Function No.	Fluid	Composition
5.	Water	$\frac{\theta_r}{\theta_s}(j\omega) = \frac{0.0536\ j\omega + 1}{0.00341(j\omega)^3 + 0.522(j\omega)^2 + 9.09j\omega + 3.42}$
5.	Oil	$\frac{\theta_r}{\theta_s}(j\omega) = \frac{0.536\ j\omega + 1}{0.00177(j\omega)^3 + 0.445(j\omega)^2 + 0.918j\omega + 0.206}$
6.	Water	$\frac{\theta_r}{\theta_s}(j\omega) = \frac{2.470}{0.00059(j\omega)^3 + 0.144(j\omega)^2 + 8.575j\omega + 3.42}$

Transfer Function No.	Fluid	Composition
6.	Oil	$\frac{\theta_r}{\theta_s}(j\omega) = \frac{3.812}{0.00115(j\omega)^3 + 2.35(j\omega)^2 + 19.9j\omega + 5.475}$

Figures 22 and 23 include plots of the theoretical transfer functions as shown by the continuous solid curves. The theoretical phase lead effect of the tank wall is clearly shown by expression No. 5 for oil. There is a pronounced dip in the attenuation curve as well as a lengthy leveling off portion of the phase lag curve. This effect is not nearly so noticeable for water because of its much smaller lead time constant. In all cases, but especially for water, the effect of the first terms in the numerators is slight because of their small coefficients. Experimental points in general lie above the theoretical attenuation curves for both fluids. This is explained in part by the use of steady state gain values at the higher frequencies which may not have been of normal accuracy. Hand pressure fluctuations were employed at the lower frequencies while the mechanical generator produced the higher frequency waves. Transients for the latter using the generator on steam flow were very difficult to obtain. In neither case do the experimental points indicate phase lead effect.

Experimental phase angle points are in good agreement with equation 6. This verifies the statement made above with regard to any wall dynamic effects. With water as the process fluid, the response to any change in steam temperature is virtually first order except at the high frequencies. In this case, coil dynamics appear to be insignificant over most of the frequency spectrum. However, for the best accuracy over

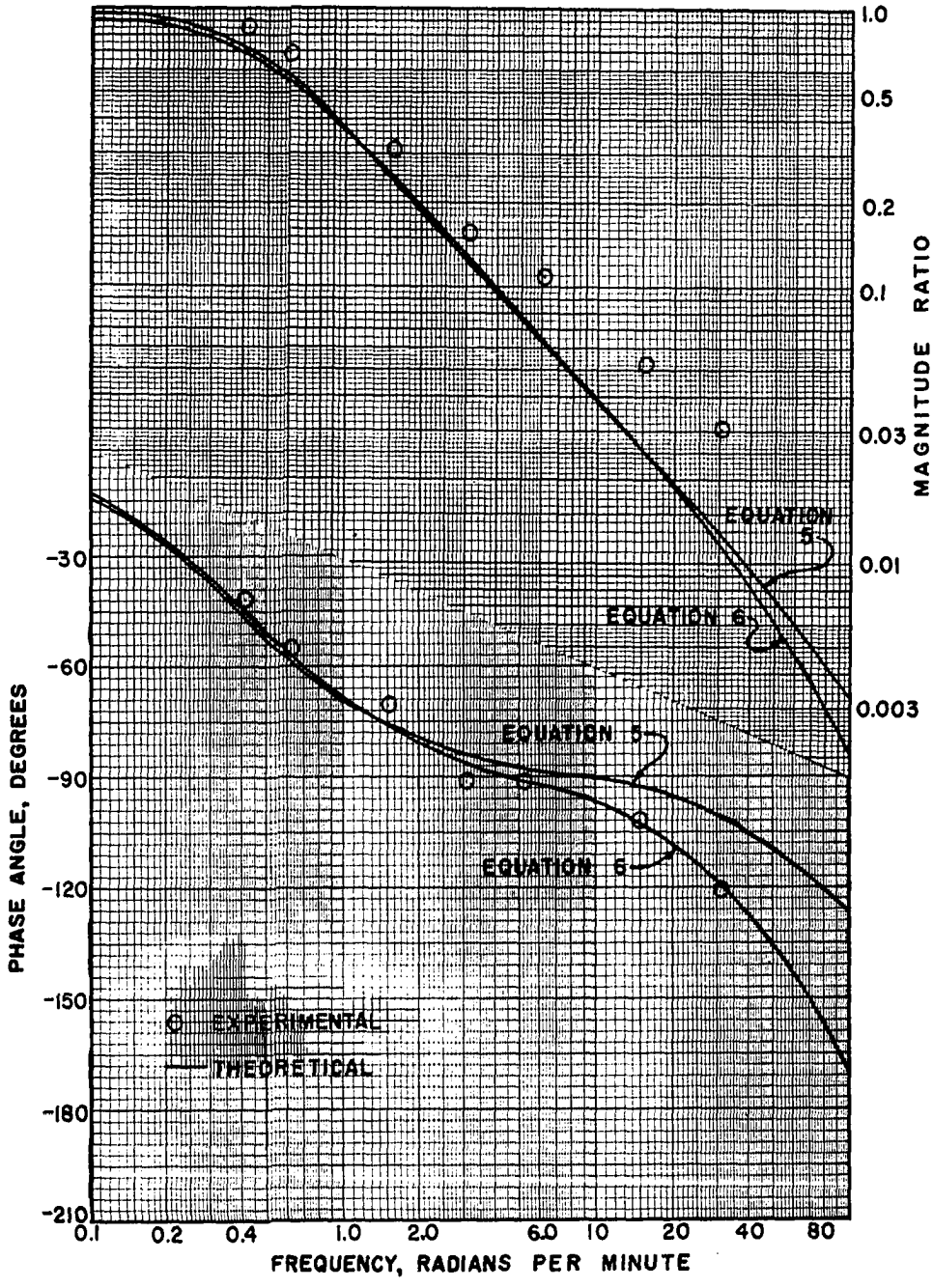


Figure 22 - Experimental and Theoretical Bode Diagrams, Arrangement Two, Water

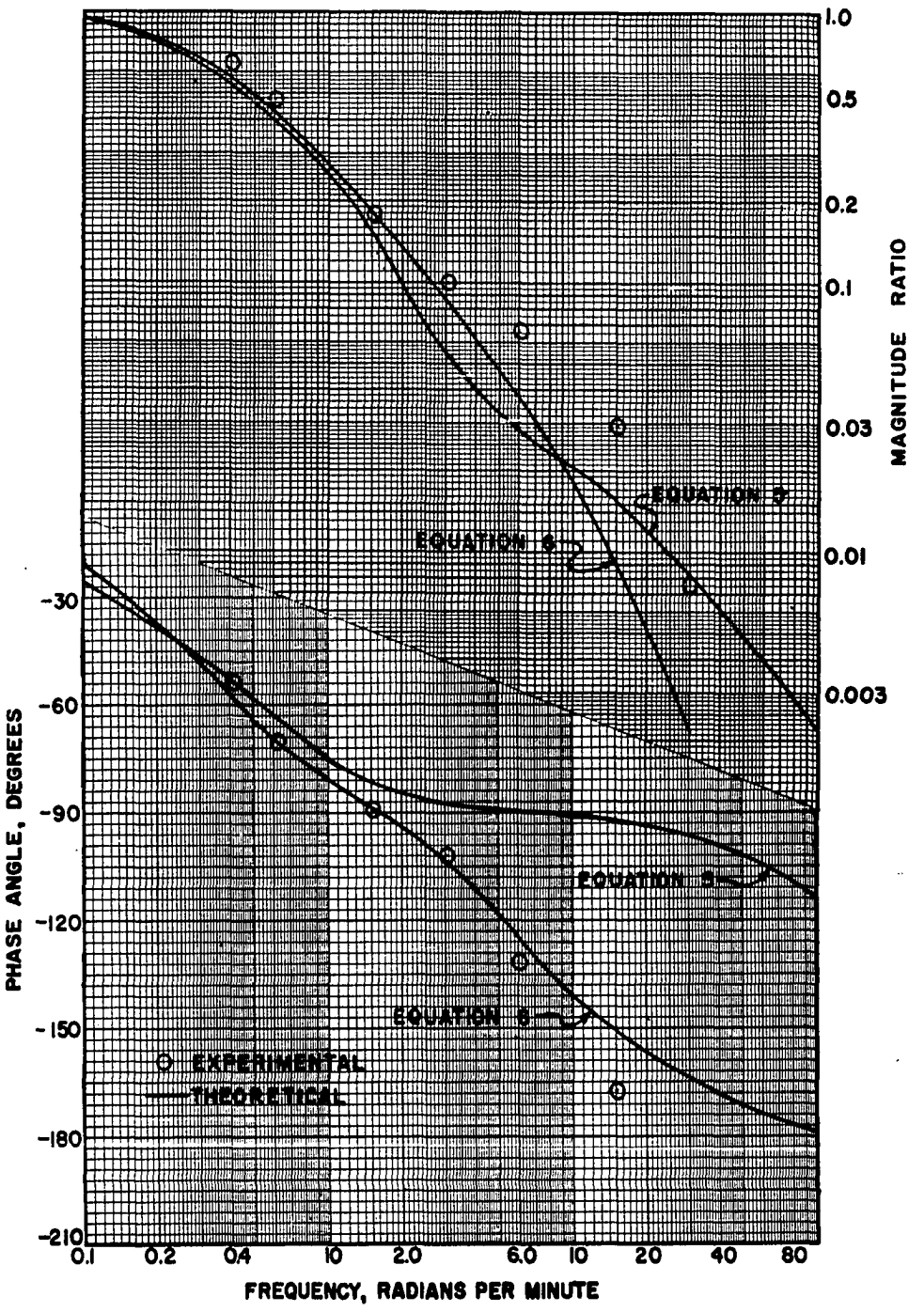


Figure 23 - Experimental and Theoretical Bode Diagrams, Arrangement Two, Oil

the entire range, transfer function No. 6 is recommended. Experimental values for oil also indicate that up to frequencies of four radians per minute, system response within engineering accuracy is described by a simple first order lag. Again, equation 6 provides good agreement, particularly for the all-important system phase lag at the higher frequencies.

The transfer function for Arrangement Three is the same as for Arrangement One except that the reactor helical coils act as a heat sink. In order to eliminate most measurement lag, the experimental work was carried out from this point on with a bare thermocouple junction as the tank fluid temperature signal source. Since 24-gauge thermocouple wire was employed, the bare junction response was probably several decades faster than any imposed experimental frequency. The chief object of this particular arrangement was to gain experience in preparation for the final and most important response study as well as to determine if the cooling coils acted as a phase lead source. In light of the preceding results, it was decided that theoretical equations 7 and 8 as listed in Table 7 should be tested against experimental results. Theoretical transfer function 9 was rejected as being far too bulky and unwieldy for what was considered to be a relatively simple response. The theoretical equations with numerical coefficients are listed below. Reasons for the difference in the two expressions are stated in Table 7.

Transfer Function No.	Fluid	Composition
7.	Water	$\frac{\theta}{W_f}(j\omega) = \frac{13.18}{2.407\ j\omega + 1}$

Transfer Function No.	Fluid	Composition
7.	Oil	$\frac{\theta}{W_f}(j\omega) = \frac{22.11}{3.70\ j\omega + 1}$
8.	Water	$\frac{\theta}{W_f}(j\omega) = \frac{0.117\ j\omega + 1}{0.117\ (j\omega)^2 + 1.0486\ j\omega + 0.213}$
8.	Oil	$\frac{\theta}{W_f}(j\omega) = \frac{0.658\ j\omega + 1}{0.658\ (j\omega)^2 + 1.178\ j\omega + 0.1902}$

These equations are plotted and identified by number in Figures 24 and 25. Both have limiting phase angles of -90 degrees and therefore are similar as regards affect on closed loop theory. In every case, it appears that the first equation more nearly coincides with the experimental data. It is noteworthy that erroneously high magnitude ratios at the higher frequencies do not appear in this set of data. It is believed that more accurate dynamic data can be obtained with exchange of heat between two fluids than with condensing steam. Additional experience also brought about refinements in the technique of collecting experimental frequency and transient response data.

At the highest frequency of 31 radians per minute, the experimental phase angles for both oil and water disagree with the theory. Points at lower frequencies are in relatively good agreement. However, a portion of the discrepancy may have been the result of improper instrument adjustment. It was found after the runs that the instrument gain had been inadvertently lowered from previous runs so that pen response was slightly slower. In all runs thereafter, instrument gain was raised to a point just under unstable response so that a recording speed

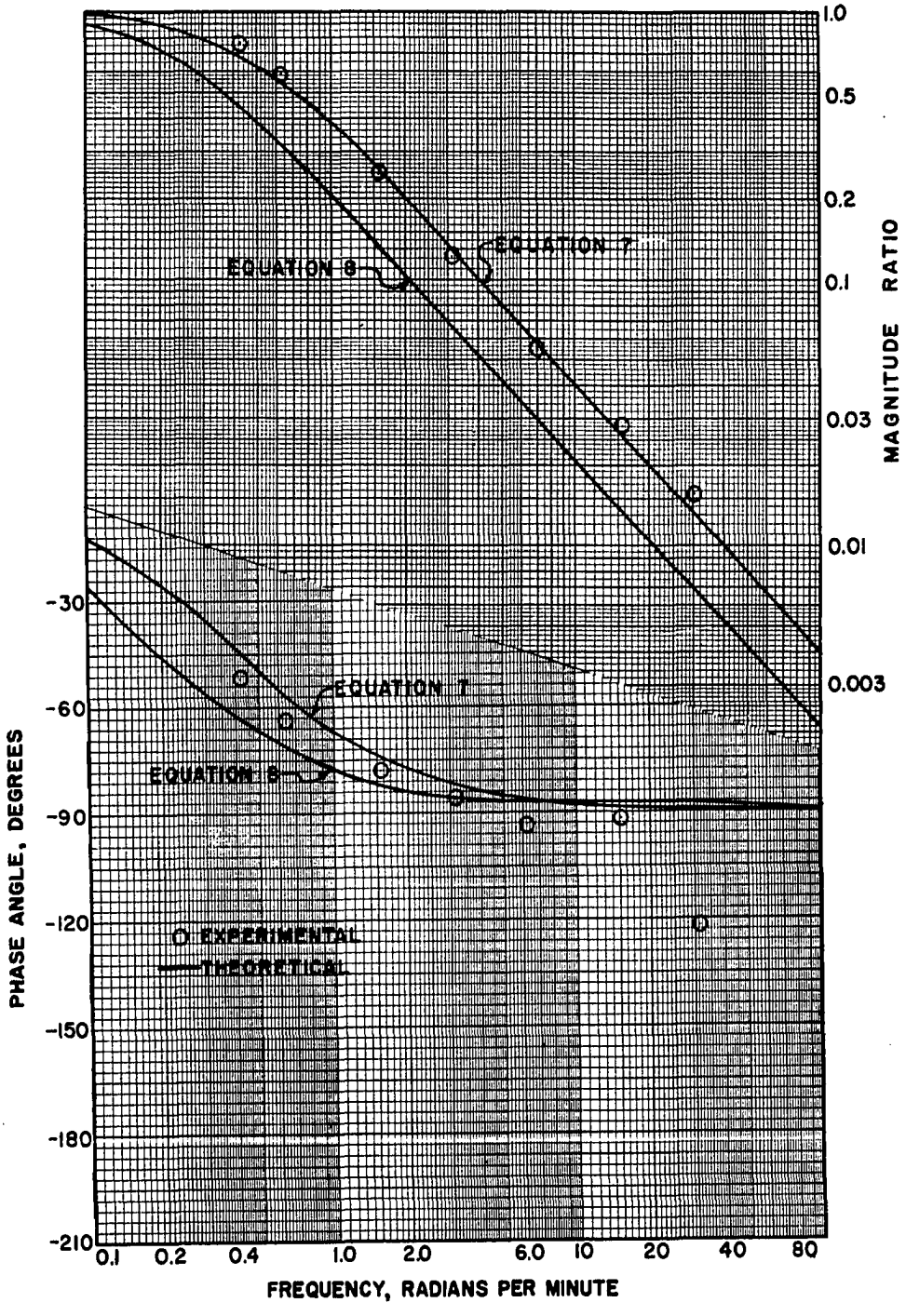


Figure 24 - Experimental and Theoretical Bode Diagrams, Arrangement Three, Water

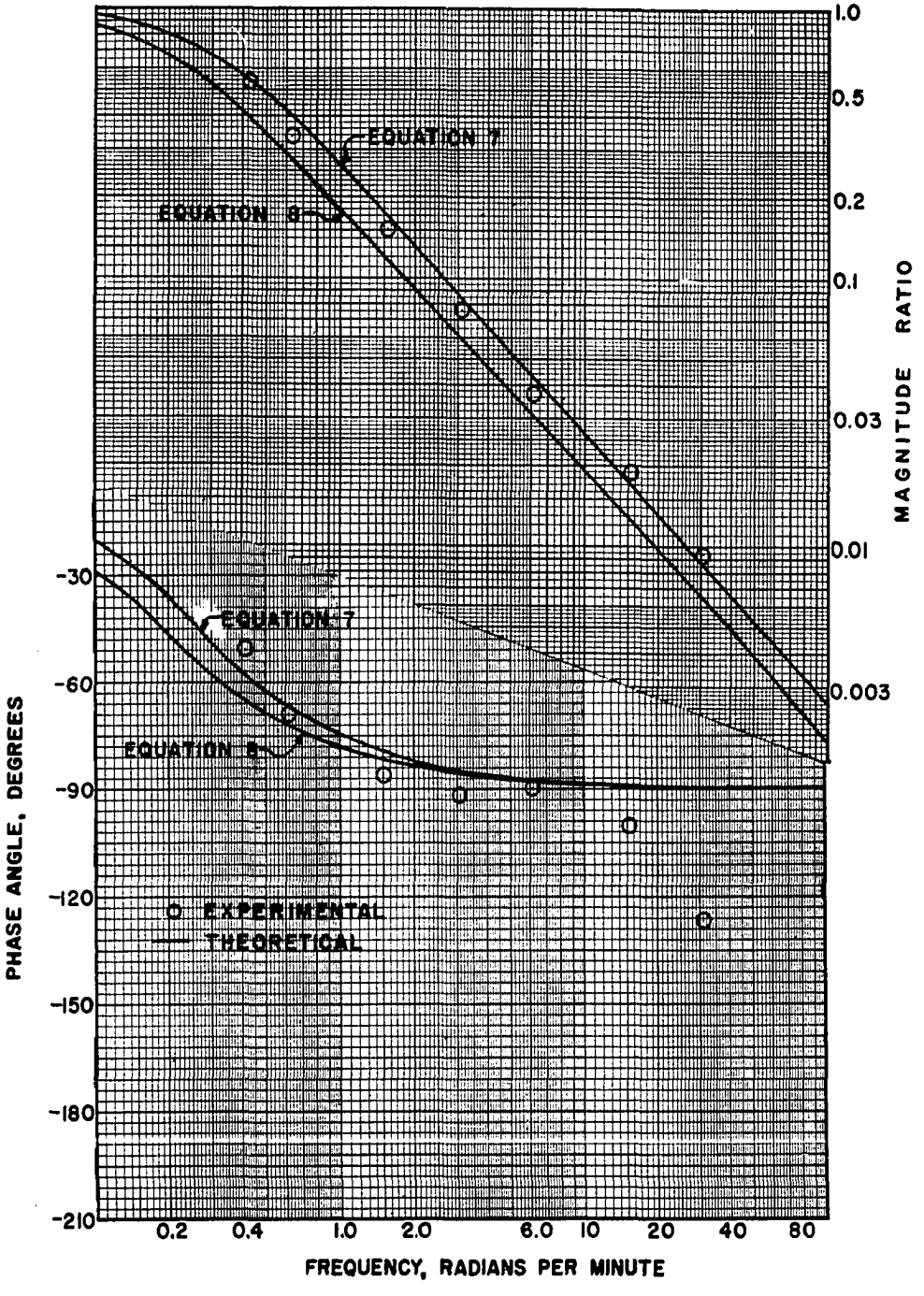


Figure 25 · Experimental and Theoretical Bode Diagrams, Arrangement Three, Oil

several orders of magnitude faster than any imposed frequency was realized. The chief point displayed by these particular response determinations is that the heat sink apparently does not act to any detectable extent as a phase lead contributor.

Equipment Arrangement Four

The transfer function in this arrangement is considerably more important than the first three both from a practical and a theoretical standpoint. It involves the dynamics of heat removal from a continuous agitated tank by manipulation of a coolant flow rate. Certain industrial control systems of tank reactors employ the same method for operation. Others control reactor temperatures by varying back pressure on a volatile coolant. In the past, most tank reactors have been of the jacketed type; however, there appears to be a trend toward cooling from an internal surface. It is therefore desirable to acquire as much information as possible relative to the dynamic characteristics of this type of process equipment. The specific objectives of this study include:

1. Determination of the effect on system dynamic response of fluid conditions both inside and outside the cooling coils.
2. Development of techniques for obtaining usable frequency response data from a non-linear process.
3. Provide recommendations regarding the derivation of theoretical transfer functions as applied to various operating conditions.

In order to determine the effect of tank fluid turbulence on

the process transfer function, frequency response runs were made at agitator speeds of 95, 200 and 350 RPM. Oil was selected as the process fluid because of its heavy, outside controlling film. The non-linear effect of equal but opposite changes in coolant flow rate on oil temperature was fully explained in Chapter V. Another of the several methods for illustrating this effect is shown in Figure 26. Initial and final cooling water temperatures are connected by a straight line. The lines are dotted because temperatures are not known at intermediate points throughout the coil. Parameters are percent of full meter flow together with steady state oil tank temperatures in parenthesis. Oil feed temperatures were 174 $\pm$ 1 F while feed rates were constant at 7.2 lbs./min. It is readily seen that at no range of coolant flow rate does equal but opposite increments of coolant rate cause equal changes in tank temperature.

In order to obtain an output wave approximately sinusoidal in nature, it was necessary to impress an input coolant wave of non-symetrical character. Good results were obtained by hand-generating a coolant wave of 20 - 40 - 70 plummet units. All the data were collected under the same operating conditions except for agitator speed. Equation VI-1 shows that the outside film coefficient h_o varies as the 0.67 power of the Reynolds number for mixing. The latter is of course directly proportional to the agitator speed. Agitator speeds were selected yielding theoretical film coefficients equal distances apart.

Figure 27 presents the experimental frequency response data. Output waves at the lowest speed were difficult to interpret because of minute drifts and distortions. No detectable response was noted beyond

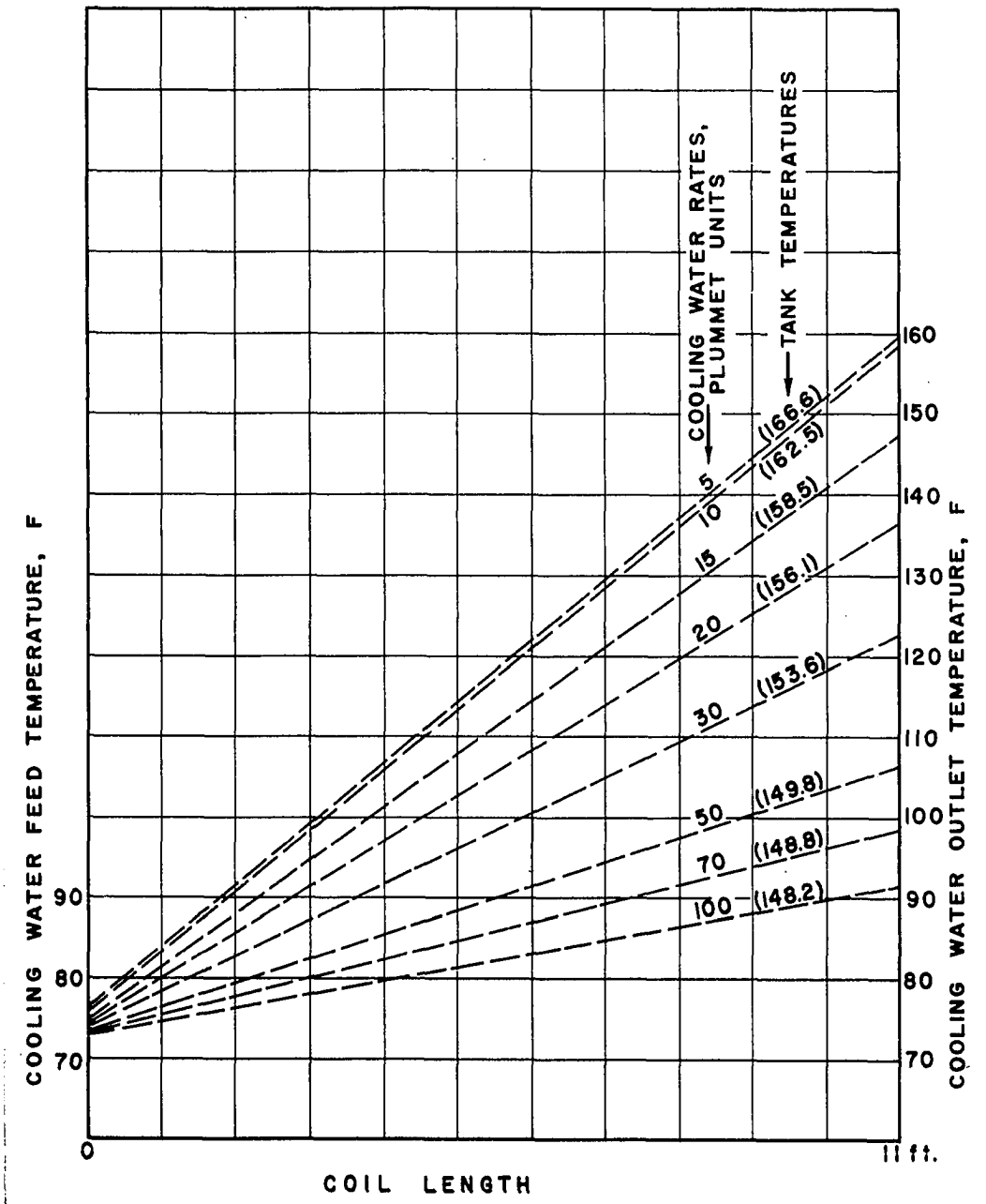


Figure 26 - Inlet and Outlet Cooling Water Temperature versus Coil Length

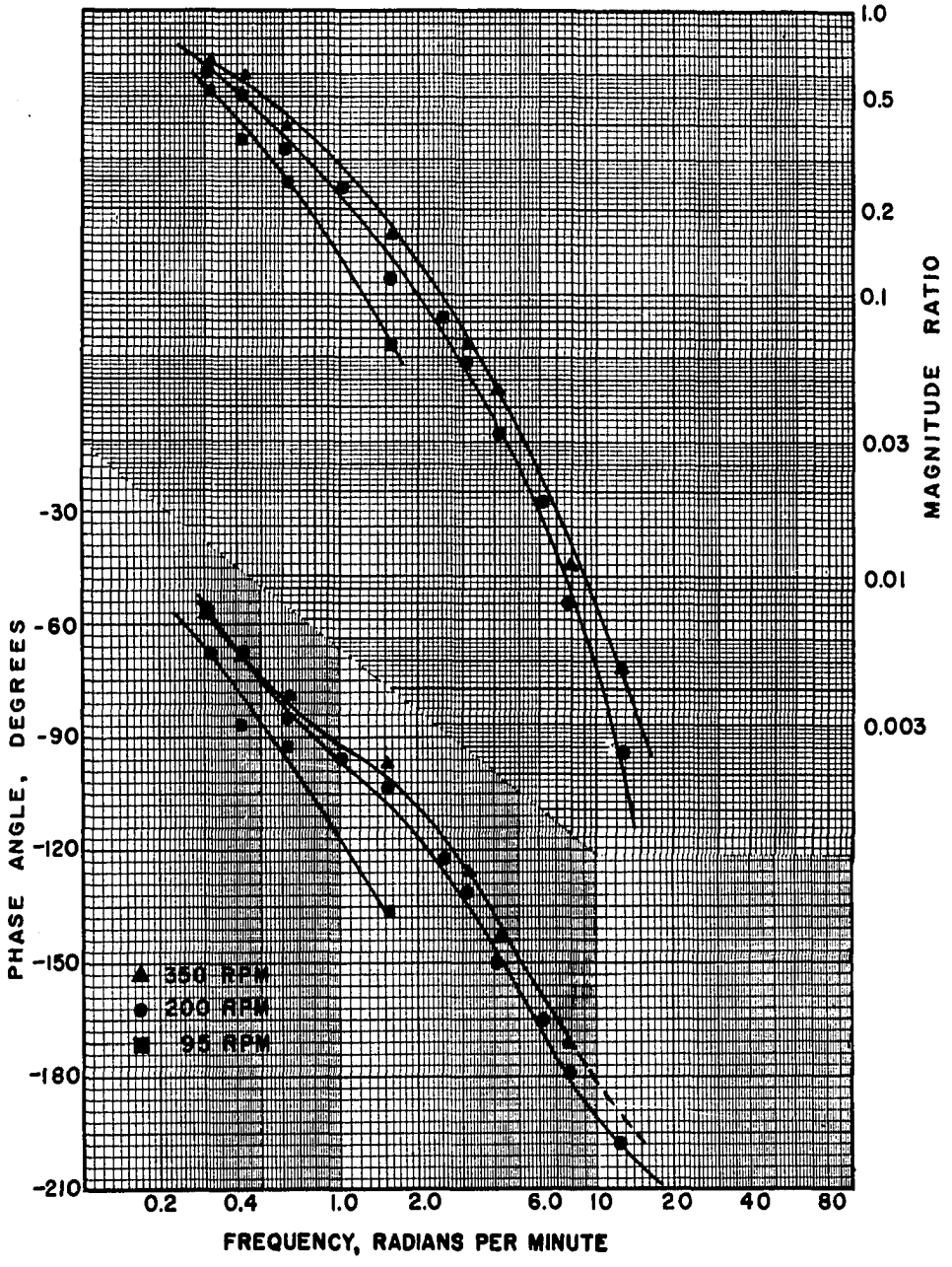


Figure 27 - Effect of Tank Fluid Conditions on Frequency Response Curves

a frequency of 1.57 radians per minute at the low speed. The data show that there is not a great deal of difference between response curves at the two higher speeds but that a sharp drop-off in system response may be expected at speeds lower than 180 RPM. This corresponds to a Reynolds number for mixing of approximately 2800 for the unit tested.

Two separate sets of frequency response data were taken in order to provide an insight into the effect on system response of different coolant flow conditions. Water was selected for testing as the process fluid so that the inner coolant film might have a proportionately greater influence on the overall heat transfer coefficient. Unfortunately, the data do not cover a wide enough range of coolant flow rates to provide complete information regarding this factor. One set of data was collected at a coolant flow range of 0.06 - 0.18 - 0.30 GPM for a minimum and maximum Reynolds number of 339 and 1690. This was classed as the laminar range although some turbulence no doubt existed at the wave peaks because of tube configuration. The other set of data were taken at a flow range of 0.36 - 0.48 - 0.60 GPM corresponding to minimum and maximum Reynolds numbers of 2025 and 3494 respectively. Fully turbulent flow probably existed over most of this range. At the flow rates listed, data could be taken with the same tank feed rate and temperature. The mean tank fluid temperature was about 15 degrees lower for the higher coolant flow rate.

Figure 28 indicates that the different rates tested have a relatively small but definite effect on the process transfer function. Points for turbulent flow consistently lie above those for the lower coolant flow rate. For a more viscous process fluid, the experimental

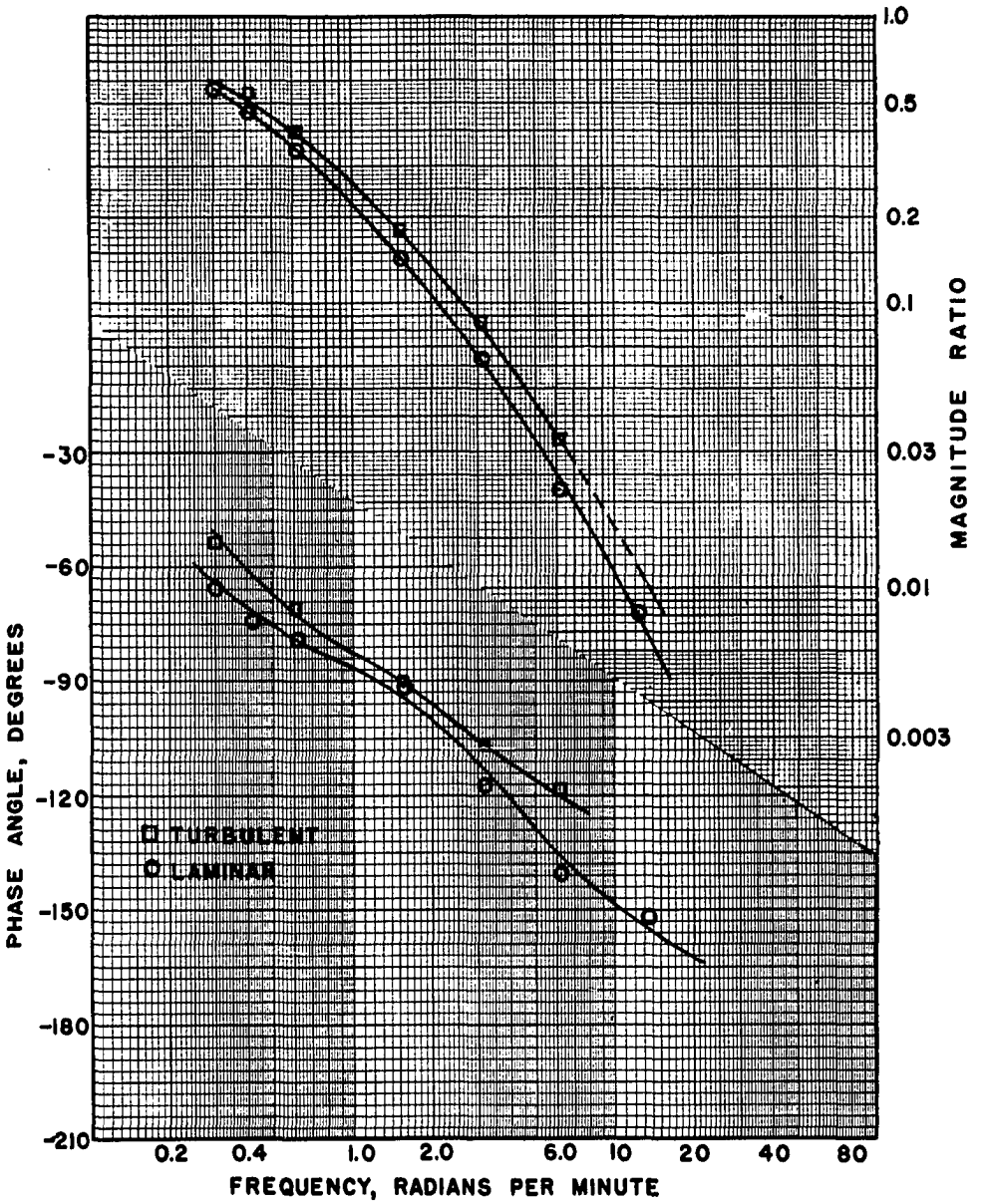


Figure 28 - Effect of Coolant Flow Conditions on Frequency Response Curves

points might be expected to lie closer together because of the lowered influence of the inner film on heat transfer rates. From this experimental work, it also might be postulated that the variation in the inner film coefficient over relatively small sinusoidal fluctuations in coolant flow rate would not be enough to introduce an error if such coefficients were treated as constants in a theoretical analysis.

The theoretical transfer functions describing process response for arrangement four have been derived in the preceding chapter. The second order response equation takes into account fluid capacitances only and employs an overall heat transfer coefficient U, calculated from steady state conditions. The third order expression considers coil capacitances and utilizes outer and inner coefficients of heat transfer. The latter is calculated by difference from the overall value and the outer coefficient. In all cases, heat transfer coefficients are treated as constants at those particular values calculated at mean steady state conditions. Substitution of the various constants into the derived equations yields the following numerical expressions for the theoretical transfer functions.

Transfer Function No.	Fluid	Composition
10.	Water	$\frac{\theta}{W_w}(j\omega) = \frac{165.0}{(j\omega)^2 + 23.7\ j\omega + 9.31}$
10.	Oil	$\frac{\theta}{W_w}(j\omega) = \frac{85.4}{(j\omega)^2 + 5.34\ j\omega + 1.153}$
11.	Water	$\frac{\theta}{W_w}(j\omega) = \frac{179.5}{0.0089(j\omega)^3 + 1.287(j\omega)^2 + 25.27j\omega + 1.09}$

Transfer Function No.	Fluid	Composition
11.	Oil	$\frac{\theta}{W_w}(j\omega) = \frac{86.8}{0.0336(j\omega)^3+1.381(j\omega)^2+ 5.54(j\omega)+ 1.77}$

All experimental data, including steady state parameters, gains, magnitude ratios and phase angles are included in Appendix C.

The theoretical curves are denoted by number in Figures 29 and 30. For both sets of theoretical attenuation curves, the loci do not differ appreciably up to a frequency of about ten radians per minute. Percentage divergence for oil is considerably greater than for water as frequencies are increased. Of interest is the shape of theoretical equation 11 when plotted as phase lag. All of the previous phase lag curves showed marked tendencies to level out asymptotically around -90 degrees before dropping thereby indicating a dominant first order response at the low and medium frequencies. Equation 11 for oil is practically a straight line up to a lag of -120 degrees. At this point, it curves downward and approaches a lag of -270 degrees asymptotically. Theoretical equation 10 phase lag curve for oil reacts in somewhat the same manner except for a slight leveling tendency at -90 degrees and a limiting phase angle of -180 degrees. With water as the process fluid, both theoretical curves show pronounced leveling tendencies at -90 degrees before continuing on to their respective limiting phase angles.

In order to help insure against misinterpretation caused by meager and widespread experimental data, about twice as many frequencies were tested as was normally the case. Response output waves were examined very carefully, especially for phase lag angles. This was because

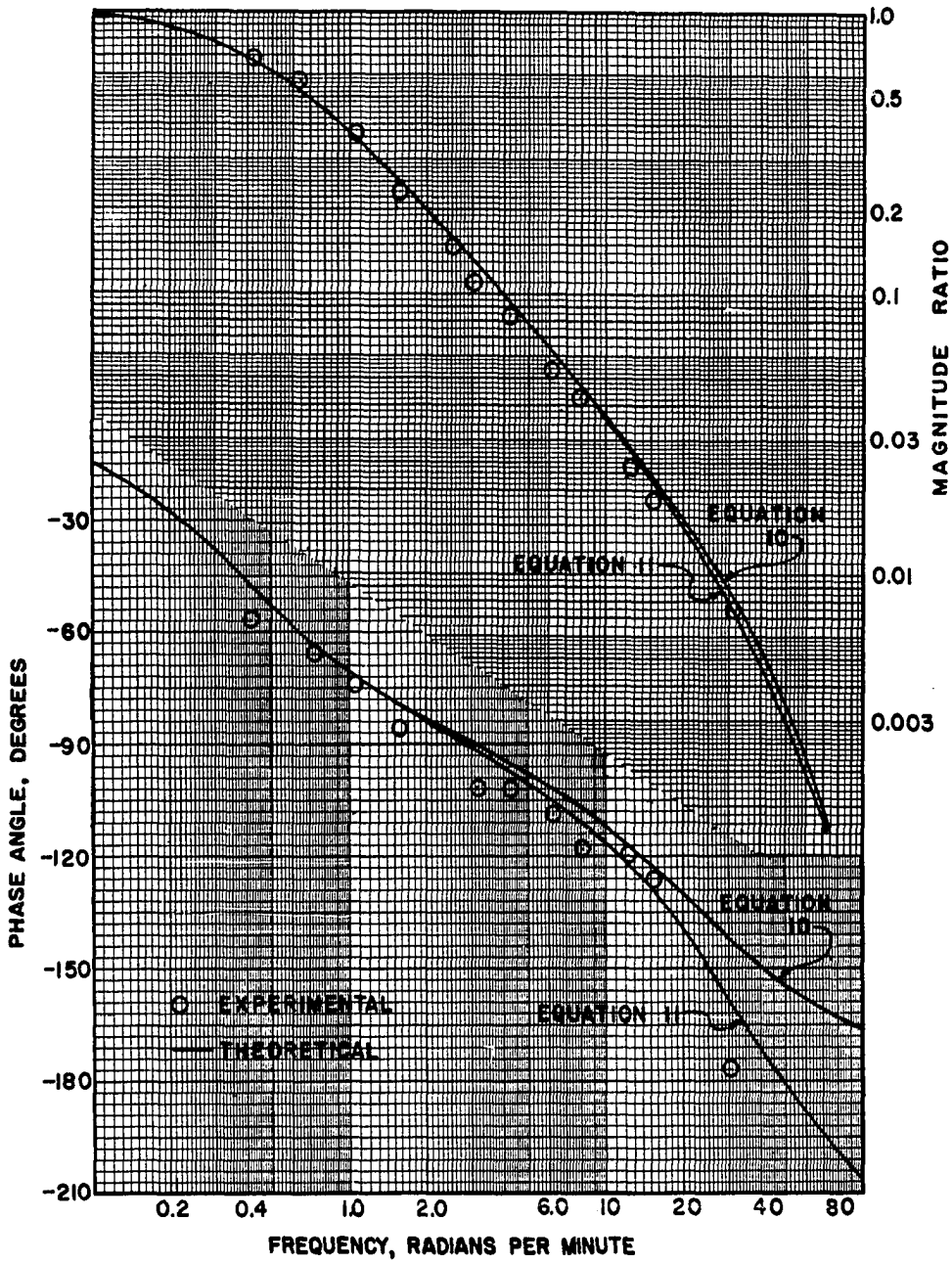


Figure 29 - Experimental and Theoretical Bode Diagrams, Arrangement Four, Water

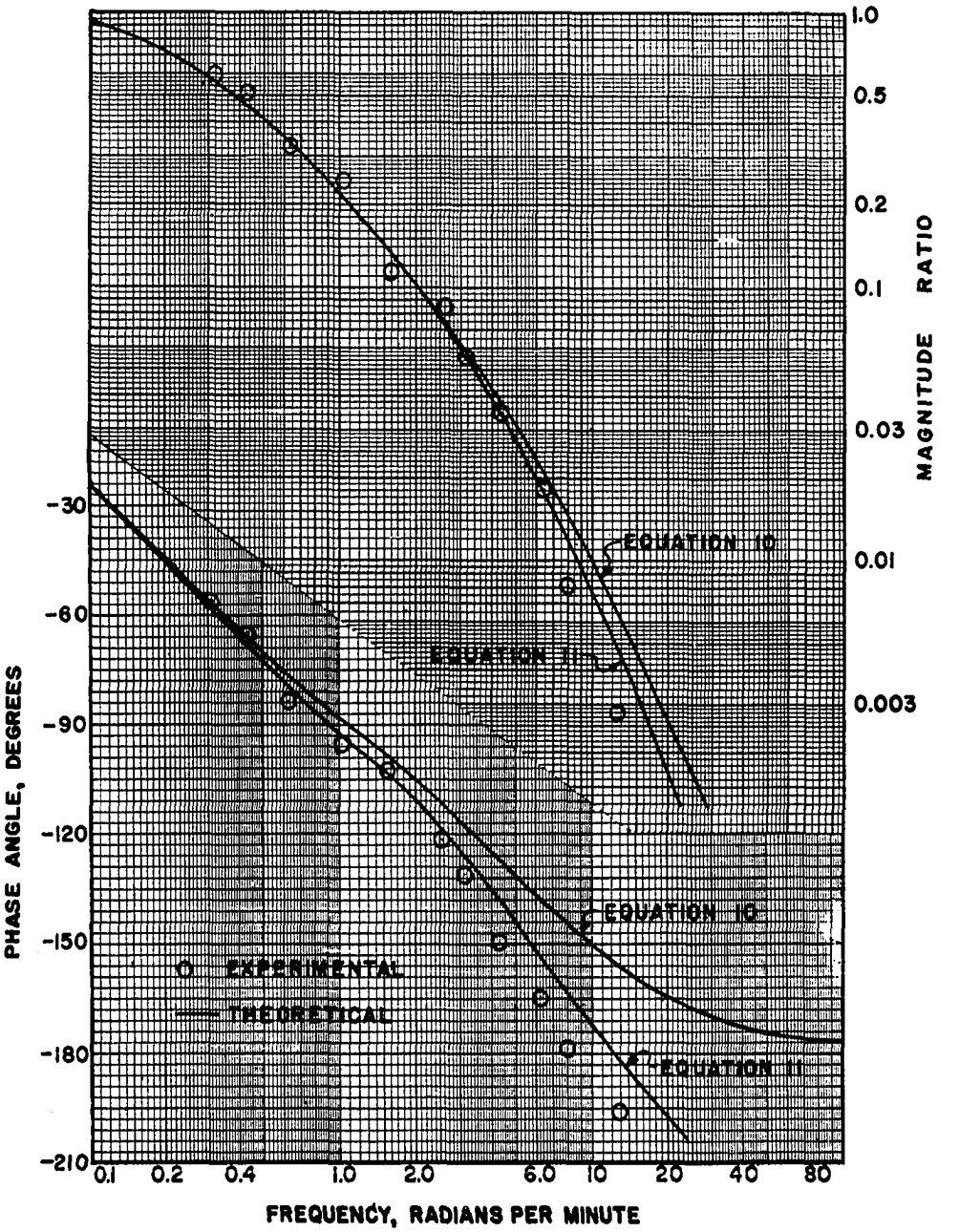


Figure 30 - Experimental and Theoretical Bode Diagrams, Arrangement Four, Oil

of the extreme importance of phase lag data and because of the sharper contrast in theoretical phase lag curves as compared with attenuation curves. The agreement between theory and experiment is quite satisfactory, especially for oil. From the theoretical and experimental investigation, it may be concluded that the response of tank fluid temperature to a change in coolant flow rate is definitely of higher order. Within limits of engineering accuracy, a second order transfer function represents the response for water over most of the frequency spectrum. However, for oil the third order expression is definitely recommended.

SUMMARY

A theoretical and experimental investigation has been made relative to the dynamic heat transfer characteristics of a continuous agitated tank reactor of 12-inch diameter. Dynamic response characteristics of the given equipment have been determined by transient and frequency response techniques. Data were taken for four different equipment arrangements in which fluids of widely varying physical properties were charged. A total of eleven different theoretical transfer functions have been developed and comparisons made with experimental data.

Sine Wave Generator

A relatively simple mechanical device was designed for the purpose of imparting a sinusoidal wave of flow to certain input variables. The key components of this unit are a variable speed Scotch yoke drive attached atop a linear diaphragm control valve. Careful experimental checking of the input wave indicated that a near-perfect sinusoid of input flow is imparted by the mechanical sine wave generator. Such a generator was employed throughout a large portion of the experimental frequency response determinations. In some cases, however, periodic wave motion was obtained manually by manipulation of a needle valve.

Variation of Equipment Response with Fluids Charged

For all equipment arrangements, duplicate runs were made with fluids of unlike physical properties. Experimental results vividly demonstrate the sharp contrast in process response characteristics with the different fluids tested. This is illustrated quantitatively by Figure 19. From the standpoint of reactor heat exchange, process dynamics will vary significantly with physical properties of the fluids processed. Such variations must be taken into account in writing theoretical process transfer functions.

Secondary Lags

The comparison of experiment with theory in Arrangement Two has demonstrated that certain small secondary lags may react in such a manner as to have appreciable effect on attenuation and phase lag curves at the higher frequencies. In this particular case, transfer of heat through the small metal capacitances of transfer coils and a thermocouple well is sufficient to cause definite response effects at frequencies of 5 to 10 radians per minute or higher. Again, fluid properties dictate the manner and frequencies at which such lags become significant.

Phase Lead Effect of Tank Walls

Concentrated experimental effort was devoted to a determination of reactor wall phase lead effect. Theoretical transfer functions 4, 5, 8, and 9 exhibit phase lead characteristics. A comparison of equations 5 and 8 with experimental results indicates that for relatively small process upsets around the operating point, any reactor tank wall phase lead effect is so small as to be insignificant at all frequencies tested.

Tank Fluid Conditions

An approximate general rule was experimentally established relative to the effect of reactor tank fluid conditions on the dynamic response of this equipment type. A pictorial illustration is best afforded by inspection of Figure 27. For the process conditions under study, the effect of fluid turbulence on system dynamics is significant at Reynolds numbers for mixing below 2800. Above this figure, system response increases slowly with an increase in the mixing Reynolds number. The point at which a further increase in the Reynolds number ceased to effect equipment response was not established.

Coolant Fluid Flow Conditions

Figure 28 illustrates the effect of dynamic response on coolant fluid flow conditions for Arrangement Four. All process parameters except coolant flow rates were held constant. An attempt was made to obtain response data at definite conditions of laminar and turbulent coolant flow. Even with these unlike flow types, the response curves were similar, with somewhat faster response, of course, being realized by turbulent coolant flow. Differences in response characteristics for various levels of coolant turbulence may then be assumed to be very slight.

Recommended Theoretical Transfer Functions Describing the Dynamics of Reactor Heat Removal

The manner and rate of change in tank temperature brought about by a change in coolant flow rate was the subject of intensive study. With oil as the process fluid, system response was significantly

non-linear. In order to obtain an output wave amenable to interpretation, frequency response determinations were completed using inputs which were not precisely sinusoidal in nature. Good checks between experiment and theory were nevertheless obtained. With water as the process fluid, a second order transfer function is in suitable agreement with the data. The equation considers only fluid capacitances and utilizes an overall film coefficient of heat transfer. The theoretical expression is:

$$\frac{\theta}{W_w}(j\omega) = \frac{2K_7/T_{16}}{(j\omega)^2 + \left[\frac{T_{15} + T_{17}}{T_{15}T_{17}}\right] j\omega + \frac{1}{T_{15}T_{17}} - \frac{1}{T_{14}T_{16}}} \qquad \text{VII-1}$$

With oil as the process fluid, a more complicated expression was necessary in order to bring theory and experiment within satisfactory agreement. In so doing, it was found that the outside film coefficient as obtained from the correlation of Oldshue and Gretton was suitable under dynamical conditions. Coil capacitance was considered in this derivation in addition to tank fluid and coolant capacitances. Theoretical results are:

$$\frac{\theta}{W_w}(j\omega) = \frac{2K_9K_{10}/T_{23}}{I(j\omega)^3 + J(j\omega)^2 + L(j\omega) + M} \qquad \text{VII-2}$$

The coefficients are functions of several time constants and are defined on page 73. The above theoretical transfer function fits the experimental results very satisfactorily for both fluids. It must be used to represent system response during the charging of oil since the data indicate experimental phase lags in excess of 180 degrees.

BIBLIOGRAPHY

1. Bechtol, I. C, Petroleum Refiner, 36, 132 (1957)

2. Berger, D. E. and Campbell, G. G., Chem. Eng. Prog. 51, 348 (1955)

3. Berger, D. E. and Short, G. R., Ind. Eng. Chem. 48, 1027 (1956)

4. Bilous, O., Block, H. D. and Piret, E. L., Am. Inst. Chem. Eng. 2, 249 (1957)

5. Brown, G. S. and Campbell, D. P., Principles of Servomechanisms, John Wiley and Sons, New York (1948)

6. Campbell, D. P., Ind. Eng. Chem. 47, 409 (1955)

7. Catheron, A. R. and Hainsworth, B. D., Ind. Eng. Chem. 48, 1042 (1956)

8. Ceaglske, N. H., Automatic Control for Chemical Engineers, John Wiley and Sons, New York (1956)

9. Ceaglske, N. H, and Eckman, D. P., Ind. Eng. Chem. 45, 1879 (1953)

10. Chilton, T. H., Drew, T. B., and Jebens, R. H., Ind. Eng. Chem. 36, 510 (1944)

11. Chestnut, H. and Mayer, R. W., Servomechanisms and Regulating System Design, Vol. 1., John Wiley and Sons, New York (1951)

12. Cohen, W. C. and Johnson, E. F., Ind. Eng. Chem. 48, 1031 (1956)

13. Cummings, C. H. and West, A. S., Ibid, 42, 2303 (1950)

14. Dunlap, I. R. and Rushton, J. H., Chem. Eng. Prog. Symposium Series, 49, 5 (1953)

15. Eckman, D. P. and Moise, J. C., Ind. Eng. Chem. 45, 1879 (1953)

16. Franks, R. G. and Worley, G. W., Ibid, 48, 1074 (1956)

17. Hass, R. H. and Saver, P. J., Ind. Eng. Chem. 47, 398 (1955)

18. Isakoff, S. E., Ibid. 47, 413 (1955)

19. Johnson, E. F., Ibid. 43, 2708 (1951)

20. Johnson, E. F., Ibid. 47, 396 (1955)

21. Johnson, E. F. Chem. Eng. Prog. 51, 353 (1955)

22. Johnson, E. F. and Bey, T., Ind. Eng. Chem. 47, 403 (1955)

23. LaJoy, M. H., Industrial Automatic Controls, Prentice Hall, New York, (1954)

24. Laspe, C. G. in Automation in Business and Industry, Editor, Grabbe, E. M., John Wiley and Sons, New York, (1957)

25. Lees, S., and Hougen, J. O., Ind. Eng. Chem. 48, 1064, (1956)

26. Levenstein, H., Control Engineering, 4, 90 (1957)

27. Mason, C. E., Trans. Am. Soc. Mech. Eng. 60, 327 (1938)

28. McKnight, C. W. and Worley, G. W., Nat. Instr. Soc. Am., Paper 53-6-1 (1953)

29. Minneapolis Honeywell, Brown Inst. Div., Bulletin 1170.

30. Mozley, J. M., Ind. Eng. Chem. 48, 1035 (1956)

31. Nixon, F. E., Principles of Automatic Controls, Prentice Hall, New York (1953)

32. Oldshue, J. Y., and Gretton, A. T., Chem. Eng. Prog. 50, 615 (1954)

33. Powell, B. E., Control Engineering, 4, 101 (1957)

34. Reswick, J. B., Control Engineering, 2, 50 (1955)

35. Stanton, B. D. and Hoyt, P. R., Texas A. and M. Symposium on Instrumentation, Jan. (1953)

36. St. Clair, P. W., Erath, L. W., and Gillespie, S. L., Trans. Am. Soc. Mech. Eng. 76, 1177 (1954)

37. Takahashi, Y. in Automatic and Manual Control, Academic Press, New York, (1952)

38. Thaler, G. J. and Brown, R. G., Servomechanism Analysis, McGraw-Hill, New York (1953)

39. Vannah, W. E. and Slater, L. E., Ind. Eng. Chem. 48, 1000 (1956)

40. Velguth, F. W. and Anderson, R. C., Nat. Instr. Soc. Am. Paper 53-6-3 (1953)

41. Wilks, P. A., Chem. Eng. Prog. 52, 357 (1955)

42. Wilhelm, R. H., Johnson, W. C., Wynkoop, R., and Collier, D. W., Ibid. 44, 105 (1948)

43. Williams, T. J., Petroleum Refiner 35, 211 (1956)

44. Williams, T. J., and Rose, A., Ind. Eng. Chem. 47, 2284 (1955)

45. Williams, T. J., Harnett, R. T., and Rose, A., Ind. Eng. Chem. 48, 1008 (1956)

46. Williams, T. J. and Harnett, R. T., Chem. Eng. Prog. 53, 220 (1957)

47. Williams, T. J. and Young, J. M., Petroleum Refiner, 36, 229 (1957)

48. Zoss, L. M., Gollin, N. W. and Edelman, R. I., Ind. Eng. Chem. 48, 1069 (1956)

49. Aris, R. and Amundson, N. R., Chem. Eng. Prog. 53, 227 (1957)

50. Young, A. J., An Introduction to Process Control System Design, Longmans, Green and Co., London. (1955)

APPENDIX A

Nomenclature

Individual Symbols

A = Surface Area, Ft.^{2}

C = Heat Capacitance, B.T.U./^oF

c_p = Specific Heat, B.T.U./(lb.)(^oF)

d = Tube diameter, Ft.

D = Impeller diameter, Ft.

F = Frequency, cycles/minute

h = Individual heat transfer coefficient, B.T.U./(Min.)(ft.^{2})(F)

j = $\sqrt{-1}$

k = Thermal conductivity, B.T.U./(Min.)(ft.^{2})(^oF/ft.)

K_1 = Proportional mode controller constant

K_2 = Derivative mode controller constant

K = Control element gain

K_r = Process gain

K_t = Measuring element gain

$L[f(t)]$ = Laplace transform of given function

M = Magnitude ratio, mass in pounds

N = Agitator speed, RPS

s = Laplace transorm complex variable

T = Time constant, minutes

t = Time, minutes and tank diameter, ft.

U = Overall heat transfer coefficient, B.T.U./(Min.)(ft.^{2})(F)

V = Cooling water velocity, Ft./sec.

W = Fluid flow rate, lb./min.

Δ = Small change of process variable around a steady state

θ = Temperature, F

ω = Frequency, radians/minute

ϕ = Phase angle, degrees

ρ = Density, lbs./ft.^{3}

μ = Viscosity, B.V.U.

Subscripts

a = Average area

c = Coils

f = Process fluid

i = Inside area

o = Outside area

r = Thermocouple well

s = Steam

t = Tank

w = Cooling water

w_i = Cooling water in

w_o = Cooling water out

Time Constants and Ratios of Time Constants

Constant	Composition	Constant	Composition
T_1	$\frac{C_c}{h_s A_s}$	$\frac{1}{T_{11}}$	$\frac{1}{T_3} + \frac{1}{T_6} + \frac{1}{T_9}$
T_2	$\frac{C_c}{h_f A_f}$	T_{12}	$\frac{A_o c_p \rho}{U \pi d}$
T_3	$\frac{C_c}{h_f A_f}$	T_{13}	$\frac{C_w}{\bar{W}_w c_p}$
T_4	$\frac{C_f}{h_t A_t}$	T_{14}	$\frac{C_w}{U A_a}$
T_5	$\frac{C_f}{W_f c_p}$	$\frac{1}{T_{15}}$	$\frac{2}{T_{13}} + \frac{1}{T_{14}}$
T_6	$\frac{C_t}{h_t A_t}$	T_{16}	$\frac{C_f}{U A_a}$
$\frac{1}{T_7}$	$\frac{1}{T_1} + \frac{1}{T_2}$	$\frac{1}{T_{17}}$	$\frac{1}{T_5} + \frac{1}{T_{16}}$
$\frac{1}{T_8}$	$\frac{1}{T_3} + \frac{1}{T_4} + \frac{1}{T_5}$	T_{18}	$\frac{C_w}{h_i A_i}$
T_9	$\frac{C_f}{h_r A_r}$	$\frac{1}{T_{19}}$	$\frac{2}{T_{13}} + \frac{1}{T_{18}}$
T_{10}	$\frac{C_r}{h_r A_r}$	T_{20}	$\frac{C_c}{h_o A_o}$

Time Constants and Ratios of Time Constants - Continued

Constant	Composition	Constant	Composition
T_{21}	$\frac{C_c}{h_1 A_1}$	K_4	$\frac{T_8}{T_4}$
$\frac{1}{T_{22}}$	$\frac{1}{T_{20}} + \frac{1}{T_{21}}$	K_5	$\frac{T_{11}}{T_9}$
T_{23}	$\frac{C_f}{h_o A_o}$	K_6	$\frac{T_{11}}{T_3}$
$\frac{1}{T_{24}}$	$\frac{1}{T_5} + \frac{1}{T_{23}}$	K_7	$\frac{\theta_{w_i} c_p}{C_w}$
$\frac{1}{T_{25}}$	$\frac{1}{T_3} + \frac{1}{T_5} + \frac{1}{T_{14}}$	K_8	$\frac{T_{22}}{T_{20}}$
$\frac{1}{T_{26}}$	$\frac{1}{T_2} + \frac{1}{T_{21}}$	K_9	$\frac{T_{22}}{T_{21}}$
$\frac{1}{T_{27}}$	$\frac{1}{T_5} + \frac{1}{T_{16}}$	K_{10}	$\frac{c_p \theta_f}{c_p W_f + h_f A_f}$
K_1	$\frac{T_7}{T_1}$	K_{11}	$\frac{\theta_f c_p}{C_f}$
K_2	$\frac{T_7}{T_2}$	K_{12}	$\frac{\theta_{w_i} c_p}{C_w}$
K_3	$\frac{T_8}{T_3}$		

APPENDIX B

Equipment Calibration Data

TABLE 9

Calibration Data for Water-Series 1700, 6.66 GPM
Fischer Porter Flowrator

Plummet Reading	Fluid Charged, lbs.	Fluid Temperature, °F	Avg. Time, Min.	Avg. Rate lbs./min.
8	55	96.7	11.778	4.63
10	55	77.2	9.626	5.71
15	55	78.0	7.735	8.12
20	55	78.0	5.113	10.76
30	110	78.7	6.825	16.17
40	110	79.0	5.090	21.54
50	110	79.0	4.733	27.07
60	110	79.0	3.394	32.39
70	110	79.0	2.893	38.11
80	110	79.2	2.506	43.96

TABLE 10

Calibration Data for Water-Series 1700, 6.6 GPM
Fischer Porter Flowrator

Plummet Reading	Fluid Charged, lbs.	Fluid Temperature, °F	Avg. Time, Min.	Avg. Rate lbs./min.
8	50	170.2	11.112	4.48
10	50	169.0	8.991	5.58
15	60	171.0	7.538	7.79
20	60	170.5	5.660	10.61
25	60	169.0	4.559	13.18
30	80	169.0	5.053	15.84
35	80	170.0	4.313	18.58
40	80	170.0	3.784	21.13

TABLE 11

Calibration Data for Oil-Series 1700, 6.6 GPM
Fischer Porter Flowrator

Plummet Reading	Fluid Charged, lbs.	Fluid Temperature, °F	Avg. Time, Min.	Avg. Rate lbs./min.
8	25	87	11.327	2.21
10	25	85	7.657	3.26
15	25	83	3.927	6.37
20	30	83	3.128	9.59
25	60	83	4.802	12.49
30	70	83	4.637	15.10
40	70	83	3.403	20.57
50	70	83	2.813	24.88
8	25	107.7	7.848	3.19
10	40	107.1	7.894	5.07
15	50	107.0	6.223	8.04
20	55	107.1	5.108	10.77
25	60	107.0	4.525	13.26
30	70	107.0	4.458	15.70
40	70	107.0	3.377	20.73
50	70	107.0	2.743	25.52

TABLE 12

Calibration Data for Oil-Series 1700, 6.6 GPM
Fischer Portor Flowrator

Plummet Reading	Fluid Charged, lbs.	Fluid Temperature, °F	Avg. Time, Min.	Avg. Rate lbs./min.
8	25	120.7	6.377	3.92
10	40	120.3	7.413	5.40
15	40	120.0	4.872	8.21
20	50	120.0	4.633	10.79
25	60	120.6	4.513	13.29
30	70	120.2	4.433	15.79
40	70	120.7	3.383	20.69
50	70	120.2	2.727	25.67
8	25	139.0	5.732	4.36
10	40	139.5	7.153	5.59
15	40	139.8	4.880	8.20
20	50	139.0	4.636	10.78
25	60	138.3	4.533	13.24
30	70	139.2	4.452	15.72
40	70	139.2	3.390	20.65
50	70	139.5	2.713	25.80

TABLE 13

Calibration Data for Bristol Recording Potentiometer

Tank Fluid Temp. °F	Avg. Strip Cht. Reading, Cht. Divs.	Tank Fluid Temp. °F	Avg. Strip Cht. Reading, Cht. Divs.
120	0	120	0
130	24.31	130	24.25
140	49.00	140	49.92
150	74.32	150	72.43
160	99.13	160	96.40

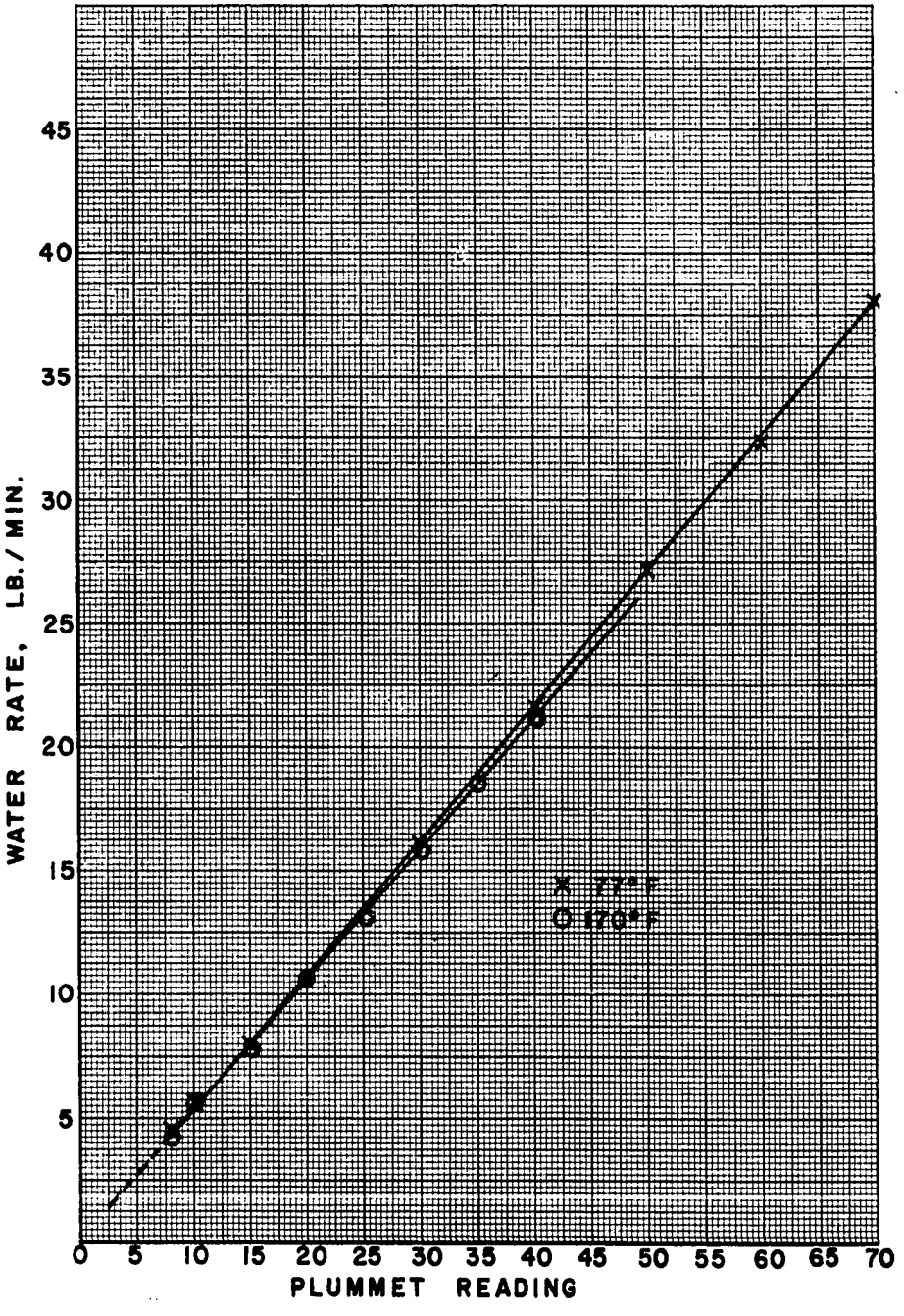


Figure 31 - Calibration Curves on Fischer Porter Flowrator for Various Temperatures

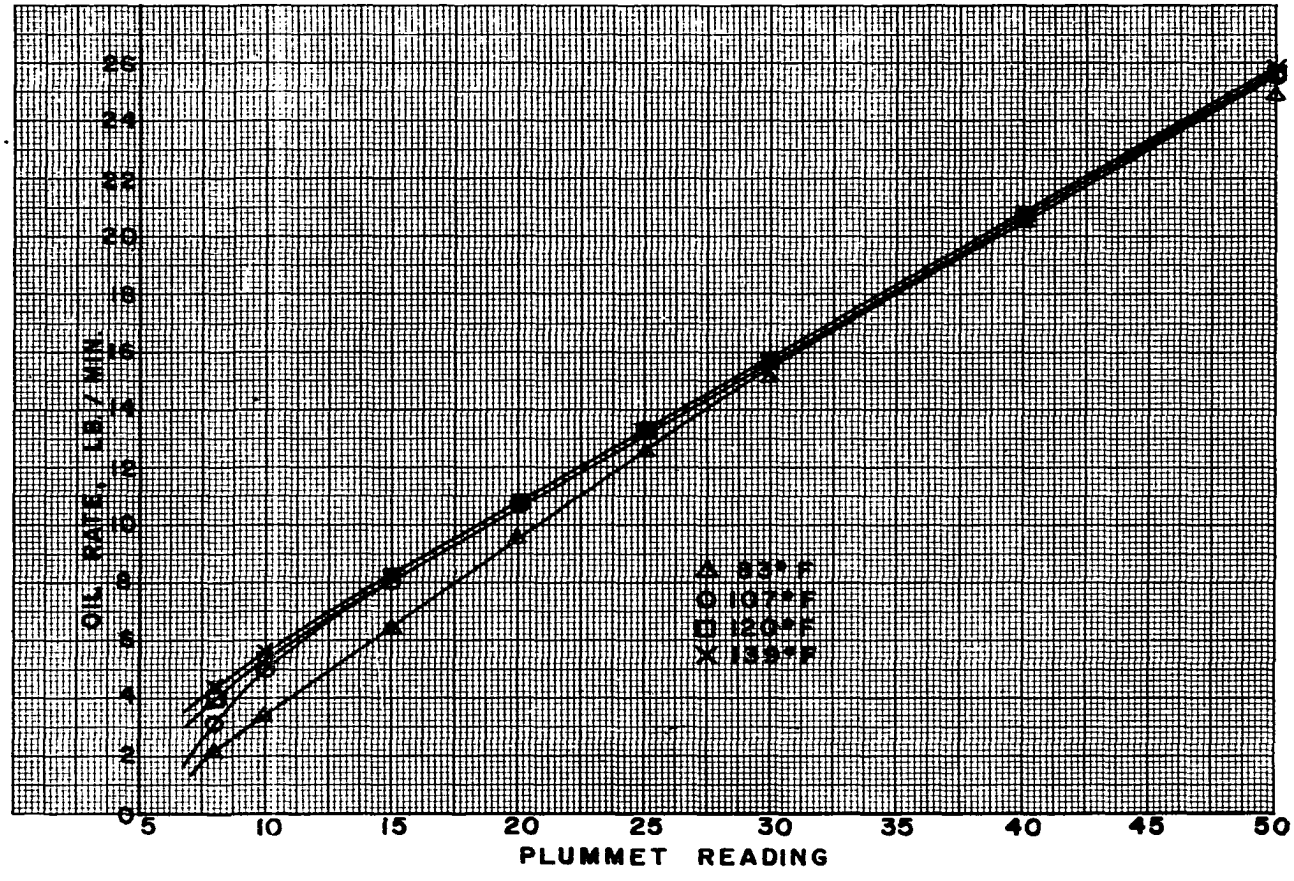


Figure 32 - Calibration Curves on Fischer Porter Flowrator for Oil at Various Temperatures

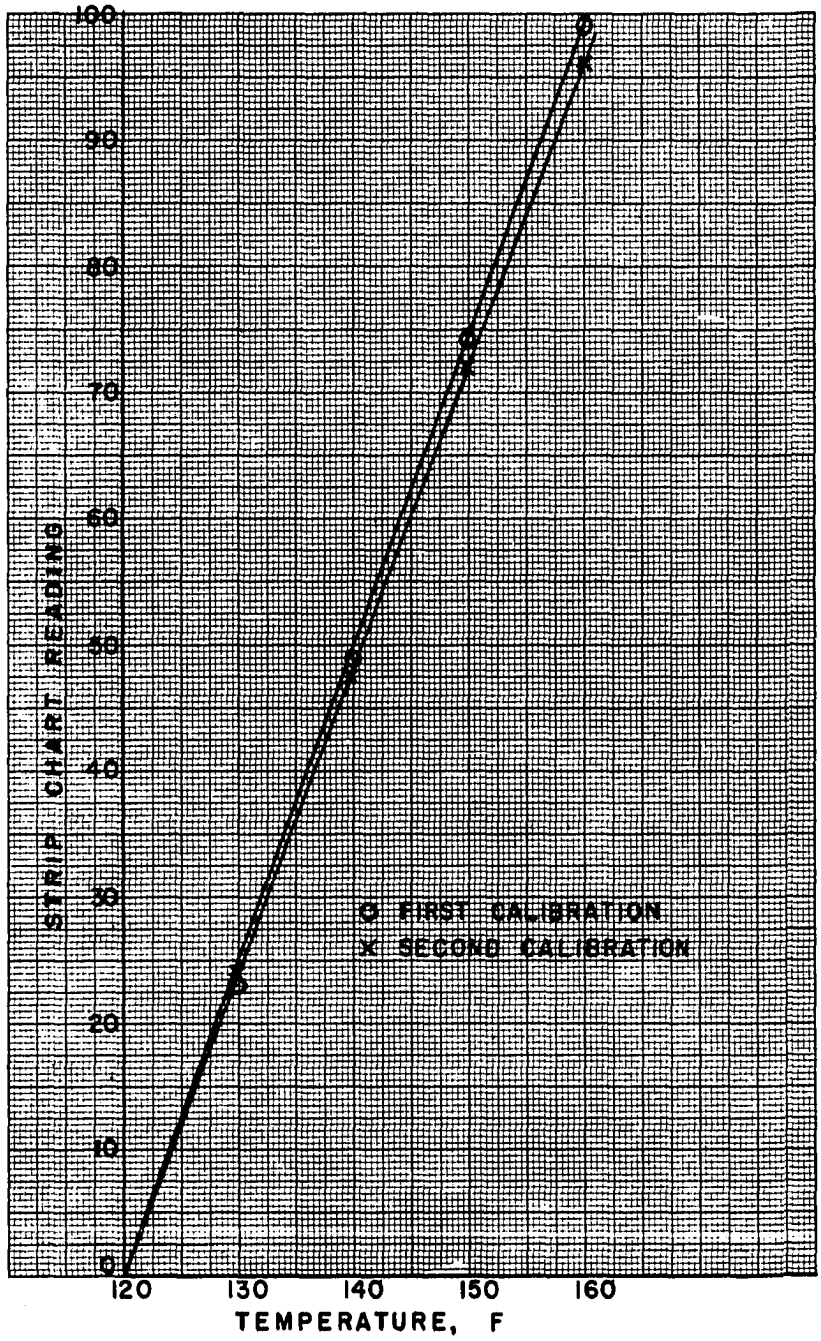


Figure 33 - Calibration Curve for Bristol Continuous Recording Potentiometer

APPENDIX C

Dynamic Response Data

TABLE 14

Steady State Conditions for Equipment Arrangement One
Fluid Feed Rate Forcing
Process Fluid-Water

Run No.	Radians / Minute	Water Feed, °F, θ_f	θ	Steam Pressure, Psig, Header	Reducer	Tank
A-33	31.4	77.0	142	44	44	1.5
A-34	15.7	76.2	139.5	44	44	1.5
A-35	6.28	78.0	140.5	45	42	1.5
A-36	3.14	77.8	141.3	48	43	1.5
A-37	1.57	78.0	139.5	46	43	1.5
A-38	0.628	78.8	140.0	44	40	1.5

Parameters: Feed Rate, Steady State: 13.51 $\frac{\text{lb.}}{\text{min.}}$

Feed Rate Forcing Range: 8.0 - 13.51 - 19.0 $\frac{\text{lb.}}{\text{min.}}$

Agitator RPM: 200

TABLE 15

Processed Frequency Response Data, Equipment Arrangement One
Fluid Feed Rate Forcing
Process Fluid-Water

Run No.	Radians / Minute	Steady State Gain, Chart Divs.	°F	Average Amplitude, Chart Divs.	°F	Magnitude Ratio	Phase Angle, Degrees
A-33	31.4	54.0	24.0	2.41	1.07	0.0445	-135
A-34	15.7	54.0	24.0	3.47	1.54	0.064	-102.7
A-35	6.28	54.0	24.0	5.94	2.64	0.110	- 90
A-36	3.12	54.0	24.0	11.14	4.95	0.206	- 77
A-37	1.57	54.0	24.0	22.9	10.15	0.423	- 69.4
A-38	0.628	54.0	24.0	42.8	19.00	0.792	- 63.1

TABLE 16

Steady State Conditions for Equipment Arrangement One
Fluid Feed Rate Forcing
Process Fluid - Oil

Run No.	Radians / Minute	Water Feed, °F θ_f	Water Feed, °F θ	Steam Pressure, Psig, Header	Steam Pressure, Psig, Reducer	Steam Pressure, Psig, Tank
B-7	31.4	100.6	131.1	69	45	1.5
B-8	15.7	100.6	131.0	69	45	1.5
B-9	6.28	102.0	131.0	69	45	1.5
B-10	3.14	101.0	131.1	69	45	1.5
B-11	1.57	100.0	131.0	69	45	1.5
B-12A	0.628	102.0	134.0	60	43	1.5
B-13	0.413	100.0	134.1	57	43	1.5

Parameters: Feed Rate, Steady State: 10.5 lb./min.

Feed Rate Forcing Range: Variable, approx.

7.2 - 10.5 - 13.8 lb./min.

Agitator RPM: 200

TABLE 17

Processed Frequency Response Data, Equipment Arrangement One
Fluid Feed Rate Forcing
Process Fluid-Oil

Run No.	Radians / Minute	Steady State Gain, Chart Divs.	Steady State Gain, °F	Average Amplitude, Chart Divs.	Average Amplitude, °F	Magnitude Ratio	Phase Angle, Degrees
B-7	31.4	29.2	13.0	0.10	0.044	0.0034	
B-8	15.7	29.2	13.0	0.40	0.178	0.0137	
B-9	6.28	30.4	13.5	0.95	0.422	0.0312	
B-10	3.14	31.7	14.1	3.44	1.53	0.109	-120
B-11	1.57	31.7	14.1	5.61	2.49	0.177	-98
B-12A	0.628	30.4	13.5	17.7	7.85	0.587	-77
B-13	0.413	30.4	13.5	20.8	9.25	0.686	-54.7

TABLE 18

Steady State Conditions for Equipment Arrangement Two
Steam Pressure Forcing
Process Fluid-Water

Run No.	Radians / Minute	Water Feed, °F θ_f	Water Feed, °F θ	Steam Pressure, Psig, Reducer	Steam Pressure, Psig, Tank
A-39	0.421	77.6	151.8	53	6
A-40	0.628	77.5	151.8	49	6
A-41	1.570	77.8	151.8	47	6
A-42	3.14	78.0	152.1	45	6
A-43	6.28	78.1	151.5	46	6
A-46	15.70	78.0	151.0	58	8.2
A-47	31.40	78.0	151.0	58	8.2

Parameters: Feed Rate, Steady State: 13.51 lb./min.

Steam Pressure Forcing Range: Variable,
Avg. of 2-6-10 Psig

Agitator RPM: 200

TABLE 19

Processed Frequency Response Data, Equipment Arrangement Two
Steam Pressure Forcing
Process Fluid-Water

Run No.	Radians / Minute	Steady State Gain, Chart Divs.	Steady State Gain, °F	Average Amplitude, Chart Divs.	Average Amplitude, °F	Magnitude Ratio	Phase Angle, Degrees
A-39	0.421	25.91	11.51	30.1	13.4	0.859	-42
A-40	0.628	20.89	9.28	30.1	13.4	0.692	-54
A-41	1.57	9.46	4.21	30.1	13.4	0.314	-71
A-42	3.12	4.79	2.13	30.1	13.4	0.159	-91
A-43	6.28	4.07	1.81	37.8	16.8	0.107	-91
A-46	15.7	2.96	1.27	54.0	24.0	0.0528	-103
A-47	31.4	1.70	0.754	54.0	24.0	0.0314	-121

TABLE 20

Steady State Conditions for Equipment Arrangement Two
Steam Pressure Forcing
Process Fluid-Oil

Run No.	Radians / Minute	Oil Feed, °F θ_f	Oil Feed, °F θ	Steam Pressure, Psig, Reducer	Steam Pressure, Psig, Tank
B-14	31.4	102.0	143.3	30	10.2
B-15	15.70	101.8	142.2	30	8.9
B-16	6.28	99.0	140.5	30	8.9
B-17	3.14	100.0	140.9	30	10
B-18	1.57	100.2	144.3	33	10
B-19	0.628	101.0	142.8	33	10
B-20	0.421	100.5	142.6	33	10

Parameters: Feed Rate, Steady State: 10.6 lb./min.

Steam Pressure Forcing Range: Variable,
Avg. of 3-10-17 Psig

Agitator RPM: 200

TABLE 21

Processed Frequency Response Data, Equipment Arrangement Two
Steam Pressure Forcing
Process Fluid - Oil

Run No.	Radians / Minute	Steady State Gain, Chart Divs.	Steady State Gain, °F	Average Amplitude, Chart Divs.	Average Amplitude, °F	Magnitude Ratio	Phase Angle, Degrees
B-14	31.4	12.6	5.6	0.10	0.0444	0.00794	
B-15	15.7	18.0	8.0	0.55	0.244	0.0305	-173
B-16	6.28	27.0	12.0	1.82	0.81	0.0675	-132
B-17	3.12	26.8	11.9	2.70	1.20	0.101	-102
B-18	1.57	26.8	11.9	4.70	2.09	0.176	-90
B-19	0.628	26.8	11.9	13.1	5.83	0.491	-72
B-20	0.421	26.8	11.9	17.7	7.86	0.662	-54

TABLE 22

Steady State Conditions for Equipment Arrangement Three
Fluid Feed Rate Forcing
Process Fluid-Water

Run No.	Radians / Minute	Water Feed, °F θ_f	θ	Cooling Water, θ_{w_i}	θ_{w_o}
A-53	0.421	170.0	141.5	75	125.1
A-54	0.628	170.1	141.5	75.4	125.9
A-55	1.57	170.0	141.3	76.0	125.9
A-56	3.12	170.1	141.5	76.1	126.0
A-57	6.28	170.1	141.8	76.2	126.2
A-58	15.7	170.1	141.5	77.5	126.9
A-59	31.4	170.0	142	76.9	126.9

Parameters: Coolant Flow, 5.52 lb./min.

Feed Rate Forcing Range: Avg. 6.5-10.8-15.1 lb./min.

Agitator RPM: 200

TABLE 23

Processed Frequency Response Data, Equipment Arrangement Three
Fluid Feed Rate Forcing
Process Fluid-Water

Run No.	Radians / Minute	Steady State Gain, Chart Divs.	Steady State Gain, °F	Average Amplitude, Chart Divs.	Average Amplitude, °F	Magnitude Ratio	Phase Angle, Degrees
A-53	0.421	22.5	10.0	29.4	13.1	0.764	-52
A-54	0.628	17.1	7.59	29.4	13.1	0.580	-64
A-55	1.57	7.28	3.24	29.4	13.1	0.248	-79
A-56	3.12	3.56	1.58	29.4	13.1	0.121	-86
A-57	6.28	1.64	0.729	29.4	13.1	0.0556	-94
A-58	15.7	1.25	0.554	43.8	19.5	0.0284	-92
A-59	31.4	0.755	0.336	43.8	19.5	0.172	-122

TABLE 24

Steady State Conditions for Equipment Arrangement Four
Fluid Feed Rate Forcing
Process Fluid-Oil

Run No.	Radians / Minute	Oil Feed, °F		Cooling Water,	
		θ_f	θ	θ_{w_i}	θ_{w_o}
B-24	0.421	172.0	140.8	78.3	90.0
B-25	0.628	170.8	141.5	79.3	90.6
B-26	1.57	171.0	140.9	78.8	89.7
B-27	3.12	170.5	140.9	77.5	89.8
B-28	6.28	172.1	141.0	78.0	89.0
B-29	15.7	171.0	140.1	78.0	89.0
B-30	31.4	172.0	140.0	78.0	89.0

Parameters: Coolant Flow: 10.8 lb./min.

Feed Rate Forcing Range: Avg. 4.2-8.1-12 lb./min.

Agitator RPM: 200

TABLE 25

Processed Frequency Response Data, Equipment Arrangement Three
Fluid Feed Rate Forcing
Process Fluid - Oil

Run No.	Radians / Minute	Steady State Gain, Chart Divs.	°F	Average Amplitude, Chart Divs.	°F	Magnitude Ratio	Phase Angle, Degrees
B-24	0.421	50.0	22.2	25.6	11.4	0.512	-51
B-25	0.628	50.0	22.2	16.8	7.46	0.334	-69
B-26	1.57	50.0	22.2	7.42	3.30	0.148	-86
B-27	3.12	50.0	22.2	3.75	1.67	0.075	-92
B-28	6.28	50.0	22.2	1.84	0.818	0.0368	-90
B-29	15.7	65.0	28.9	1.20	0.533	0.0185	-101
B-30	31.4	65.0	28.9	0.60	0.27	0.0092	-127

TABLE 26

Processed Frequency Response Data, Arrangement Four
Effect of Agitator RPM on Response Curves
Cooling Water Rate Forcing
Process Fluid - Oil

Run No.	Agitator RPM	Radians / Minute	Average Amplitude, Chart Divs.	Average Amplitude, °F	Steady State Gain, Chart Divs.	Steady State Gain, °F	Magnitude Ratio	Phase Angle, Degrees
B-48	95	0.314	7.2	3.2	13.8	6.13	0.52	-68°
B-49	95	0.42	4.9	2.2	13.8	6.13	0.355	-87
B-50	95	0.628	3.45	1.53	13.8	6.13	0.250	-93
B-51	95	1.57	0.92	0.41	13.8	6.13	0.0677	-137
B-34	200	0.314	14.95	6.65	24.6	10.9	0.610	-56°
B-35	200	0.420	12.55	5.58	24.6	10.9	0.510	-68°
B-36	200	0.628	8.10	3.60	24.6	10.9	0.330	-84°
B-41	200	1.048	6.10	2.71	24.6	10.9	0.248	-95°
B-37	200	1.57	2.84	1.26	24.6	10.9	0.115	-103
B-42	200	2.52	2.10	0.93	24.6	10.9	0.0854	-122°
B-38	200	3.12	1.42	0.63	24.6	10.9	0.058	-131
B-43	200	4.19	0.80	0.35	24.6	10.9	0.0325	-150
B-39	200	6.28	0.45	0.20	24.6	10.9	0.0183	-165°
B-44	200	7.85	0.20	0.089	24.6	10.9	0.00813	-179°
B-45	200	12.56	0.07	0.0031	24.6	10.9	0.00284	-197°

TABLE 26 Continued

Processed Frequency Response Data, Arrangement Four
Effect of Agitator RPM on Response Curves
Cooling Water Rate Forcing
Process Fluid - Oil

Run No.	Agitator RPM	Radians / Minute	Average Amplitude, Chart Divs.	Average Amplitude, °F	Steady State Gain, Chart Divs.	Steady State Gain, °F	Magnitude Ratio	Phase Angle, Degrees
B-52	350	0.314	16.7	7.33	25.5	11.3	0.655	-57
B-53	350	0.420	14.9	6.63	25.5	11.3	0.584	-67.5
B-54	350	0.628	10.11	4.50	25.5	11.3	0.396	-79
B-55	350	1.570	4.12	1.83	25.5	11.3	0.161	-97
B-56	350	3.120	1.65	0.735	25.5	11.3	0.0647	-126
B-57	350	4.190	1.10	0.489	25.5	11.3	0.0432	-143
B-58	350	7.85	0.22	0.120	25.5	11.3	0.0106	-172
B-59	350	12.56	0.12		25.5	11.3	0.00470	-185

TABLE 27

Processed Frequency Response Data, Arrangement Four
Effect of Coolant Flow Conditions on System Response
Laminar Coolant Flow

Run No.	Radians / Minute	Average Amplitude, Chart Divs.	°F	Magnitude Ratio	Phase Angle, Degrees
A-82	0.314	18.65	8.29	0.565	-65
A-83	0.420	15.30	6.80	0.463	-74
A-84	0.628	11.25	5.00	0.341	-80
A-85	1.57	4.70	2.09	0.142	-92
A-86	3.12	2.10	0.93	0.0636	-118
A-87	6.28	0.80	0.18	0.0242	-141
A-88	12.56	0.27	0.12	0.00818	-152

Parameters: Steady State Gain: 33 Chart Divisions

Fluid Feed Rate: 7.97 lb./min.

Coolant Flow Forcing Range: 0.06-0.18-0.30 GPM

Agitator RPM: 200

TABLE 28

Processed Frequency Response Data, Arrangement Four
Effect of Coolant Flow Conditions on System Response
Turbulent Coolant Flow

Run No.	Radians / Minute	Average Amplitude, Chart Divs. °F	Magnitude Ratio	Phase Angle, Degrees
A-91	0.314	8.7	0.568	-53
A-92	0.420	8.3	0.543	-61
A-93	0.628	6.0	0.392	-71
A-94	1.57	2.75	0.179	-91
A-95	3.12	1.15	0.0751	-107
A-96	6.28	0.50	0.0327	-118
A-97	12.56	Indeterminant		

Parameters: Steady State Gain: 15.3 Chart Divisions

Fluid Feed Rate: 7.97 lb./min.

Coolant Flow Forcing Range: 0.36-0.48-0.60 GPM

Agitator RPM: 200

TABLE 29

*Effect of Agitator Speed on Theoretical Steady State Value of h_o

	Water		Oil	
Impeller Speed	Re. No. for Mixing $ND^2\rho/\mu$	h_o, $\frac{BTU}{(hr.)(ft.^2)(^oF)}$	Re. No. for Mixing $ND^2\rho/\mu$	h_o $\frac{BTU}{(hr.)(ft.^2)(^oF)}$
40	14,400	240	612	14.2
50	18,050	285	767	28.4
60	21,600	314	919	31.6
80	28,800	378	1225	38.8
100	35,800	438	1530	44.7
120	43,200	498	1840	50.9
140	50,400	558	2145	56.0
160	57,600	601	2450	61.6
180	64,800	658	2760	66.0
200	72,000	763	3060	72.0
240	86,400	787	3680	80.5
280	101,000	887	4280	88.6
320	115,400	953	4900	98.6

APPENDIX D

Miscellaneous Data

TABLE 30

Physical Properties of Process Fluids

Special Low V.I. Oil			
Temperature, F	100	147	210
Specific Gravity	0.891	0.875	0.852
Viscosity, Centipoise	26.3	9.64	3.83
Thermal Conductivity, (B.T.U.)/ (hr.)(sq.ft.)(°F/ft.)	0.070	0.069	0.067
Specific Heat, B.T.U./(lb.)(°F) (at one atm.)	0.457	0.484	0.510
Water			
Temperature, F	100	147	200
Specific Gravity	0.993	0.981	0.963
Viscosity, Centipoise	0.71	0.41	0.28
Thermal Conductivity, (B.T.U.)/ (hr.)(sq.ft.)(°F/ft.)	0.350	0.373	0.402
Specific Heat, B.T.U./(lb.)(°F) (at one atm.)	1.000	1.000	1.003

TABLE 31

Volumes and Weights of Equipment

Weight of Reactor Tank	17.469 lbs.
Weight of Coils for Arrangement One, Two and Three	1.313 lbs.
Surface Area of Above Coils	135.01 $in.^2$
Volume of Tank with Above Coils	0.7869 $ft.^3$
Weight of Coil for Arrangement Four	2.914 lbs.
Surface Area of Above Coils	264.83 $in.^2$
Volume of Tank with Above Coils	0.7671 $ft.^3$
Volume of Above Coils	0.0178 $ft.^3$

APPENDIX E

Explanation of Basic Principles

OUTLINE OF SERVO-THEORY AS APPLIED TO THE PRESENT PROBLEM

Because of the very recent interest in the field of control development by chemical engineers, a condensed description of some of the fundamentals of modern process control theory will be presented as they specifically affect the present problem. No attempt will be made to go into all the various facets of servo-theory. The excellent recent textbooks and technical articles can be consulted in the event a more detailed coverage is desired.

The following diagram presents a typical continuous agitated tank reactor with a possible mode of effluent temperature control. It is pointed out here that the system is hypothetical and is presented for illustrative purposes only:

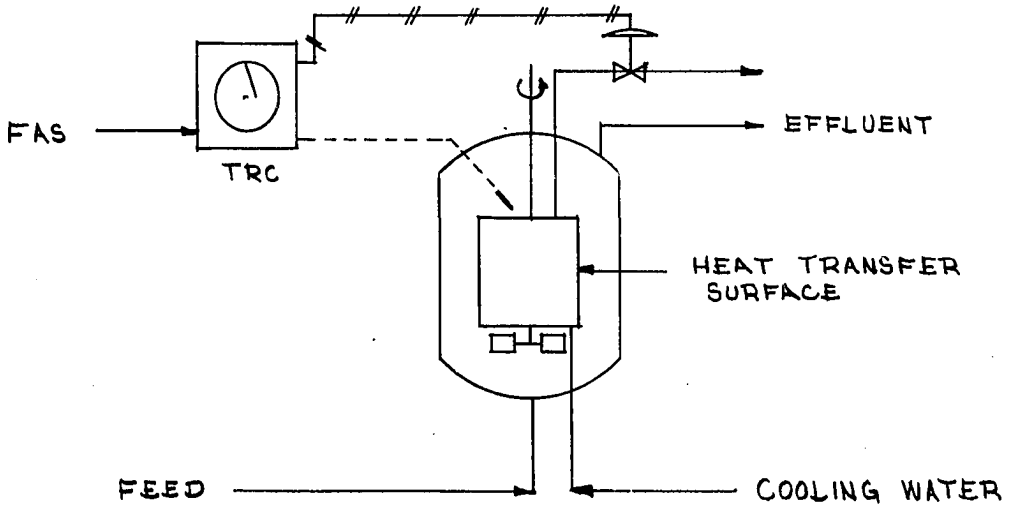


Figure 34

The unreacted feed enters the bottom of the reactor where, assuming perfect mixing, it immediately assumes the temperature and composition of the reactor fluid and the effluent. If the system is on proper control, the temperature remains constant at the desired setpoint. Also, effluent composition remains relatively constant. The cooling water rate remains at the value required to maintain reactor fluid temperature constant by removing the heat generated by the exothermic chemical reaction. The system has thus reached steady state operation, i.e., none of the process variables are changing with time at the various points in the system.

As has been the practice for many years, the process design of this unit is normally carried out on the basis of assumed steady state operation. The time rate of change of the various process parameters with a change in energy supply, feed rate or energy removal are ordinarily not given attention in the original process design. As a rule there is no information available as to the effect on a given variable with a sudden or periodic change in another variable. Under such conditions, the control system installed for the purpose of automatically correcting upsets may not perform its assigned task in the manner most desired. In a majority of cases, there is sufficient flexibility in controller adjustments and in system self-regulation to realize acceptable control. However in the forthcoming era of faster processes and computer control, such empirical techniques will not suffice. A basic, systematic and mathematically proven method must then be employed in completely characterizing control system dynamics.

Probably the most basic building block of modern control theory

is the so-called transfer function. Its meaning and utility must be understood in order to obtain the maximum information from the body of this work. Basically, the transfer function is a differential equation written with distinctive notation. It describes the manner in which a given variable changes with time when a related variable is changed. As a very simple example, consider the system described in Figure 34. For the sake of illustration, it will be assumed that there is no heat of reaction or heat transfer surface in the reactor. The fluid feed rate is also constant. Thus at steady state conditions the vessel and effluent temperature are identical to the feed temperature. If for some reason or another, the feed temperature is suddenly increased, the vessel and effluent temperature will also increase; but there will be a definite time lag because of the holding time in the vessel. The rate of change of the effluent temperature Θ is easily obtained from a simple unsteady state heat balance:

$$\frac{M}{W}\frac{d\Theta}{dt} = \Theta_f(t)-\Theta(t) \qquad \text{A-1}$$

M represents the mass of fluid in the vessel, W is the mass flow rate and Θ_f is the temperature of the feed. The units of $\frac{M}{W}$ are time, often represented by the symbol T. In order to obtain the final conventional form of a transfer function, the preceding differential equation is transformed by the Laplace transformation which is defined as:

$$L\left[f(t)\right] \triangleq \int_0^\infty f(t)e^{-st}dt \qquad \text{A-2}$$

If all initial conditions are assumed to be zero, the describing differential equation is then converted to:

$$T\Theta\, s + \Theta = \Theta_f \qquad \text{A-3}$$

On rearranging, this results in:

$$\frac{\theta}{\theta_f}(s) = \frac{1}{Ts + 1} \qquad \text{A-4}$$

This expression represents a first order transfer function relating the effluent temperature to the feed temperature. A classical solution of the defining differential equation will show that the variables are related by a simple exponential time lag. As stated before, the transfer function is then a special notation for a differential equation wherein some function of the operator, s, relates the variables in question.

Another basic concept which must be appreciated is that of the block diagram as is now very commonly used in all areas of control work. The control block diagram for the system illustrated in Figure 34 is now constructed:

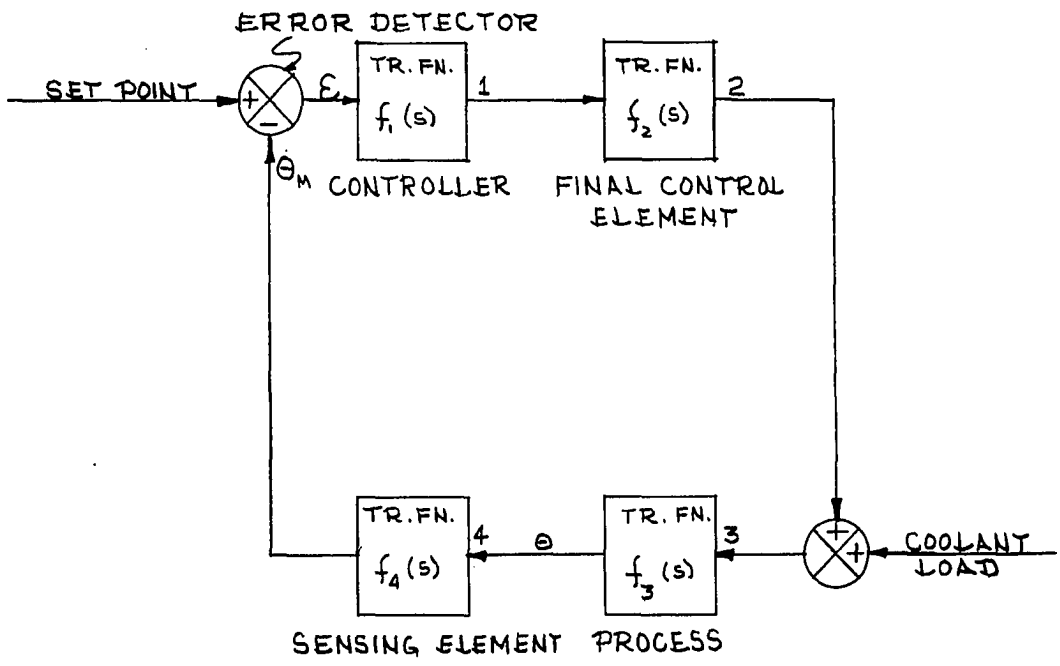


Figure 35

The various squares represent discrete points in the control system wherein output and input variables are represented by transfer functions. All transfer functions are composed of some function of s, various time constants and certain other constants made up of various process or control parameters. All describe the relationship between the output and input signal to the block in question in the schematic loop. Referring again to Figure 34 as a case in point, assume that there is a sudden increase in cooling water pressure in the line feeding the reactor tubes. This causes a decrease in reactor temperature. The error detector senses the deviation and transmits an error signal to the controller. Certain action is taken on the signal depending upon controller settings. A command, usually in the form of a pneumatic signal, is relayed to the final control element. A transfer function must relate its input and output also for the final control element cannot act instantaneously on a controller signal. The motor valve then decreases the flow of coolant to the reactor. Again, the result upon θ is far from instantaneous and the input and output signals are related by a transfer function which is often complicated and difficult to evaluate accurately. Finally, the sensing element must detect any rise in θ and transmit this information to the error detector. The same condition holds for signals to and from the sensing element.

The control system just described is one of the simplest feedback types possible since it may be represented by a single loop. Many systems are much more complicated, involving cascading and other types of multiple loop configurations. However, the basic principles of servo-theory remain the same and certain mathematical manipulations are

equally applicable for all systems. From the illustration just presented, it may be seen that a knowledge of the various transfer functions is essential to a complete understanding of system control dynamics. This may perhaps be demonstrated more clearly by a discussion of certain mathematical rules applicable in combining the various transfer functions making up the control loop.

At least one mathematical expression of considerable interest is that of the control ratio. For Figure 35, this ratio is Θ_M/Θ_i where Θ_M is the measured value of the reactor fluid temperature and Θ_i is the controller setpoint or desired value of the same variable. This ratio is equal to the entire closed-loop system equation:

$$\frac{\Theta_M}{\Theta_i} = \text{System Equation} \qquad \text{A-5}$$

In this case, block diagram algebra allows the combining by multiplication of the first three transfer functions up to the output signal Θ.

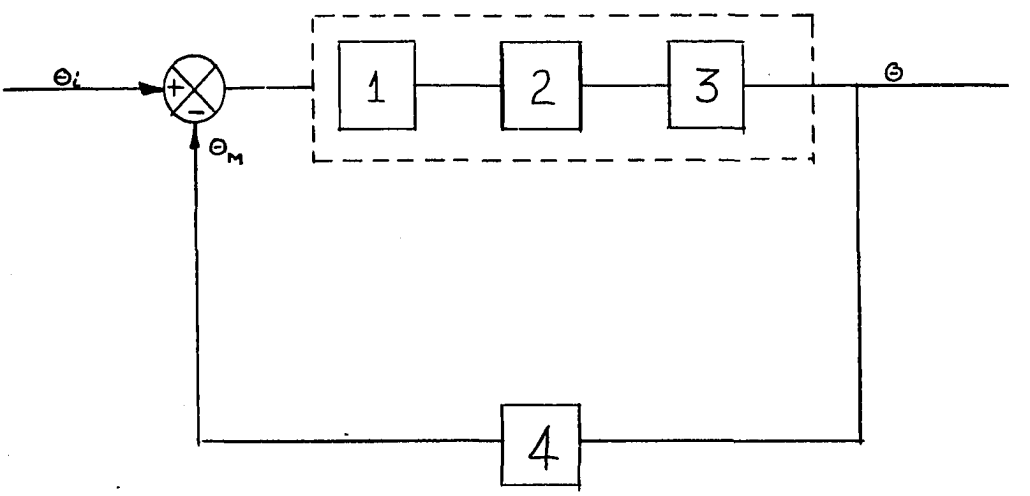


Figure 36

Simple arbitrary expressions are assigned to all transfer functions at this point in order to complete the discussion:

Number

$$\text{Controller Transfer Function} = K_1 + K_2/s = \frac{K_1 s + K_2}{s} \qquad (1)$$

$$\text{Control Element Transfer Function} = \frac{K_d}{T_d s + 1} \qquad (2)$$

$$\text{Process Transfer Function} = \frac{K_r}{T_r s + 1} \qquad (3)$$

$$\text{Measuring Element Transfer Function} = \frac{K_t}{T_t s + 1} \qquad (4)$$

Thus, referring to Figure 36, the three transfer functions within the dotted rectangle may be multiplied together (assuming the system is linear) to form the following:

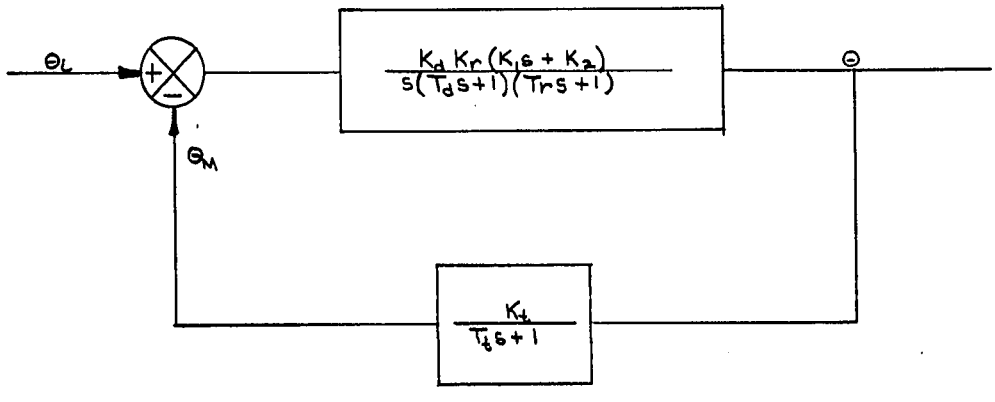


Figure 37

It is quite common to denote the constant portion of a given transfer function by the symbol K and the frequency variant portion by

the symbol G. In this particular case, a lag is introduced into the feedback loop by the measuring element. This transfer function will be denoted by the symbol K_tG_t. It may easily be demonstrated that the control ratio as previously defined may be represented by:

$$\frac{\Theta_M}{\Theta_i} = \frac{KG}{1 + (KG)(K_tG_t)} \qquad \text{A-6}$$

Thus by simple substitution, the system equation for the above loop is described in the following manner:

$$\frac{\Theta_M}{\Theta_i} = \frac{\dfrac{K_dK_r(K_1s + K_2)}{s(T_ds + 1)(T_rs + 1}}{1 + \dfrac{K_dK_rK_t(K_1s + K_2)}{s(T_ds + 1)(T_rs + 1)(T_ts + 1)}} \qquad \text{A-7}$$

The system equation is then a fourth order expression relating Θ_M, the measured value of the reactor temperature to Θ_i, the controller setpoint in the s domain. An analytical expression for the effect of Θ_i on Θ_M may be obtained by rearranging the system equation, assuming some type of forcing function for Θ_i and obtaining its inverse in the time domain. Thus, if a solution is obtainable and it is assumed that the system is forced by a unit step function applied to Θ_i, it may be readily observed as to the time variation of Θ_M. It could be overdamped, critically damped, underdamped or oscillatory depending on the values of the various constants in the equation. This method, although offering an ultimate solution, is not generally recommended. Even for such a simple system as the one described, the solution is quite tedious. It may be appreciated that for more involved systems, hand mathematical methods soon become prohibitively unwieldy. Another objection to such analytical

methods is the fact that it cannot be easily ascertained as to how system parameters may be changed in order to realize desired performance. Analytical methods such as those described are not often used except as methods for instruction.

It may be readily proven that if s is replaced by $j\omega$ in a system equation or any individual transfer function, the resulting expression characterizes the dynamic variation in the output variable when forced by a sinusoidal variation in the input. Such a substitution is theoretically restricted to linear systems; however for small variations around steady state values, it is often a close approximation for non-linear systems. After such a substitution is made, a well-known graphical method may be used very effectively in either analysis or synthesis of the control network in question. The resulting graphs are known as Bode or attenuation diagrams.

In a graphical analysis, the first step is usually that of plotting the process transfer function on a Bode diagram. Referring to the arbitrarily assigned transfer functions, it is assumed for simplicity that K_r of the process transfer function is equal to unity. Thus:

$$\frac{\theta_{ro}}{\theta_{ri}} = \frac{1}{T_r\,(j\omega) + 1} \qquad \text{(Transfer Function No. 3)}$$

The logarithm of the ratio on the left is then plotted against the logarithm of the frequency to form one portion of the Bode diagram. It is noted that the denominator of the transfer function is a vector quantity with both magnitude and phase angle. The other portion of the diagram consists of a plot of this phase angle with the logarithm of assumed frequencies. The control element transfer function may be plotted

in the same manner. Figure 38 illustrates the preceding statements.

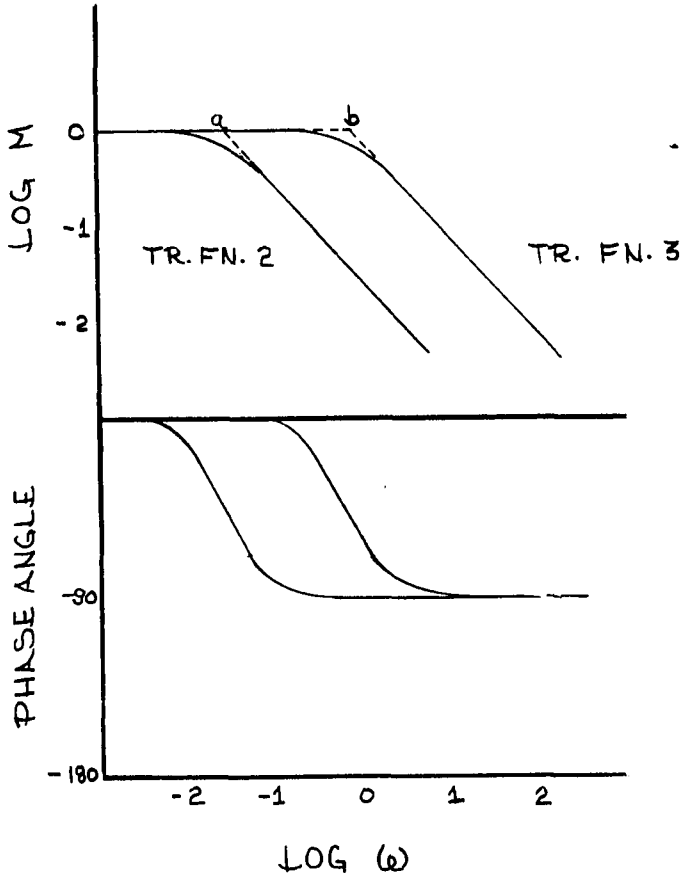


Figure 38

Points a and b in the top plot represent the "break" frequencies of transfer functions 2 and 3 respectively. The points are equal numerically to the reciprocals of respective time constants T_r and T_d in radians per unit time. For purposes of illustration, time constants have been selected more nearly equivalent in numerical value than would actually by the case for the particular transfer functions involved. The great utility of the Bode diagram lies in the fact that since logarithms have been plotted, the transfer functions may be in effect multi-

plied together by the simple procedure of addition on the diagrams. Thus, transfer functions 2 and 3 may be resolved to single curves as shown in Figure 39.

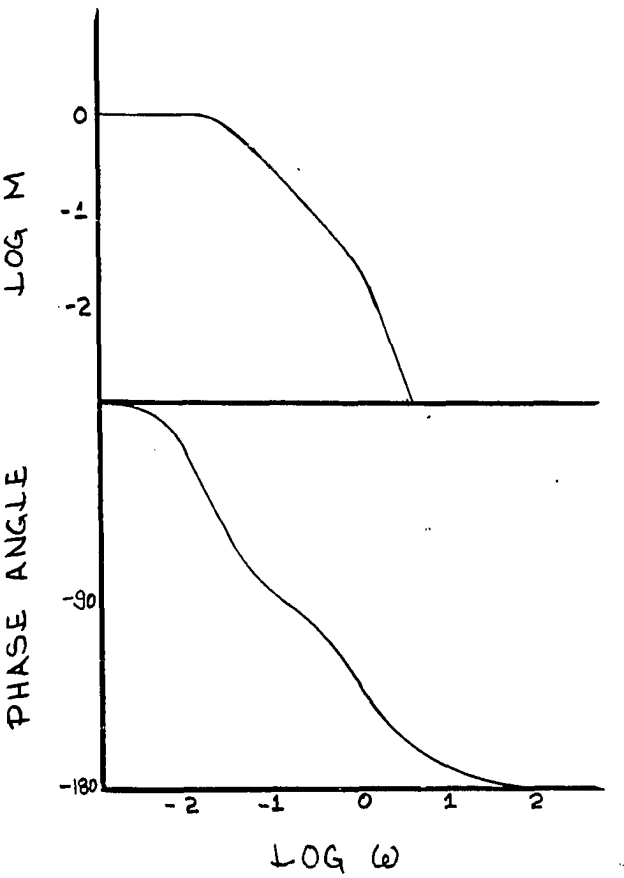


Figure 39

Other control loop transfer functions may be combined in the same general manner. Various controller constants can then be applied in determining the overall effect of these on the system response curves. This approach to system analysis, though graphical, yields a wealth of information. The problem of control loop stability is readily handled by these techniques. Such methods, or modifications thereof, are widely

employed in the broadening field of cybernetics.

One of the chief objectives of a theoretical approach to process control problems is that of being able to determine judicious combinations of control components with the process in question so that a rapidly-responding, stable control system is realized. This same information is necessary in the event a process or several processes are to be controlled by a centralized electronic computer system. The basic elements of analytical and graphical methods for such a study have been demonstrated.

THEORY OF FREQUENCY AND TRANSIENT RESPONSE TECHNIQUES AS APPLIED TO CHEMICAL PROCESSES

Transient Response

The transient response of a given process refers to a graph showing the change in time of one process variable after another variable by which it is affected is suddenly changed a given amount. For linear systems, the direction or magnitude of the input charge always results in output reaction curves which are dynamically similar. For non-linear systems, the size and direction of the input can result in output curves which are not similar. A considerable amount of information may be obtained from the knowledge of a process's transient response; however, this information is in general qualitative. Quantitative information may be obtained only by a very approximate graphical procedure, curve fitting or certain other numerical methods. Nevertheless, transient response analysis is utilized extensively because of the information available from it and the relative ease with which the reaction curves may be generated.

The majority of chemical processes may be represented by one of three general types of transient reaction curves. These are (a) the first order transient, (b) a transient composed of two or more non-interacting exponential lags, and (c) some combinations of (a) or (b) with a true time delay or pure dead time. Typical curves are shown in Figure 40.

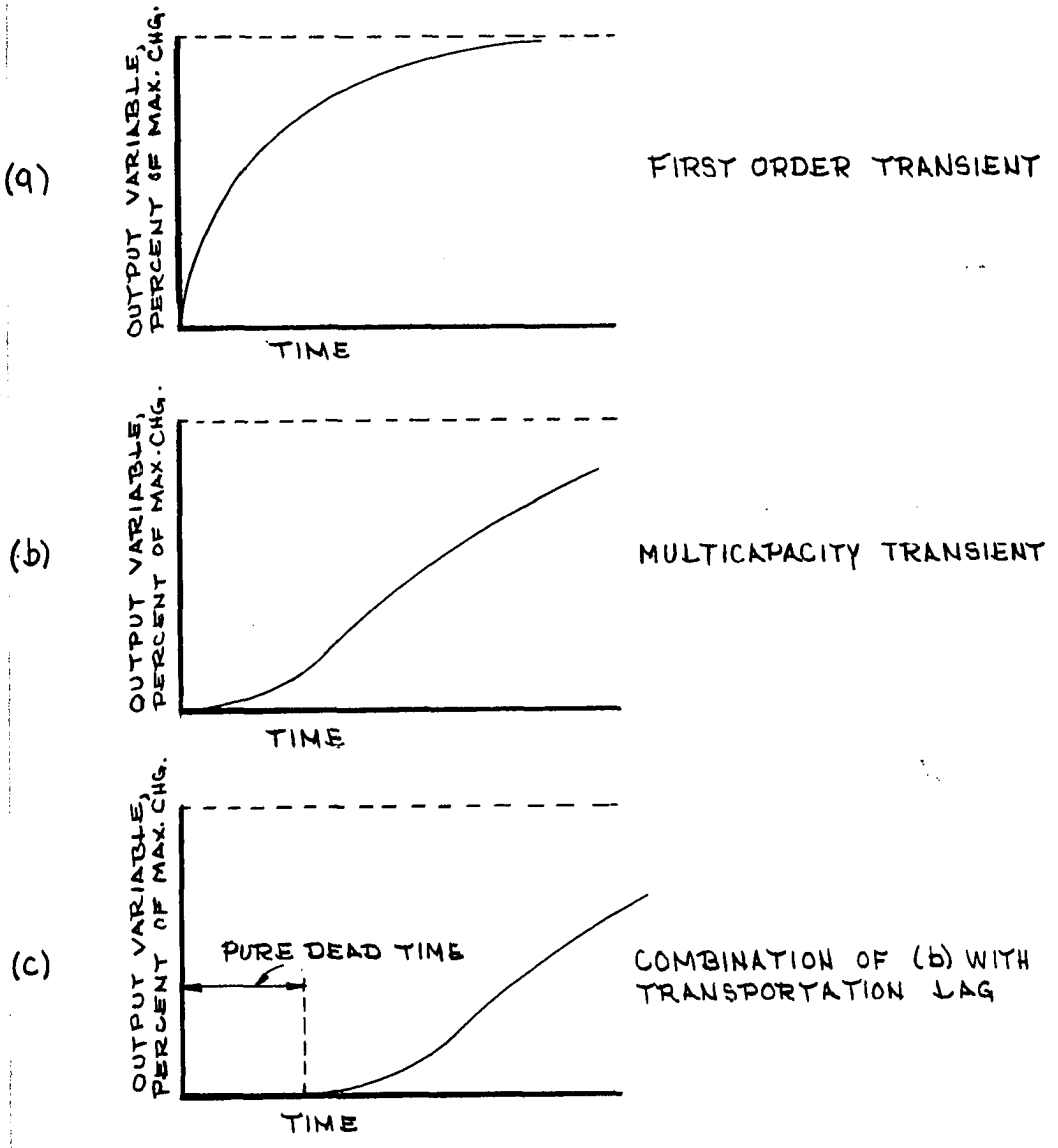


Figure 40

Type (c) curve is of special interest because it is encountered quite often in control problems peculiar to the chemical process control field. This is brought about by the multitude of piping present in most process plants. The transmission of, for example, a temperature signal by the flow of a fluid through a long conducting pipe involves true time delay

or pure dead time. The open loop transients for such processes as heat exchange, distillation, absorption and others may be represented by some arrangement of the curves presented. All are overdamped, i.e., there is present some degree of self-regulation. However, for exothermic chemical reactions, this regulation may not be present in which case the familiar s-shaped transient would not be obtained.

Type (b) curves may be analyzed graphically by the method of Oldenbourg and Sartorius for the case of the response curve for two series sequenced exponential time stages. It is cautioned that the method is graphical and therefore quite approximate as Figure 41 shows:

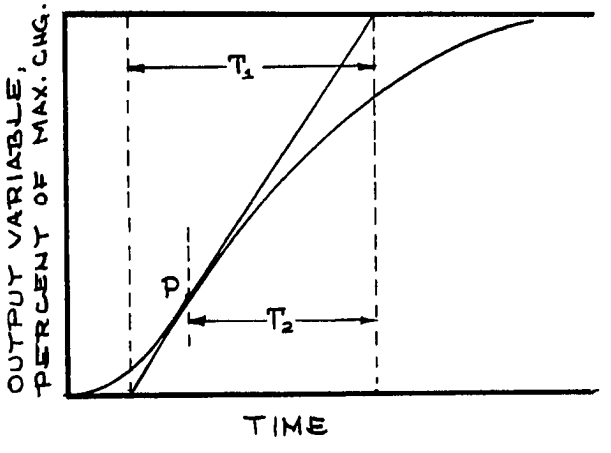


Figure 41

The time T_1 is the reflection on the time axis of the tangent line through the response curve point of inflection P. Time T_2 is the distance from the point of inflection to a position where the tangent line strikes the 100 per cent reaction point. A knowledge of these values then allows an estimation of the time constants T_a and T_b associated

with the transient in question. For the average response curve, the position of P and the slope of the tangent line through this inflection point is not very definite. The method is then subject to considerable inaccuracy although it is often used to advantage as a first approximation.

Analysis of the individual process by means of transient response is not at present used a great deal. Considerably more information is available by a study of the transient response of the closed loop. However, some open loop studies have been made by transient response techniques. Johnson and Bey (23) applied transient analysis as a portion of a study concerning a pneumatic analog. The method of Oldenbourg and Sartorius was employed by Cohen and Johnson (12) in the investigation of the dynamics of a long concentric pipe heat exchanger. In this case, the process was distributed rather than lumped. From the transient reaction curve they were able to obtain values for the time constants applicable to a second order staged system. This information, together with the inclusion of a term taking into account the transportation lag, resulted in a process transfer function which agreed fairly well with the experimental data. Levenstein (26) demonstrates a modification of an older method for obtaining a system's transfer function from a knowledge of the transient response. This numerical approach applies linear difference equations in converting the system transient to an expression approximating the transfer function. Such methods have been little investigated regarding process transients and offer a challenge as a new procedure for studying process dynamics.

Transient response has its most intensive application in the

study of closed-loop systems. Here, the effect of the all-important controller parameters on the overall control system may be observed. As previously mentioned, one procedure in the analysis of a complicated control situation is to make use of the analog computer. Differential equations relating the important process variables are derived and programmed into the computer along with those for the controller. The response of the output in question is then noted for a given set of controller constants. The effect of these is noted, then plotted in a systematic manner. The final result is a battery of diagrams from which optimum controller settings for the given system may be determined. Williams and co-workers (41, 42) used such an approach in the dynamical analysis of a five-plate distillation column. Williams and Young (44) also describe the results using the same technique in the analysis of a shell and tube multipass heat exchanger. It should be pointed out that in the use of these methods, no attempt is made to analyze the response curves except to note whether the response is overdamped, underdamped, oscillatory or unstable. Nevertheless, the procedure is of considerable value. Since control constants and process parameters are generally programmed in the form of potentiometer settings, the effect of any changes in these may be rapidly and systematically observed.

In summarizing, it may be stated that the chief value of transient response for the open loop case is the rapid and relatively simple method it possesses in providing a qualitative answer as to the speed and nature of a process response. Classical and numerical techniques for resolving the response curve into transfer function form are at present, time consuming and unwieldy. Graphical analysis of the response curve

may be applied to relatively simple systems but must be used with caution because of inherent inaccuracies. However, a transient analysis supplies the most direct information regarding closed loop stability. It is often used in this capacity as a means of analysis in electronic simulation of control processes.

Frequency Response

The dynamic characteristics of any block or combination of blocks in the feedback loop may be determined by frequency response analysis. Here, the input signal is forced in a periodic manner in place of the step function utilized in transient response analysis. The mathematical relationships involved may best be demonstrated by application of the following basic operational calculus:

The transformed input wave is: $L(K \sin\omega t) = K \frac{\omega}{s^2 + \omega^2}$

The assumed first order process transfer function is:

$$\frac{\theta}{\theta_i}(s) = \frac{1}{s + \alpha}$$

Multiplying these:

$$\theta(s) = \frac{1}{s + \alpha} \cdot \frac{K\omega}{s^2 + \omega^2}$$

This may be rearranged to:

$$\theta(s) = -\frac{K\omega}{\alpha^2 + \omega^2} \left[\frac{s - \alpha}{s^2 + \omega^2} - \frac{1}{s + \alpha} \right]$$

Neglecting the transient term and using transform tables to obtain a steady state solution in the time domain:

$$\theta(t) = \frac{K}{\sqrt{\alpha^2 + \omega^2}} \sin(\omega t - \phi)$$

Thus it is proven mathematically that the output of a linear system will be a sinusoid of the same frequency as the input wave but will lag it by the angle ϕ. The output will also be reduced in amplitude by an amount dependent upon the applied frequency ω.

The value of frequency response lies in the fact that it provides information directly in the form most readily utilized. For example, in the case of a chemical process, a selected input variable is forced sinusoidally at a conveniently low frequency. The output variable then changes in a periodic manner--a sine wave also, if the system is linear. The relationship between two variables is said to be linear if, at a given frequency, the ratio of the input and output waves do not change with a variation in the input wave amplitude. Although this constitutes a theoretical restriction to the utility of frequency response techniques, it holds in the great majority of cases for small variations around steady state values. It is convenient if the two variables are both traced on the same strip chart. From such records the key information obtained is the ratio of the amplitudes for the two waves, known as the magnitude ratio. Also, the distance between corresponding points on the waves is obtained in degrees. This is the phase lag. The values for both phase lag and magnitude ratio are both very much dependent upon the impressed frequency of the input variable as has been proven mathematically. The manner in which these quantities change with input frequency depends upon the response characteristics of the system under study. A plot of log magnitude ratio and phase lag versus log impressed frequency defines the so-called Bode or attenuation diagrams as previously discussed. The diagrams are actually graphical expressions for

differential equations and are different for all unlike systems. Figure 42 illustrates the basic fundamentals of frequency response.

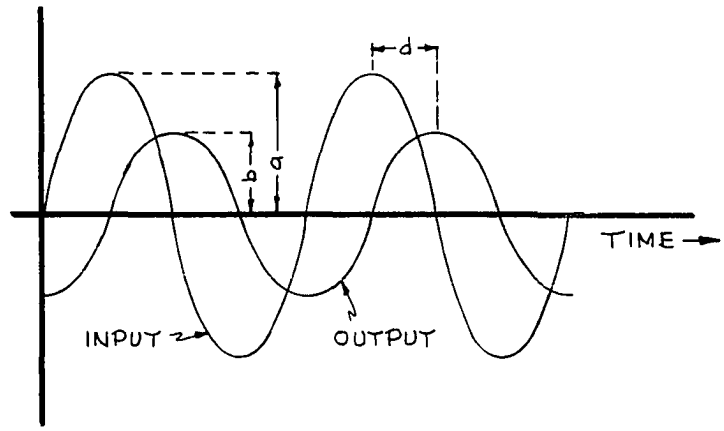


Figure 42

The numerical values of the ratio b/a together with the lag d as functions of frequency make up the raw data from a frequency response study. It should be kept in mind that, at least for chemical processes, the units describing the input and output variables are usually not the same. For example, the output might be effluent concentration of a key component in lb. mols per cubic foot as forced by variations in steam pressure to a reactor in the units of force pounds per square inch. Or it could be liquid level in feet when acted upon by a periodic variation in flow rate in gallons per minute. The units are subject to much more heterogeneity than is the case for electrical and mechanical systems. This makes it advisable to determine a steady-state gain at the outset of a frequency response analysis. Amplitude limits for the input variable are then based upon the resulting information. The value chosen is the smallest value which will permit an intelligible recording of the

output variable over a reasonable extended frequency spectrum.

In the present work, the process transients were obtained as part of the determination of the steady state gains. Thus if the cooling water rate were changed suddenly (in both positive and negative directions) the transient and steady state condition of the output variable was continuously recorded. The ratio of the input and output final values represents the magnitude ratio at zero frequency. All other magnitude ratios are then divided by this figure so that the resulting Bode diagram is in effect standardized at a numerical value of unity at zero frequency. This may be represented mathematically as follows:

$$\text{Magnitude Ratio} = \frac{\left[\frac{\Delta\theta_f}{\Delta W_c}\right]_{F = F}}{\left[\frac{\Delta\theta_f}{\Delta W_c}\right]_{F = 0}} \qquad \text{A-8}$$

It is not mandatory to apply such procedures, however it does permit standardization and a convenient method for comparing attenuation diagrams.

All attenuation and phase lag diagrams have certain common factors, particularly for chemical processes. As input frequencies are increased, the magnitude ratio progresses continually to lower values. If the makeup of the process is such that any capacitance acts as a phase lead contributor, the magnitude ratio curve levels out or in some cases rises during short bands of frequency change. In any event however, the magnitude ratio decreases to zero at infinite frequency, for no real system can transfer a signal at infinite frequency. Furthermore, the phase lag always increases to some definite limiting value for

series sequenced stages as the frequency increases indefinitely. As previously stated, the factor of key importance is the path which these curves take throughout the applied frequency.

An easily visualized method for describing the frequency variation of magnitude ratio and phase lag is that of the Nyquist diagram. The Nyquist diagram for a second order process is presented in Figure 43 for illustration:

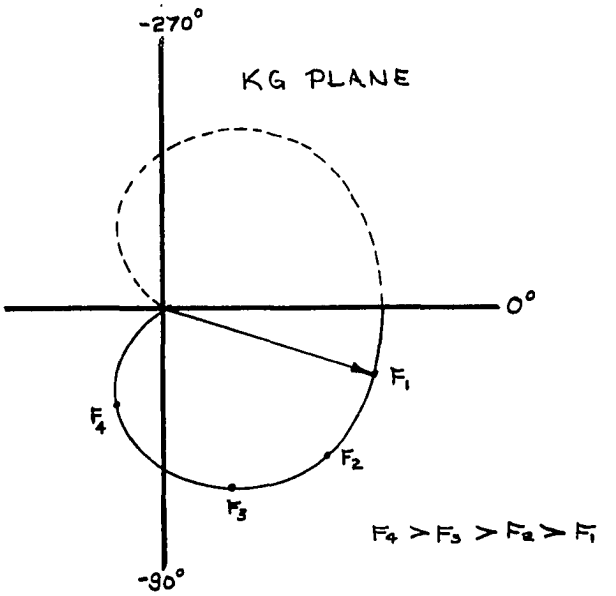


Figure 43

Here, the magnitude ratio is plotted on polar graph paper as a vector. For example, a magnitude ratio represented by line L is plotted at an angle corresponding to that of the appropriate phase lag for the frequency F_1. Points corresponding to F_2, F_3, F_4, etc., are also plotted and the resulting locus is the Nyquist diagram. It is readily observed that as the frequency increases to large values, the magnitude ratio approaches zero and the phase lag approaches some limiting angle for series sequenced time lags. For transportation lags however, the

phase angle does not approach a limiting figure but increases (negatively) indefinitely. The science of servomechanisms has been perfected to such a degree that with the above types of information and curves available, many conclusions regarding an individual block or the complete control system may be drawn. All the details of such techniques are too involved and lengthy for discussion here; any one of several texts on servo-theory (5, 11, 35) may be consulted for the desired information. It should be mentioned however, that the phase lag contributed by the process is of paramount importance in the stability of the final control loop. The ability to predict this lag accurately for a given process is then of prime concern.

Chemical process control development differs from most classical chemical engineering research endeavors in that an explicit solution to the describing differential equations is not necessary. The mathematical expression relating the change in a given variable with time when forced by another is rarely sought for two reasons: (1) Except for the simplest control loops, integration of the system equation by the inverse Laplace transformation is invariably too tedious and difficult for practicability and (2) all the information required for resolution of the control loop may be realized from transfer functions themselves either by graphical solution or by simulation. Thus, insofar as a knowledge of control dynamics is concerned, the transfer function represents a solution to the dynamical characteristics of the process.

Equipment For Response Analysis

The imposition of the sine wave to an input variable in a

given process is fraught with many difficulties. This perhaps accounts for the scarcity of experimental response data for processes in the literature. Such data are readily available however for various electronic and mechanical components such as amplifiers, servo units, controllers, valves, etc. The prime requisite, of course, is the equipment at hand for the introduction of a sine wave into some process variable. Sine wave generators have been available from commercial suppliers since about 1954. The usual arrangement is to supply a power source consisting of a synchronous electric motor with some wide-range, sensitive and accurate speed reduction mechanism for providing a variable output shaft rotation. Rotational motion is then converted to translational by the use of an eccentric. Through appropriate transducers, the position signal is converted to a pneumatic signal with the conventional 3 to 15 psig range. The desired pressure levels and pressure amplitudes may be obtained by adjustment. All settings are continuous on the more expensive instruments. A test may then be run on the process in question by connecting the pressure output signal from the generator onto the diaphragm valve used in controlling the desired input variable. St.Clair, et. al. (34) present a comprehensive discourse on sine wave generators. In addition to their interesting descriptions they provide listings of sources wherein more specific information may be obtained. Eckman and Moise (15) provide a description of the construction, operation, and analysis of data from a sine wave generator. At the present time, brochures are available from instrument manufacturers describing their particular type of generator (29).

The use of a commercial generator with a variable pressure

output is a very convenient method for conducting frequency response tests since process lines do not have to be dismantled for the insertion of special equipment. The only input connection is the air line at the control valve diaphragm. However, a disadvantage arises here since the resulting graphs include valve dynamics as well as the dynamics of the process, assuming that the air pressure variation at the generator is recorded as the input. Usually this is insignificant because of the large difference between valve and process break-points. In certain cases involving a fast process and a high friction valve, the interpretation of experimental results could be misleading. This is not meant as a criticism of pneumatic generators, however the true dynamics of the process itself can best be achieved by mechanically manipulating the control valve stem. The same result would of course be realized from a pneumatic signal if the input wave is obtained by transducers directly from the valve stem. The disadvantage of a purely mechanical system is the difficulty in regulating valve stem levels and input amplitudes.

An attempt has been made to present a clear, concise explanation of modern control theories and techniques as specifically applied to the present problem. It is hoped that it will be of value as introductory information to the material found in the body of the text.